

Summer 2017

BIOGEOCHEMICAL INTERACTIONS IN FLOODED UNDERGROUND MINES

Renee Schmidt
Montana Tech

Follow this and additional works at: http://digitalcommons.mtech.edu/grad_rsch

 Part of the [Geochemistry Commons](#)

Recommended Citation

Schmidt, Renee, "BIOGEOCHEMICAL INTERACTIONS IN FLOODED UNDERGROUND MINES" (2017). *Graduate Theses & Non-Theses*. 129.
http://digitalcommons.mtech.edu/grad_rsch/129

This Thesis is brought to you for free and open access by the Student Scholarship at Digital Commons @ Montana Tech. It has been accepted for inclusion in Graduate Theses & Non-Theses by an authorized administrator of Digital Commons @ Montana Tech. For more information, please contact sjuskiewicz@mtech.edu.

BIOGEOCHEMICAL INTERACTIONS IN FLOODED UNDERGROUND
MINES

by
Renée Schmidt

A thesis submitted in partial fulfillment of the
requirements for the degree of

Master of Science in Geoscience:
Geochemistry Option

Montana Tech
2017



Abstract

This study presents a biogeochemical analysis of microbial communities in flooded underground mines in Butte, Montana, USA. Samples were collected from nine mineshafts representing three distinct geochemical zones. These zones consist of the East, West, and Outer Camp mines. The East Camp mines, bordering the Berkeley Pit Superfund site, have the highest concentrations of dissolved metals and the most acidic pH values. Dissolved metal concentrations in the West Camp are one to three orders of magnitude lower than in the East Camp and have nearly neutral pH values. The Outer Camp mines have similar metal concentrations to the West Camp but are neutral to alkaline in pH. Sulfide levels also differ between the zones. In the East Camp, sulfide levels were below detection limits, whereas the West and Outer Camp mines had sulfide concentrations ranging from 10^{-6} to 10^{-4} mol/L. δD and $\delta^{18}O$, major cations and anions, dissolved inorganic carbon (DIC) with $\delta^{13}C_{DIC}$, dissolved organic carbon (DOC) with $\delta^{13}C_{DOC}$, and trace elements characterized the microbial habitat in each mine. DNA from planktonic biomass was assessed for phylogenetic diversity using 16S and 18S rRNA gene sequencing. Biological trends were predicted to parallel the geochemical zones; however, the microbial communities showed characteristics unique to each site. The East Camp and Orphan Boy from the Outer Camp had the greatest microbial diversity. The Emma and Travona from the West Camp had similar microbial communities, but the Ophir had the least diversity and bacterial phyla not found in the other sites. Both the geochemical and microbial findings from the Ophir suggest that mine water is mixing with a surficial source or from storm water input. This thesis provides a foundation for future biological work involving metabolic potential (metagenomic) and activity (proteomic) analysis in anoxic mine waters. Additionally, these results have relevance to industrial applications in bioleaching and bioremediation.

Keywords: water-rock-microbe interactions, biogeochemistry, underground mines, 16S rRNA gene, 18S rRNA gene, microbial diversity, Butte, Montana

Acknowledgements

Thank you, Dr. Alysia Cox, for being such a wonderful adviser and mentor. Thank you to the following individuals who assisted me in sample collection and analyses: Laboratory Exploring Geobiochemical Engineering and Natural Dynamics (LEGEND) members Georgia “Like a Boss” Dahlquist, “J-Dawg” Jordan Foster, and “Co-captain” McKenzie Dillard; faculty and staff from the Montana Bureau of Mines and Geology (MBMG) Gary Icopini, Ted Duaine, Matt Berzel, Jeremy Harwood, Ashley Huft, and Jackie Timmer. Dr. Chris Gammons and Joe Griffen provided a wealth of knowledge about the Butte water systems and assisted in sample collection. Dr. Steve Parker and Gary Wyss provided hours of instrument training. Mark Mariano, Joao Nascimento, and Anna Nugent provided extra helping hands during some excruciatingly cold and windy days. I also want to thank my family, especially Peter Hofacker for their love, support and help. Thank you to my committee members Drs. Chris Gammons, Katie Hailer, and Marisa Pedulla.

Funding for this project was made possible by: the Montana Tech Faculty Development and Faculty Seed Grants to Dr. Alysia Cox; the Montana Research and Economic Development Initiative (MREDI) Grant to Drs. Jerome Downey, Edward Rosenberg, Hsin-Hsiung Huang, and Alysia Cox; the NASA Exobiology Award (#NNX-16AJ-616) to Drs. Everett Shock, Alysia Cox, Jayson Raymond, Jordan Okie, Kris Fecteau, and Grayson Boyer.

Table of Contents

ABSTRACT	II
ACKNOWLEDGEMENTS	III
LIST OF TABLES	VI
LIST OF FIGURES.....	VII
LIST OF EQUATIONS	IX
GLOSSARY OF ABBREVIATIONS	X
1. INTRODUCTION	1
1.1. <i>Statement of Purpose</i>	1
1.2. <i>History</i>	1
1.3. <i>Site Description</i>	2
1.3.1. Geology	2
1.3.2. Geochemistry and Groundwater Divides	3
1.4. <i>Microbiology</i>	6
1.5. <i>Previous Work</i>	7
1.6. <i>Thesis Objectives</i>	10
2. METHODS	11
2.1. <i>Field Methods</i>	11
2.1.1. Sample Collection.....	11
2.1.2. Water Filtration and Preservation.....	12
2.1.3. Planktonic Biomass Collection.....	13
2.1.4. Geochemical Parameters	14
2.1.5. Field Spectrophotometry	14
2.1.5.1. Silica (SiO ₂).....	14
2.1.5.2. Ferrous Iron (Fe ²⁺)	15
2.1.5.3. Total Dissolved Sulfide (H ₂ S, HS ⁻)	15

2.2.	<i>Analytical Methods</i>	16
2.3.	<i>Biological Methods</i>	17
2.3.1.	DNA Extraction	17
2.3.1.1.	PCR and Gel Electrophoresis.....	20
2.3.1.2.	Sequencing	22
3.	RESULTS.....	24
3.1.	<i>Mine Water Chemistry</i>	24
3.2.	<i>PCR and Gel Electrophoresis</i>	43
3.3.	<i>Sequencing Results</i>	44
3.3.1.	Domain Distribution	44
3.3.2.	16S rRNA Gene: Archaea	46
3.3.3.	16S rRNA Gene: Bacteria	47
3.3.4.	18S rRNA Gene: Eukarya	50
4.	DISCUSSION.....	52
4.1.	<i>Defining the Habitat</i>	52
4.1.1.	Physico-chemical Parameters	52
4.1.2.	Stable Isotopes	55
4.1.3.	Major Cations, Major Anions, and Trace Elements	57
4.1.4.	pH Dependent Speciation	60
4.1.5.	Microbial Communities	62
4.1.6.	Microbial diversity in the Ophir.....	66
4.1.7.	Natural Amelioration?.....	67
5.	CONCLUSION AND FURTHER STUDIES	68
	REFERENCES CITED	70
6.	APPENDIX A: RAW DATA.....	77
7.	APPENDIX B: SUPPLEMENTAL DATA	85

List of Tables

Table I: Preservation and storage specifications for chemical composition.....	13
Table II: Methods and reagents for dissolved silica	15
Table III: Methods and reagents for FerroZine.....	15
Table IV: Methods and reagents for dissolved sulfide	16
Table V: Polymerase chain reaction (PCR) primer sequences	20
Table VI: Nucleotide mixed base pairs.....	20
Table VII: Archaeal phyla and classes.....	47
Table VIII: Reducing and oxidizing bacteria genera	49
Table IX: Hydrolab field parameters for mines, Silver Bow and Blacktail Creeks.	77
Table X: Spectrophotometry data.	78
Table XI: Stable isotopes.....	78
Table XII: Dissolved carbon concentrations in mines and Silver Bow and Blacktail Creeks.	79
Table XIII: Major cation concentrations in mines.....	80
Table XIV: Major anion concentrations in mines.....	80
Table XV: Trace element concentrations in mines.....	81
Table XVI: Log K values for carbonic acid reaction in equation 4.....	82
Table XVII: Nanodrop results and DNA yields	82
Table XVIII: Domain distribution by sequence count.....	82
Table XIX: Archaeal classes and phyla sequence counts.....	83
Table XX: Bacterial phyla sequence counts.	84
Table XXI: Eukaryotic phyla and domain sequence counts.....	84

List of Figures

Figure 1: Mineralization zones in Butte, MT (from Gammons <i>et al.</i> , 2009).....	3
Figure 2: Butte, MT relevant sites and groundwater flow.	4
Figure 3: Cell count and culture isolates adapted from Metesh and Duaiame, 2002.	9
Figure 4: Total organic carbon in mines adapted from Metesh and Duaiame, 2002.....	9
Figure 5: Water bath setup for Sterivex DNA extraction.	18
Figure 6: DNA extract and chloroform/isoamyl alcohol layer.	18
Figure 7: Sterivex filters after DNA extraction.	25
Figure 8: Conductivity and pH trends in Silver Bow and Blacktail Creeks and mines.....	27
Figure 9: Conductivity and temperature trends in Silver Bow and Blacktail Creeks and mines.	28
Figure 10: δD and $\delta^{18}O$	29
Figure 11: $\delta^{13}C_{DIC}$ and $\delta^{13}C_{DOC}$	31
Figure 12: DIC and temperature trends.	32
Figure 13: Total concentration and major cation relative abundances.	34
Figure 14: Total concentration and major anion relative abundances.	35
Figure 15: Total concentration and trace element relative abundances.	36
Figure 16: Carbonic acid speciation.	38
Figure 17: C-O-H Eh-pH diagram.	38
Figure 18: Sulfate and sulfide pH trends.	39
Figure 19: S-O-H Eh-pH diagram.....	40
Figure 20: Total concentrations of elements vs. pH.	41
Figure 21: Total concentrations of elements vs. pH.	42

Figure 22: Fe-O-H Eh-pH diagram.....	43
Figure 23: Domain sequence counts and relative abundance.....	45
Figure 24: Relative abundance of archaeal phyla.....	46
Figure 25: Relative abundance of Euryarchaeota classes.....	47
Figure 26: Relative abundance of bacterial phyla.....	48
Figure 27: Sulfate reducing and sulfur oxidizing bacterial sequence counts.....	49
Figure 28: Iron reducing and oxidizing bacterial sequence counts.....	50
Figure 29: Eukaryotic domains and phyla.....	51
Figure 30: Gel electrophoresis of mine samples (set 1).....	85
Figure 31: Gel electrophoresis of mine samples (set 2).....	86
Figure 32: East Camp trace element concentrations.....	87
Figure 33: West Camp trace element concentrations.....	88
Figure 34: Outer Camp trace element concentrations.....	89

List of Equations

Equation 1: Carbon dioxide to carbonic acid.....	37
Equation 2: Carbonic acid to bicarbonate.....	37
Equation 3: Bicarbonate to carbonate.....	37
Equation 4: Equilibrium calculation for carbon speciation.....	37
Equation 5: Pyrite oxidation with oxygen.....	58
Equation 6: Pyrite oxidation with ferric iron.....	58
Equation 7: Calcite dissolution in acidic water.....	58
Equation 8: Carbonic acid to carbon dioxide.....	59
Equation 9: Sulfate reducing bacteria metabolic reaction.....	60

Glossary of Abbreviations

Abbreviation	Definition
BC	Blacktail Creek
DEB	DNA extraction buffer
DIC	Dissolved inorganic carbon
DOC	Dissolved organic carbon
DNA	Deoxyribonucleic acid
GWIC	Ground Water Information Center
ICP-MS	Inductively coupled plasma mass spectrometry
ICP-OES	Inductively coupled plasma optical emission spectrometry
LEGEND	Laboratory Exploring Geobiochemical Engineering and Natural Dynamics
Ma	Mega-annum (million years)
MBMG	Montana Bureau of Mines and Geology
MR DNA	Molecular Research DNA, Limited Partnership
MT	Montana
OTU	Operational taxonomic unit
PCR	Polymerase chain reaction
RNA	Ribonucleic acid
rRNA	Ribosomal ribonucleic acid
SBC	Silver Bow Creek
SEWS	Salt water ethanol solution
TOC	Total organic carbon
VPDB	Vienna Pee Dee Belemnite
VSMOW	Vienna Standard Mean Ocean Water
WCEW	West Camp Extraction Well

1. Introduction

1.1. Statement of Purpose

This thesis project aims to ascertain the microbial diversity present in flooded underground mineshafts. This project is the first culture independent study of planktonic biomass in the flooded underground mines of Butte, Montana. The goals of this thesis are to:

1. Define the habitat based on chemical potential.
2. Discover what microbes exist in these habitats.
3. Inquire into the relationships between microbial communities and their geochemical habitats.
4. Establish a foundation for future microbiological work involving metabolic potential (metagenomics) and microbial activity (proteomics) in Butte's flooded underground mines.

1.2. History

Mining in Butte, Montana began in the early 1860s, and mineral extraction continues today with only brief interruptions over the past 150 years. By the 1890s, Butte had become a leading producer in copper, mining up to 1.13×10^8 kg per year (Jenkins and Lorengo, 2002). Mineshafts reached a depth of 1600 m below the surface, which challenged the mining techniques of the day. Prior to open pit mining in 1955, the mine workings made up a total of 10,000 km of adits and 67 km of vertical shafts (Duaine *et al.*, 2004). Butte ore had exceptionally high concentrations of copper, with a grade of 0.99% copper in the Kelley mine. In 1955, mining moved to the surface using the open pit technique. The Berkeley pit produced up to 1.24×10^8 kg of copper annually, but excavation stopped in 1982 due to a fall in copper prices. The Anaconda Company shut off the dewatering pumps located 1160 m below the surface of the

Kelley and water from the aquifer immediately started to flood the underground mines (Pitwatch, 2013). The mines' water quality is of environmental concern due to high dissolved metal concentrations and acidic pH ranges. The Montana Bureau of Mines and Geology (MBMG) began monitoring the flooded mine system and Berkeley Pit water immediately after the closure. The MBMG annually reports chemical and water level changes of the flooded mine system and provides these data to the public through the Ground Water Information Center (GWIC) (MBMG, 2016).

1.3. Site Description

1.3.1. Geology

Enriched ore deposits in the Butte area occurred from multiple porphyry mineralization events. Butte granite, the predominant host rock, predated the mineralization events at 76 Ma. The host rock primarily consisted of plagioclase, quartz, and K-feldspar with 15-20% composition biotite/hornblende and trace minerals such as apatite, magnetite, titanite, and ilmenite (Gammons *et al.*, 2009). At 66 Ma, the pre-Main Stage mineralization event deposited a low-grade porphyry copper-molybdenum system. This deposition altered the granite by converting hornblende to biotite and plagioclase to K-feldspar. The second hydrothermal event, known as the Main Stage, occurred at 62 Ma and formed veins up to 10 m thick, 3 km long, and 1 km deep (Gammons *et al.*, 2009). The Main Stage mineralization event created zones, typical of a porphyry deposit (Figure 1).

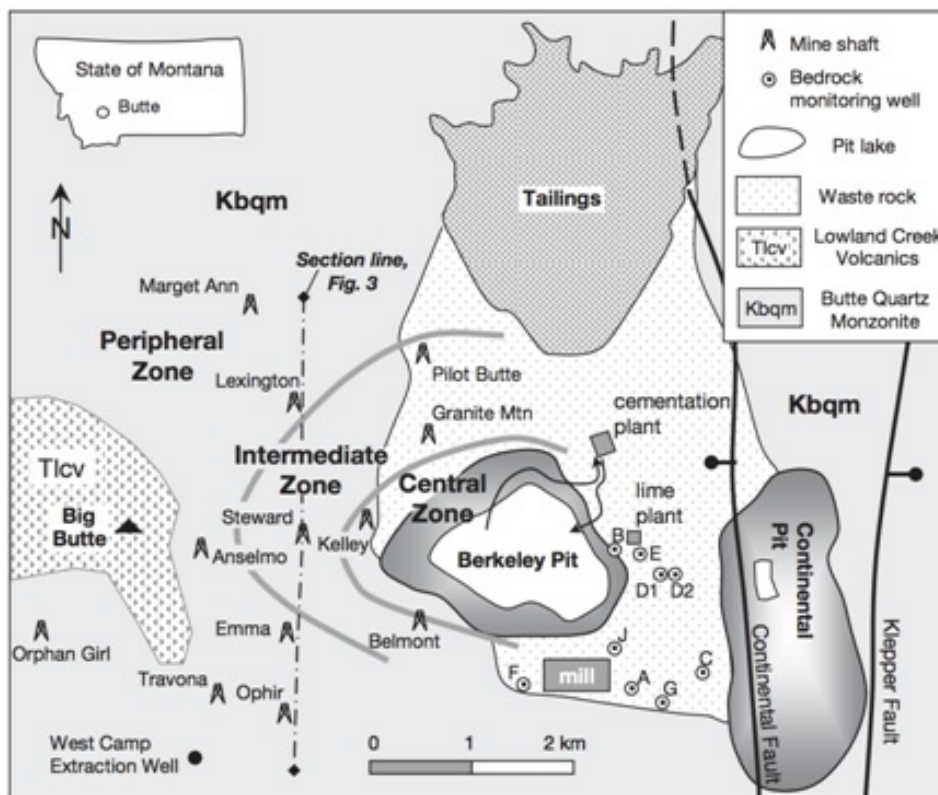


Figure 1: Mineralization zones in Butte, MT (from Gammons *et al.*, 2009).

The Butte porphyry deposit exhibits a gradation of copper concentrations and mineral alteration, with the central zone containing the highest abundance of copper-bearing sulfides (Meyer *et al.*, 1968). Copper grades remain high into the intermediate zone, where zinc was also mined. The ore in the peripheral zone includes higher concentrations of zinc, lead, silver, and manganese but very little copper. In the intermediate and peripheral zones, rhodochrosite provided the main source of manganese. This carbonate mineral also contributes to the buffering capacity of the flooded waters. Therefore, these flooded mines have neutral to alkaline pH (Gammons *et al.*, 2009).

1.3.2. Geochemistry and Groundwater Divides

Like the geology, zonation also occurs in the geochemistry of the flooded mine water (Gammons *et al.*, 2009) (Figure 2). Waters in the central and intermediate geologic zones contain the East Camp mines (Anselmo, Kelley, Pilot Butte, and Steward). These sites have elevated

concentrations of dissolved metals, especially iron, and are acidic. The waters in the Kelley mine are elevated in temperature. The warmer temperature in this mine may be due to the exothermic nature of pyrite oxidation from ferric iron rather than hydrothermal heating (Pellicori *et al.*, 2005). Waters in both the West Camp (Emma, Travona, and Ophir) and Outer Camp (Orphan Boy and Orphan Girl) are lower in metal concentrations with nearly neutral pH values. The geochemistry of the Outer Camp mines is distinct from the East Camp as they have a higher buffering capacity due to the increased alkalinity concentrations from carbonate minerals (calcite and rhodochrosite) and have notable hydrogen sulfide concentrations attributed to sulfate reducing bacteria (Roesler *et al.*, 2007; Gammons *et al.*, 2009).

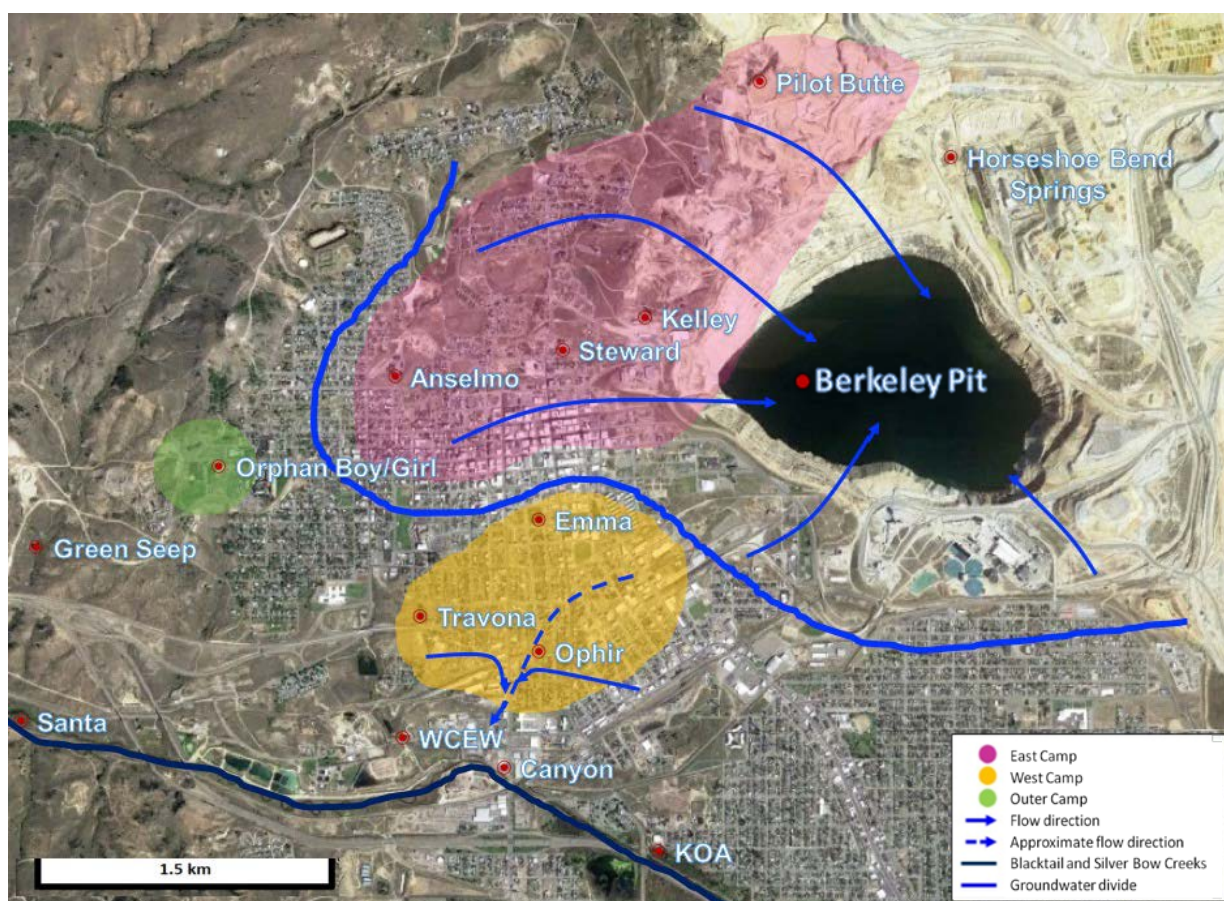


Figure 2: Butte, MT relevant sites and groundwater flow.
(flow lines adapted from Gammons *et al.*, 2009, map from Google Maps).

Groundwater divides separate the East, West, and Outer Camps. The East Camp mine waters are part of one interconnected mine pool (Snyder, 2012). When mining began in the Berkeley Pit, concrete bulkheads isolated active from inactive portions of the underground mines. Bulkhead placements reduced the volume of mine openings requiring ventilation and groundwater pumping. The bulkheads also isolated the West Camp (Travona, Emma, and Ophir) as water from these mines began flooding nearby basements. This water is redirected to the West Camp Extraction Well (WCEW), mixed with alluvial groundwater, and treated with lime before discharging into Silver Bow Creek (Gammons *et al.*, 2009).

Mine water from Orphan Boy and Orphan Girl, known as the Outer Camp, have reached the pre-mining water table elevation (Gammons *et al.*, 2009). The water from these mines flows out as a spring known as Green Seep, which the MBMG monitors annually for water quality. A groundwater divide separates the East Camp from the West Camp. Mine waters located in the East Camp flow into the Berkeley Pit. The West Camp mines flow in the opposite direction. The dashed groundwater flow arrow in the West Camp area is a general direction of groundwater flow (Figure 2).

Surficial water surrounding the underground mining area includes the Berkeley Pit, Horseshoe Bend springs, and Silver Bow Creek. The Berkeley Pit has the lowest pH values in the area and highest metal concentrations. Early reports from the MBMG show that the water in the pit was at a pH of 2.64 and has increased to a pH of 3.41 (MBMG, 1987; MBMG, 2016). The water is currently at a level of 1626 m above sea level and lime treatment will begin when the water reaches a level of 1649 m (Pitwatch.org, 2016). Located northeast of the Berkeley Pit is Horseshoe Bend, which is a natural spring affected by mining operations with a pH of 3.04 and elevated metal concentrations in arsenic, aluminum, cadmium, copper, iron, strontium, and zinc

(MBMG, 2016). The spring is rerouted to the Horseshoe Bend wastewater plant which treats 3.4 million gallons of water per day (Pitwatch.org, 2016). Sludge produced from the treatment is discarded into the pit. Silver Bow Creek, the headwaters of the Clark Fork River, is located south of uptown Butte and flows east to west. The water level in the Berkeley Pit must remain lower than the elevation of Silver Bow Creek to prevent mine water seepage into the creek.

1.4. Microbiology

Microbiota exist in all locations of the mining environment. Niches include bed sediments, ore and host rock, and water. Microorganisms are found both microscopically or macroscopically as snottite, streamers, and mats (Bond *et al.*, 2000). In surficial waters, dissolved oxygen (DO) concentrations range from saturated to anoxic depending on the location of the microbial niche, whereas underground mine water is anoxic. Previous studies have found that factors such as pH, conductivity, temperature, and metal concentration locally affect the taxonomic diversity, but DO and electron potential are the factors that primarily determine the overall type of existing community within each niche, especially in macroscopic growth (Ziegler *et al.*, 2013; Mendez-Garcia *et al.*, 2014).

Microbial communities are well explored and understood in acid mine drainage (AMD) systems (Zettler *et al.*, 2003; Baker and Banfield, 2003; Bruneel *et al.*, 2006). AMD typically contains pH values less than three and temperature ranges between 10-60°C. AMD sites where microbial habitats and communities have been extensively studied include, but are not limited to, the Rio Tinto in Spain, Richmond mine in California, and Carnoulès mine in France. At each of these sites, the predominant organisms belonged to the Bacteria and Archaea, although Eukarya existed in lower amounts (Zettler *et al.*, 2003; Baker and Banfield, 2003; Bruneel *et al.*, 2006). In AMD systems, the predominant bacterial phyla are Proteobacteria,

Nitrospirae, Actinobacteria, Firmicutes, and Acidobacteria (Mendez-Garcia *et al.*, 2015). The predominant archaeal order in AMD is typically from the Thermoplasmata class (Mendez-Garcia *et al.*, 2015). These organisms are both acidophiles and thermophiles that thrive in pyrite rich, high conductivity waters and contribute to AMD by oxidizing iron (Edwards *et al.*, 2000).

Studying the microbial communities in underground mines is an important part of understanding element cycling and has relevant applications to the mining industry. Element cycling occurs from chemical, geological, and biological factors. Microbes can increase chemical reaction rates and water-rock interactions by metabolizing both organic and inorganic components in a system. In effect, these interactions affect the speciation of elements in an environment, which can lead to either an increase or reduction of dissolved metals in water. In mine waters, microbes can act as catalysts in redox reactions, alter mineral compositions, sequester or release toxic metals, and change net pH as a product of their metabolism. Redox reactions induced by microbial activity are essential under controlled conditions in the mining industry as microbes can enhance the yields of minerals extracted from ore through bioleaching or remediate water by precipitating dissolved metals (Hamidian *et al.*, 2000).

1.5. Previous Work

The geochemistry of flooded underground mines in Butte, MT is well studied (Metesh, 1990; Duaiame *et al.*, 1998; Pellicori *et al.*, 2005; Gammons *et al.*, 2006; Roesler *et al.*, 2007; Gammons *et al.*, 2009; Snyder, 2012; Duaiame, 2015) The Montana Bureau of Mines and Geology has collected water quality data and has produced monitoring reports since the Berkeley Pit ceased operations in 1982 (earliest publication is Duaiame *et al.*, 1998, latest publication is Duaiame, 2015). All raw water quality data are published and available to the public through the

Ground Water Information Center (GWIC). Previous studies have determined the chemistry, local meteoric water line and stable isotope composition of Butte water, groundwater flow, and changes with vertical depth in the shafts (Metesh, 1990; Pellicori *et al.*, 2005; Gammons *et al.*, 2006; Roesler *et al.*, 2007; Gammons *et al.*, 2009; Snyder, 2012). These works provide a detailed view of the chemical and geological interactions that affect composition.

Little information on microbial diversity exists for these waters. Roesler *et al.*, 2007 and Gammons *et al.*, 2009 examined $\delta^{34}\text{S}$ in sulfide and sulfate isotopes in the West Camp mines and Orphan Boy. These authors suggested that sulfate reducing activity was prominent in these mines based on the depleted sulfur isotope signature of dissolved sulfide compared to sulfate. In 2002, water from several underground mines was aerobically cultured using agar (Metesh and Duaine, 2002). In this experiment, phylogenetic consistencies were found in the mines among the culture isolates (Figure 3). Samples cultured from various depths yielded similar microbes. Total organic carbon concentrations (TOC) also did not show a change in depth except for the Steward (Figure 4).

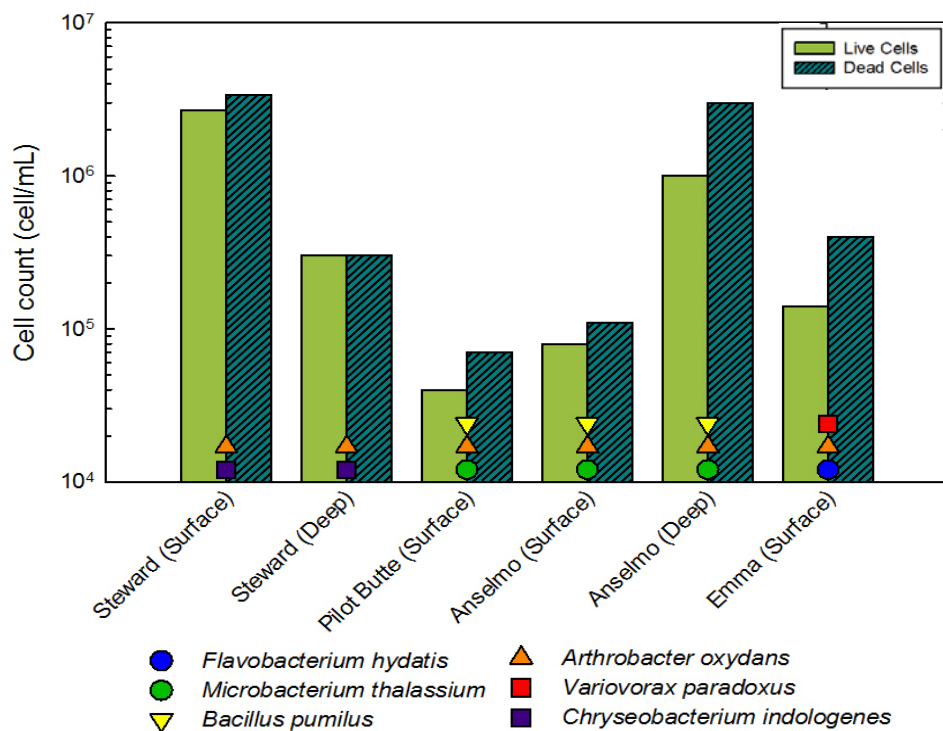


Figure 3: Cell count and culture isolates adapted from Metesh and Duaine, 2002.
Cell counts reported in logarithmic values.

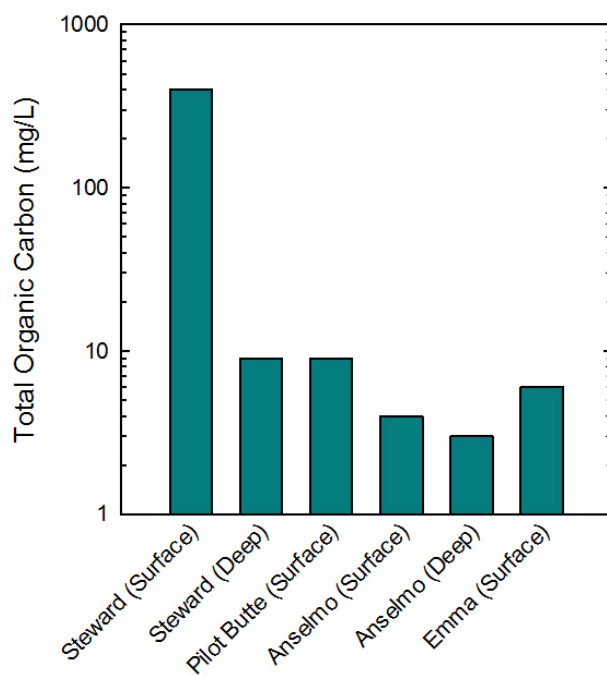


Figure 4: Total organic carbon in mines adapted from Metesh and Duaine, 2002.
Concentrations reported in logarithmic values.

This thesis expands upon Metesh and Duaine regarding microorganisms in the Butte mines by comparing 16S and 18S rRNA gene diversity to the concurrent geochemical habitat. Aerobic culturing and isolation provides a bias towards aerobic microbes whereas most organisms in the mines would be anaerobic due to the low dissolved oxygen concentration. Culture independent techniques using 16S and 18S rRNA gene primers in polymerase chain reactions (PCR) are selective to a larger range of species with less bias than culturing. This technique provides a more complete view of the entire microbial community at each sample location.

1.6. Thesis Objectives

Diversity studies combined with geochemical analysis provide a foundation for testing and understanding the physical, chemical, and ecological mechanisms in a system. A microbial diversity analysis of using 16S and 18S rRNA genes determined what members of the community existed in a particular environment. Water quality data were collected to define the microbial habitat of each mine and to establish a comparative context for taxonomic compositions. Geochemical measurements from Silver Bow and Blacktail Creeks were used as a control or comparison between surficial water and anoxic, underground mine water. In this study, microbial community compositions in diverse, aqueous habitats were determined and provided insights into the interconnected roles and patterns between microbes and water-rock interactions.

2. Methods

2.1. Field Methods

2.1.1. Sample Collection

Samples were collected in the field for both chemical composition and microbial identification (DNA extraction). Water was collected by stainless-steel, ball-check valve bailer (3" x 36", 4 L capacity) polyethylene, ball-check valve bailer (1.5" x 36", 1.5 L capacity), VWR[®] Variable Flow peristaltic pump, or purged tap depending on location. The bailers and peristaltic tubing were sterilized and trace-metal cleaned prior to sample collection with 1.2 M hydrochloric acid (HCl) (TraceMetal Grade, J.T. Baker), followed by 70% ethanol or 3% hydrogen peroxide (H₂O₂), and sterile pH 2 HCl. Following each step was a thorough rinse with sterile deionized or Q-water. HCl and water were sterilized by boiling in a microwave for 5-8 five-minute sessions for a total of 25 to 40 minutes. The stainless-steel bailer was stored in a sterile polyvinylchloride (PVC) container during transport and fitted with a trace-metal cleaned plastic cap prior to lowering into the shaft to prevent debris and water runoff from entering the sample. Sites with deep shafts required a truck-mounted winch provided and operated by the MBMG. Samples retrieved from Anselmo, Kelley, Steward, and Pilot Butte shafts were collected at a depth of 100 ft below static water level to maintain consistency with MBMG methods. Emma and Ophir wells were purged until field parameters on the DS5 Hydrolab stabilized (15-20 minutes), and water was bailed by hand using the stainless steel or polyethylene bailer. Orphan Boy and Orphan Girl samples were collected with the peristaltic pump at a depth of 20 ft below static water level. The Travona was purged for 30 minutes and collected through a faucet.

2.1.2. Water Filtration and Preservation

Water was filtered through a set of 1.2 μm and 0.8/0.2 μm PALL[®] Acrodisc[®] Supor[®] membrane (hydrophilic polyethersulfone) sterile filters to remove particulates and most microorganisms. Filtered water was collected in bottles prepped for the appropriate analysis procedure and preserved. Acrodisc[®] filters used for water filtration were frozen on dry ice in the field and stored in -80 °C for future DNA extraction. Table I provides specific cleaning and storage procedures for each sample type:

Table I: Preservation and storage specifications for chemical composition

Sample Type	Bottle Type	Cleaning	Preservation and Storage
$\delta D/\delta^{18}O$ Isotopes	Clear borosilicate glass, 8 mL, screw top vial with polyethylene cone lined caps	Rinsed with Q-water and dried at 160°C	No preservation added prior to storage. Stored at room temperature.
Cation/Anion	HDPE Nalgene™, narrow mouth, 30 mL	Filled with 1% Citranox® (v/v%) and soaked overnight. Rotated and soaked another night. Soaked in 1.2 M (10%) TraceMetal Grade HCl (J.T. Baker) (v/v%) for 3 days. Rotated and soaked another 3 days. Soaked in pH 2 HCl for 3 days. Rotated and soaked another 3 days. Each step was followed by a 7x rinse of Q-water.	2% (v/v%) HCl added prior to sample analyses if necessary. Stored with Q-water prior to collecting sample. Stored in -20°C freezer after collection.
Trace Elements	HDPE Nalgene™, narrow mouth, 30 mL	Same procedure as cation/anion.	Added 1% by volume concentrated TraceMetal Grade nitric acid (HNO ₃) (Fischer) (v/v%) prior to sample collection or immediately after collection for preservation. Stored at room temperature.
Dissolved Inorganic Carbon (DIC)	Amber VOA glass vial, 40 mL, with septa cap	Soaked in 1.2 M HCl bath for 3 days. Vials were rinsed 7x with Q-water before and after HCl bath. Muffled in tin foil at 450 °C for 4 hours. Lids were soaked in pH 2 HCl, rinsed 7x and dried in a positive pressure hood.	No preservation required. Stored at 4°C.
Dissolved Organic Carbon (DOC)	Amber VOA glass vial, 40 mL, with septa cap	Same procedure as DIC.	100 µL of 85% (v/v%) phosphoric acid (H ₃ PO ₄) (Baker) added prior to sample collection. Stored at 4°C.

2.1.3. Planktonic Biomass Collection

An aliquot of water from the bailer was transferred to a sterile, five-gallon bucket for biomass collection. Biomass was collected onto a 0.2 µm Millipore® Sterivex™ filter by pumping water through tubing using a peristaltic pump (VWR® pump, variable flow). The tubing for the peristaltic pump was trace-metal cleaned and sterilized with 70% ethanol before use. Water was filtered until the Sterivex™ was saturated with particulate or no sample remained (about 1.5-5 L). Sterivex™ filters were wrapped in aluminum foil, frozen on dry ice in the field, and transferred to a -80°C freezer.

2.1.4. Geochemical Parameters

Geochemical parameters were obtained using a DS5 Hydrolab. Measurements included pH, temperature ($^{\circ}\text{C}$), dissolved oxygen (mg/L), and conductivity ($\mu\text{S}/\text{cm}$). Dissolved oxygen and conductivity calibrations were completed the week before sampling. Each sample day, pH was calibrated using pH 4, 7, and 10 buffers. Measurements were recorded immediately after the sample reached the surface for the Anselmo, Kelley, Steward, and Pilot Butte. The Hydrolab was directly attached to the pump attached to the truck for the Emma and Ophir. Measurements from a tap were taken after 30 minutes of purging from the Travona mine. In the Orphan Boy and Girl shafts, the Hydrolab was lowered to a depth of 6.1 m and recorded directly from the shaft. For shafts that required the bailer method, the time required to bring the sample to the surface limited the accuracy of the parameter measurements. The time difference was enough to increase oxygen concentration in the water and lower temperature, which therefore altered the pH. Additionally, as the sample was brought to the surface, the water depressurized and released dissolved carbon dioxide. The loss of carbon dioxide would increase the pH. All data, except for those collected directly from the shaft should be considered estimations of the actual parameters.

2.1.5. Field Spectrophotometry

Field spectrophotometry using wet chemical tests and the HACH DR/2010 was performed for dissolved silica (SiO_2), ferrous iron (Fe^{2+}), and sulfide (H_2S , HS^-).

2.1.5.1. Silica (SiO_2)

Dissolved silica was analyzed using the Silicomolybdate EPA Method 8185 with testing limits between 17 - 1600 $\mu\text{mol}/\text{L}$ and a detection limit of $16.6 \times 10^1 \mu\text{mol}/\text{L}$. Water was filtered to 0.2 μm for both the blank and sample. Limitations to this test included interferences from high concentrations of iron and sulfide. Table II provides the reagents and methods used:

Table II: Methods and reagents for dissolved silica

Sample	Matrix	Reagents	Method
Blank	0.2 µm filtered sample water	None	Added 10 mL filtered sample water to cuvette and zeroed instrument prior to reading sample.
Sample	0.2 µm filtered sample water	HACH Molybdate Reagent Powder Pillows for HR Silica, 10 mL (sodium molybdate) HACH Acid Reagent Powder Pillows for HR Silica, 10 mL (sulfamic acid, sodium chloride) HACH Citric Acid Reagent Powder Pillows for Silica, 10 mL (citric acid)	Added molybdate reagent to 10 mL cuvette. Immediately added acid reagent. Developed reagents for 10 min. Added citric acid reagent and developed for 2 min.

2.1.5.2. Ferrous Iron (Fe²⁺)

Ferrous iron was analyzed using the FerroZine method adapted from To *et al.*, 1999.

Samples were read by absorbance at 562 nm and converted to concentration. Testing limits were between 0.05-18 µmol/L with a detection limit of 0.04 µmol/L. Collected water was filtered to 0.2 µm for the sample. Some samples required dilution prior to analysis. For the Kelley sample, a 1000x dilution was required. The dilution was made with pH 2 HCl in a 1000 mL volumetric flask. The Anselmo, Steward, and Pilot Butte samples required a 25x dilution with pH 2 HCl. The dilution was transferred to the cuvette and the reagents were added following the instructions in Table III:

Table III: Methods and reagents for FerroZine

Sample type	Matrix	Reagents used	Method
Blank	0.2 µm filtered sample water	None	Added 25 mL filtered sample water to cuvette and zeroed instrument prior to reading sample.
Sample	0.2 µm filtered sample water	4.9 x 10 ⁻³ M FerroZine reagent Ammonium acetate buffer (pH 7-7.5)	Added 20 mL of sample to a 25 mL cuvette. Added 0.5 mL of FerroZine reagent. Added 1.25 mL of buffer solution and brought sample up to 25 mL. Developed 5 min.

2.1.5.3. Total Dissolved Sulfide (H₂S, HS⁻)

Dissolved sulfide was analyzed using the Methylene Blue EPA Method 8131 and after Cline, 1969 with testing limits between 0.15-18µmol/L with a detection limit of

0.15 $\mu\text{mol/L}$. Water was unfiltered to prevent increased volatilization. Limitations to this test include interferences from turbidity, volatilization, and oxidation sensitivity with sulfide species. This sample provided a rough estimate of the dissolved sulfide concentration, as loss of species was inevitable with the bail and pump methods. Table IV includes the reagents and methods used in the sulfide test:

Table IV: Methods and reagents for dissolved sulfide

Sample type	Matrix	Reagents used	Method
Blank	Q-water	HACH Sulfide 1 Reagent (sulfuric acid) HACH Sulfide 2 Reagent (methylene blue)	Added 25 mL Q-water to cuvette. Added 1 mL of sulfide reagent 1. Added 1 mL of sulfide reagent 2. Developed 5 min before zeroing instrument.
Sample	Unfiltered sample water	HACH Sulfide 1 Reagent (sulfuric acid) HACH Sulfide 2 Reagent (methylene blue)	Added 25 mL unfiltered sample water to cuvette. Added 1 mL of sulfide reagent 1. Added 1 mL of sulfide reagent 2. Developed 5 min.

2.2. Analytical Methods

Samples collected for major cations and anions, δD and $\delta^{18}\text{O}$ isotopes, trace elements, dissolved inorganic carbon (DIC), dissolved organic carbon (DOC), and $\delta^{13}\text{C}_{\text{DIC}}$ / $\delta^{13}\text{C}_{\text{DOC}}$ were analyzed by instrumentation at Montana Tech in the MBMG. Cation data were obtained with a Thermo Scientific iCAP 6000 Series inductively coupled plasma emission spectrometer (ICP-OES) using EPA method 200.7. Anion data were obtained from the Metrohm Compact IC Plus using EPA method 300.1. Water isotopes (δD and $\delta^{18}\text{O}$) were measured using the Picarro Isotopic Water Analyzer, L2130-*i*. The isotopic values were reported in the δ notation relative to the Vienna Standard Mean Ocean Water (VSMOW). A suite of trace elements was collected using the Thermo Scientific iCAP Q inductively coupled plasma-mass spectrometer (ICP-MS) using EPA method 200.8. DIC and DOC concentrations and $\delta^{13}\text{C}_{\text{DIC}}$ / $\delta^{13}\text{C}_{\text{DOC}}$ were obtained simultaneously using the Aurora 1030W Total Organic Carbon Analyzer and Picarro G2131-*i*

analyzer using EPA method 415.1. The isotopic values were reported in the δ notation relative to the Vienna Pee Dee Belemnite standard (VPDB).

2.3. Biological Methods

2.3.1. DNA Extraction

The method used for DNA extraction was modified from Brazelton, 2010. DNA extraction buffer (DEB) was prepared prior to extraction with 0.1 M Tris-HCl (pH 8), 0.1 M sodium ethylenediaminetetraacetic acid (Na-EDTA) (pH 8), 0.1 M monosodium phosphate (NaH_2PO_4) (pH 8), 1.5 M sodium chloride (NaCl), and 1% cetrimonium bromide (CTAB). The solution was autoclaved and filter-sterilized. DEB was added directly to the Sterivex housing until the filter was completely immersed. The amount of DEB added to the filter was recorded. The filter was frozen and thawed three times at -80°C for 12 minutes and 65°C for 15 minutes in a hot water bath. For every 1 mL of DEB, 13 μL of lysozyme was added to each Sterivex and samples were incubated in a hot water bath at 37°C for 30 minutes (Figure 5). The filters were inverted every 10 minutes during incubation. Twenty-two and a half microliters of Proteinase-K and 90 μL of 20% sodium dodecyl sulfate (SDS) for every 1 mL of DEB were added to the Sterivex and incubated in a hot water for 1 hour. The filters were inverted every 10 minutes.

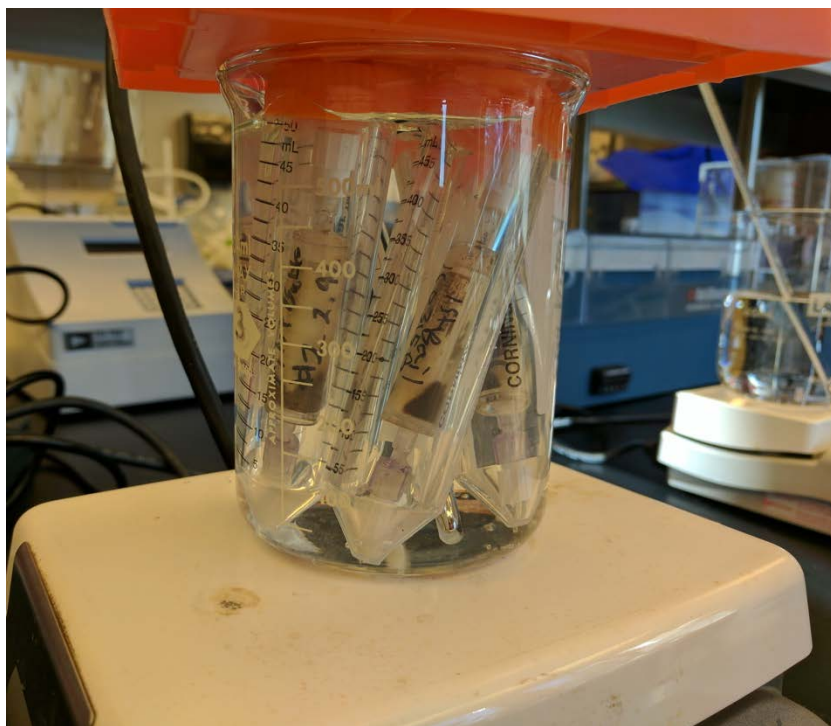


Figure 5: Water bath setup for Sterivex DNA extraction.

After lysis and incubation, the reagent was removed from the filter and added to sterile centrifuge tubes. The samples were centrifuged at 5,000 g to remove and transferred to a clean tube. Each sample was divided into 900 μL aliquots and an equal volume of cold phenol/chloroform/isoamyl alcohol (25:24:1) with alkaline buffer was added. Samples would change from clear to pink or violet with the addition of the organic reagent (Figure 6).

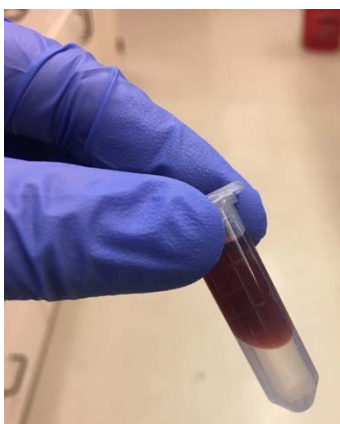


Figure 6: DNA extract and chloroform/isoamyl alcohol layer.

The sample was inverted and centrifuged at 14,000 g for 5 minutes. The supernatant was transferred to a new tube, and an equal volume of cold chloroform/isoamyl alcohol (24:1) was added. The sample was centrifuged and the supernatant was transferred in 550 μ L aliquots to new tube. One molar sodium acetate was added at 0.1 volume to each tube. Two volumes of cold isopropanol were added to the tube and inverted. The sample was placed in a -20 °C freezer for three days to allow sufficient time for precipitation. After precipitation, small crystals had formed in the solution. Each sample aliquot was combined and transferred to a 15 mL sterile, DNA-free Falcon tube. A 1 M concentration of NaCl was added to the solution. The sample was inverted and 1 mL of FastDNA[®] SPIN Kit binding matrix was added. The sample was centrifuged at 5,000 g for 1 minute. The binding matrix was suspended in the supernatant and centrifuged in a spin column. The sample was centrifuged for 1 min at 14,000 g. The binding matrix was washed with 500 μ L of FastDNA[®] SPIN Kit salt ethanol wash solution (SEWS) which is a mixture of sodium chloride and ethanol. The sample was centrifuged and SEWS was discarded. The spin column was air dried under a positive pressure hood for 5 minutes and suspended in 100 μ L of DNA free water. The sample was incubated at 55°C for 5 minutes and centrifuged at 14,000 g for 1 minute to elute the DNA. Once DNA was extracted, samples were tested for quality using the Nanodrop. The Nanodrop was blanked using 1 μ L of DNA/RNA free water and sterilized with ethanol before scanning the sample. One microliter of DNA was added to the Nanodrop and scanned for 260/280 ratios and yields (Table XVII). The DNA was stored at 4°C for up to three months until sequenced.

The Orphan Boy wood was collected at the same time as the Orphan Boy Sterivex, but processed differently. Floating pieces of wood were scooped with a net from the surface of the water. The wood was then immediately stored in a Whirl-Pak sample bag and frozen on dry ice.

The sample was stored at -80°C until extracted. For extraction, 500 mg of wood was removed from the main sample. The extraction was completed according to the directions from the FastDNA[®] SPIN Kit for soil components. After DNA extraction, the sample was stored at 4°C until analyzed.

2.3.1.1. PCR and Gel Electrophoresis

To verify the presence of amplifiable DNA, polymerase chain reaction (PCR) was performed using Universal, Bacterial, Archaeal, and Eukaryotic primers that targeted the 16s and 18s rRNA genes. Table V provides primer sequences used (after Boyd *et al.*, 2010). All primers were prepared by Integrated DNA Technologies (IDT):

Table V: Polymerase chain reaction (PCR) primer sequences

Primer	Sequence
Bacteria 1100F	5'-YAA CGA GCG CAA CCC-3'
Bacteria 1492R	5'-GGT TAC CTT GTT ACG ACT T-3'
Archaea 344F	5'-ACG GGG YGC AGC AGG CGC GA-3'
Archaea 915R	5'-GTG CTC CCC CGC CAA TTC CT-3'
Eukarya A7F	5'-AAC CTG GTT GAT CCT GCC AGT-3'
Eukarya 570R	5'-GCT ATT GGA GCT GGA ATT AC-3'
Universal 515F	5'-GTG CCA GCM GCC GCG GTA A-3'
Universal 806R	5'-GGA CTA CHV GGG TWT CTA AT-3'

The symbols in the primer are the nucleotide sequences for the gene of interest. A, T, C, and G are the DNA nucleotide bases adenine, thymine, cytosine, and guanine. The symbols H, M, V, W, and Y are part of the standard nucleotide coding system by IDT (Integrated DNA Technologies, 2011). These symbols represent mixed base pairs which are summarized in Table VI:

Table VI: Nucleotide mixed base pairs

Symbol	Mixed nucleotide
H	A, C, T
M	A, C
V	A, C, G
W	A, T
Y	C, T

For example, the forward bacterial primer contains the “YAA” codon. The codon represents both the nucleotide sequence CAA and TAA. Forward and reverse primers are used to amplify both strands of DNA.

The 16S and 18S ribosomal RNA (rRNA) genes were chosen for amplification as some DNA segments within these genes are conservative in most microorganisms and can therefore be used as a genetic marker (Janda and Abbott, 2007). The function and presence of the 16S and 18S rRNA gene have not changed over time, which suggests that any changes within these gene sequences are from evolution and can provide a measurement of time (Woese and Fox, 1977). The 16S and 18S genes distinguish differences between Prokaryotes (which include Bacteria and Archaea) and Eukaryotes. The 16S and 18S denotes the ribosomal subunit. In Bacteria and Archaea, this is the 16S portion of the 30S subunit whereas in Eukarya this is the 18S section of the 40S subunit.

Extracted DNA was combined with 12.5 μL master mix, 0.4 μL of the appropriate forward and reverse primer (concentration of 25 μM), and filled to a volume of 25 μL with sterilized and filtered Q-water (Boyd *et al.*, 2010). DNA concentrations ranged from 10 – 50 ng/ μL depending on extraction yields (see Appendix A, Table VI for nanodrop yields and 260/280 ratios). The master mix contained 80 μL of 50 mM MgCl_2 , 80 μL of 5000 nM bovine serum albumin (BSA), 400 μL of 10 x PCR buffer, 24 μL of taq polymerase, 4 μL of each dNTP, and 1400 μL of sterile water. PCR denaturation and annealing were set at the following temperatures: denaturing at 94°C for 5 minutes, and annealing at 55°C for 1 minute with a 2°C gradient for each column (Eukarya at 45°C, Universal at 5°C, Bacteria at 55°C, Archaea at 61°C), followed by an extension period of 1 minute and 30 seconds at 72°C. Ramp time between anneal temperatures and extension was 3°C/s. These steps were repeated for 34 cycles followed

by another extension period of 72°C for 20 minutes and held at 4°C until collected. PCR settings were adapted from Boyd *et al.*, 2010.

Gel electrophoresis was used to verify the presence of amplified DNA after PCR. A 1% agarose gel was made by adding 1.20 g agarose to 120 mL of tris (54 g/L)/borate (27.5 g/L)/EDTA (37.2g/L) (TBE) buffer and heated for 3 x for 30 second intervals. One and two tenths microliters of ethidium bromide were added to the solution and poured into a mold. The gel set for 30 minutes and 5 µL of PCR sample mixed with 1 µL of dye was added to the cell. Electrophoresis ran at 100 V for approximately 1 hour and DNA was visualized under ultraviolet light.

2.3.1.2. Sequencing

DNA extracts were sent to Molecular Research LP (MR DNA) in Shallowater, TX, USA for PCR amplification and 16S and 18S rRNA gene sequencing. DNA extracts with 260/280 nanodrop ratios less than 1.8 were further purified by MR DNA using the PowerClean Pro DNA Clean-UP kit. DNA extraction concentrations and 260/280 ratios were quantified using a Qubit™ before PCR amplification and sequencing. The 16S and 18S rRNA gene primers from Table V were used in PCR. Reagents used for PCR were from the HotStarTaq Plus Master Mix Kit. PCR cycles were conducted under the following conditions: 94 °C for three minutes, followed by 28 cycles of 94°C for 30 seconds, 53°C for 40 seconds and 72°C for one minute, and an elongation step of 72°C for five minutes. The results of the PCR amplification were checked with a 2% agarose gel. Samples were separated by molecular weight and DNA concentrations and purified using Ampure XP beads. Sequencing was performed on a MiSeq.

The data were processed using MR DNA's analysis pipeline. The pipeline joined overlapping sequences, removed barcodes and sequences <150bp, and deleted ambiguous base calls. The

sequences were denoised; operational taxonomic units (OTUs) were clustered at 3% divergence (97% similarity), and chimeras were removed. OTUs were taxonomically classified using nucleotide Basic Local Alignment Search Tool (BLASTn) against a curated database from the Ribosomal Database Project (RDP-II) and National Center for Biotechnology Information (NCBI) (Dowd, n.d.). Results were provided in the form of relative abundance and sequence counts.

3. Results

3.1. Mine Water Chemistry

Nine mines were sampled for δD and $\delta^{18}O$, major cations and anions, dissolved inorganic carbon (DIC), dissolved organic carbon (DOC), $\delta^{13}C_{DIC}$, $\delta^{13}C_{DOC}$, and trace elements. In the field, measurements for pH, conductivity, redox potential, temperature, and dissolved oxygen were performed *in situ* using a Hydrolab MS5 multiparameter mini sonde (see Appendix A, Table IX for measurements). Temperature and redox sensitive species SiO_2 , H_2S/HS^- , and Fe^{2+} were analyzed in the field using chemical tests and a portable spectrophotometer, and alkalinity values were determined by titration (Appendix A, Tables IX and X). These data provided the background information necessary to characterize the microbial environment. The sites sampled were separated into three geochemical zones, with the East Camp Mines (Kelley, Steward, Anselmo, Pilot Butte) having the lowest pH values (4.65-6.15) and highest dissolved metal concentrations and the West Camp (Emma, Travona, Ophir) and Outer Camp (Orphan Boy, Orphan Girl) having higher pH values (6.65-7.87), lower dissolved metals, and increased concentrations of sulfide (0.13 -0.15 mmol/L). Samples were collected from Silver Bow Creek (SBC) and Blacktail Creek (BC) in the same season as mine sampling. Geochemical data from the Silver Bow and Blacktail Creeks serves as references points for comparison between surficial waters and underground mines.

Differences in the water chemistry of each mine were readily apparent during collection. The waters from the East Camp (Kelley, Steward, Anselmo, and Pilot Butte) were bright orange to red-orange in color. Iron quickly precipitated out of unpreserved samples due to the oxygenation of iron(II) to iron(III). The water from the Kelley and Steward mine had a slight blue tint, which colored the Sterivex filter blue. Once the filter was saturated, the deposited sediment was dark

brown and looked similar in color to the filters from Anselmo and Pilot Butte. Kelley mine water had the highest recorded temperature ($32.3 \pm 0.5^\circ\text{C}$). of mines samples and effervesced during collection, which was not observed in the other mines. The West Camp's Emma, Travona, and Ophir smelled slightly of sulfide. These waters were either colorless or had a light yellow tint, but did not precipitate iron when exposed to air. The Sterivex filter was tan colored after filtering. The Outer Camps Orphan Girl and Orphan Boy were colorless, smelled strongly of sulfide, and were warmer in temperature ($26.4\text{-}26.8 \pm 0.5^\circ\text{C}$). The Sterivex filters from Orphan Girl and Boy were a light tan (Figure 7). Both the Orphan Girl and Boy had small pieces of wood floating in the water from timbers lining the shafts. A thin layer of white film covered the wood.



Figure 7: Sterivex filters after DNA extraction.

From left to right: Blank, Emma, Ophir, Travona, Orphan Boy, Pilot Butte

In situ geochemical parameters (summarized in Appendix A, Table VII) are separated by zone (East, West, and Outer) and are discussed in the order of increasing pH. Three sites from SBC and Blacktail Creek were sampled in February and May of 2016. The results showed

geochemical variability between all sites, especially in conductivity, pH, temperature, iron, and sulfide concentrations. The East Camp mines had the lowest pH range ($4.65-6.15 \pm 0.05$), greatest variation in temperature ($16.8-32.3 \pm 0.5^{\circ}\text{C}$), and highest conductivity ($2135-6634 \pm 1 \mu\text{S/cm}$). The West Camp mines were near neutral in pH ($6.34-6.55$), lower in temperature ($11.5-17.1 \pm 0.5^{\circ}\text{C}$), lowest in conductivity ($511.2-1492 \pm 1 \mu\text{S/cm}$) and smelled of sulfur (with sulfide concentrations of $0.003-0.012 \mu\text{mol/L}$). The Outer Camp mines exhibited the highest pH values ($7.07-7.87 \pm 0.05$), elevated temperatures and sulfide concentrations ($22.4-26.6 \pm 0.5^{\circ}\text{C}$ and $0.13-0.16 \mu\text{mol/L}$ respectively), and conductivity ranges that fell between those found in the East and West Camps ($1987-1990 \pm 1 \mu\text{S/cm}$). In comparison to the mines, SBC and BC had a neutral pH range ($7.33-7.98 \pm 0.05$), the coldest temperatures ($4.5-9.4 \pm 0.5^{\circ}\text{C}$), lowest conductivities ($146.8-556.6 \pm 1 \mu\text{S/cm}$), and concentrations of sulfide near detection limit ($0.14 \mu\text{mol/L}$).

Most mines had a positive oxidation reduction potential (ORP) except for the Orphan Boy and Emma. Though the Hydrolab detected dissolved oxygen concentrations, these results are not representative of mine conditions. Because of the depth of the mine, difficulty of accessing the shaft, distance between the ground level and water surface, the speed of the winch, and obstructions in the mine shaft there was a delay of about 5-20 minutes in analyzing the sample. During which, the sample was agitated between the time the bailer was filled and the sample was tested with the Hydrolab. Thus, the measured dissolved oxygen and ORP values are most likely higher than the value that would be obtained if it were possible to measure these parameters at the point of collection.

Conductivity and pH showed the greatest differences between each camp and Silver Bow and Blacktail Creeks (Figure 8). The flooded mines contained conductivity ranges that are much

higher than the surficial creek water and lower in pH, with the exception of Orphan Boy and Orphan Girl. These two mines had a similar pH to Silver Bow and Blacktail Creeks, but nearly three times greater conductivity. Generally, conductivity and pH are inversely related; however, Orphan Boy, Girl, and Pilot Butte did not follow this trend. Conductivity and temperature were positively correlated; however, Pilot Butte from the East Camp and Orphan Boy and Girl from the Outer Camp did not follow from this trend (Figure 9).

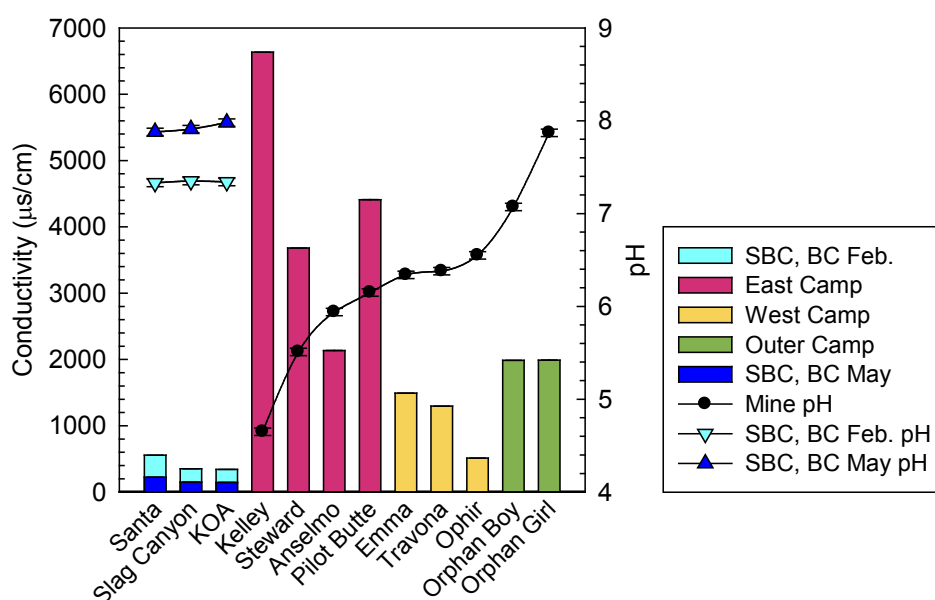


Figure 8: Conductivity and pH trends in Silver Bow and Blacktail Creeks and mines.
 Error bars on pH represents ± 0.05 from flux in meter readings. Conductivity error bars represent ± 1 $\mu\text{s}/\text{cm}$ from maximum flux in meter readings. Conductivity error bars are present but not visible due to scale.

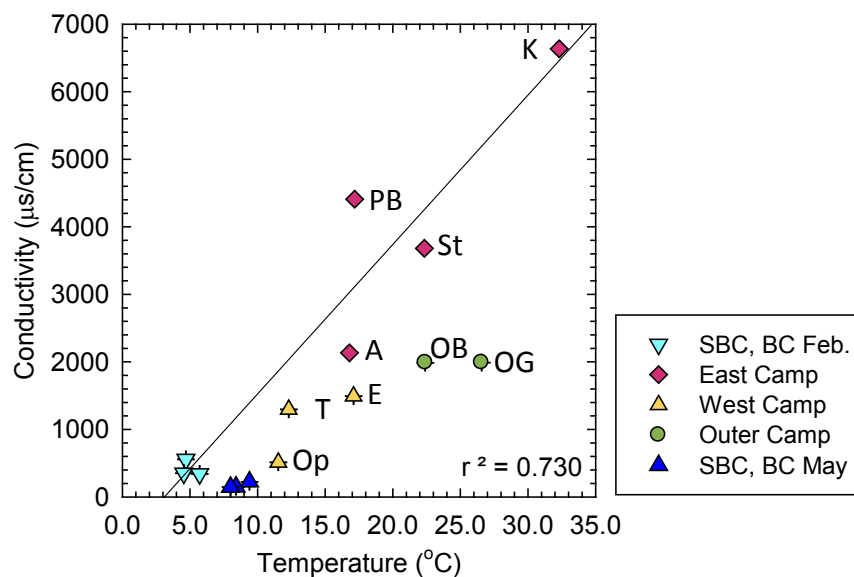


Figure 9: Conductivity and temperature trends in Silver Bow and Blacktail Creeks and mines.
 K: Kelley, PB: Pilot Butte, St: Steward, A: Anselmo, OB: Orphan Boy, OG: Orphan Girl, E: Emma, T: Travona, Op: Ophir. Conductivity error bars represent ± 1 $\mu\text{s}/\text{cm}$ and temperature error bars represent ± 0.1 $^{\circ}\text{C}$. Error bars are present but not visible since smaller than symbol size.

Results of stable isotope analyses indicated origin and source of water and carbon in the system (see Appendix A, Table XI). The Global Meteoric Water Line (GMWL) was taken from Craig, 1961 and the Butte Local Meteoric Water Line (LMWL) and Local Evaporative Line (LEL) were taken from Gammons, 2006 for δD and $\delta^{18}\text{O}$ trends (Figure 10). Silver Bow and Blacktail Creek samples showed seasonal changes in isotopic values. Water collected in May was isotopically heavier than in February.

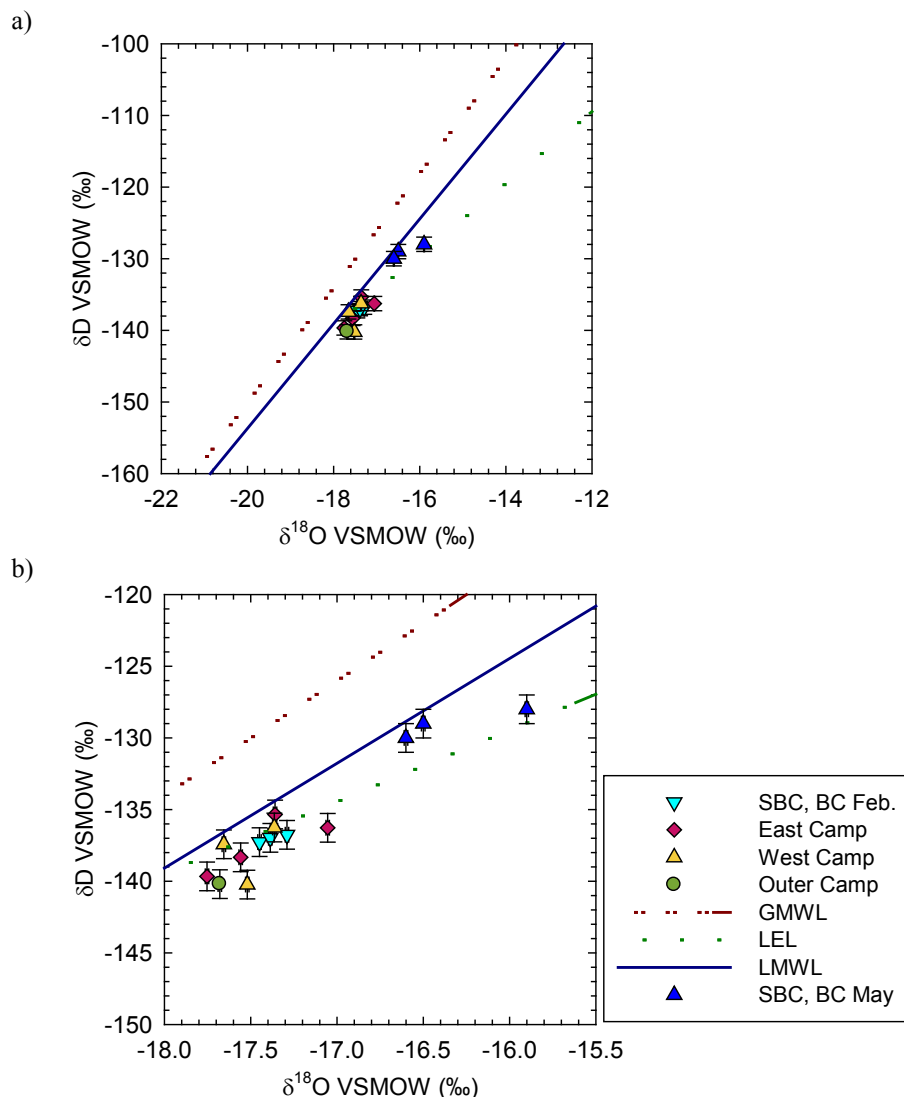


Figure 10: δD and $\delta^{18}O$.

a) Values in relation to the meteoric and evaporative water lines. b) Zoomed in. GMWL: $y = 8 \text{‰}(x) + 10 \text{‰}$; LEL: $y = 5 \text{‰}(x) - 49.5 \text{‰}$; LMWL: $y = 7.31 \text{‰}(x) - 7.5 \text{‰}$. δD and $\delta^{18}O$ relative to Vienna Standard Mean Ocean Water (VSMOW) (Craig, 1961 and Gammons, *et al.*, 2006). Error bars represent $\pm 1 \text{‰}$ for δD and $\pm 0.1 \text{‰}$ for $\delta^{18}O$.

DIC and DOC concentrations and $\delta^{13}C_{DIC}$ and $\delta^{13}C_{DOC}$ determined how distinct the mines were in terms of carbon concentrations and source. DIC values showed an inverse trend between concentration and isotopic values in the mines, but not between seasonal variations in SBC and BC (Figure 11a). DIC became isotopically lighter as the inorganic carbon concentrations increased in the mines. DOC did not show a relationship between isotopic values and

concentration (Figure 11b). The Orphan Boy and Girl mines had the highest concentration of DOC in the mines but did not have the lightest $\delta^{13}\text{C}_{\text{DOC}}$ values.

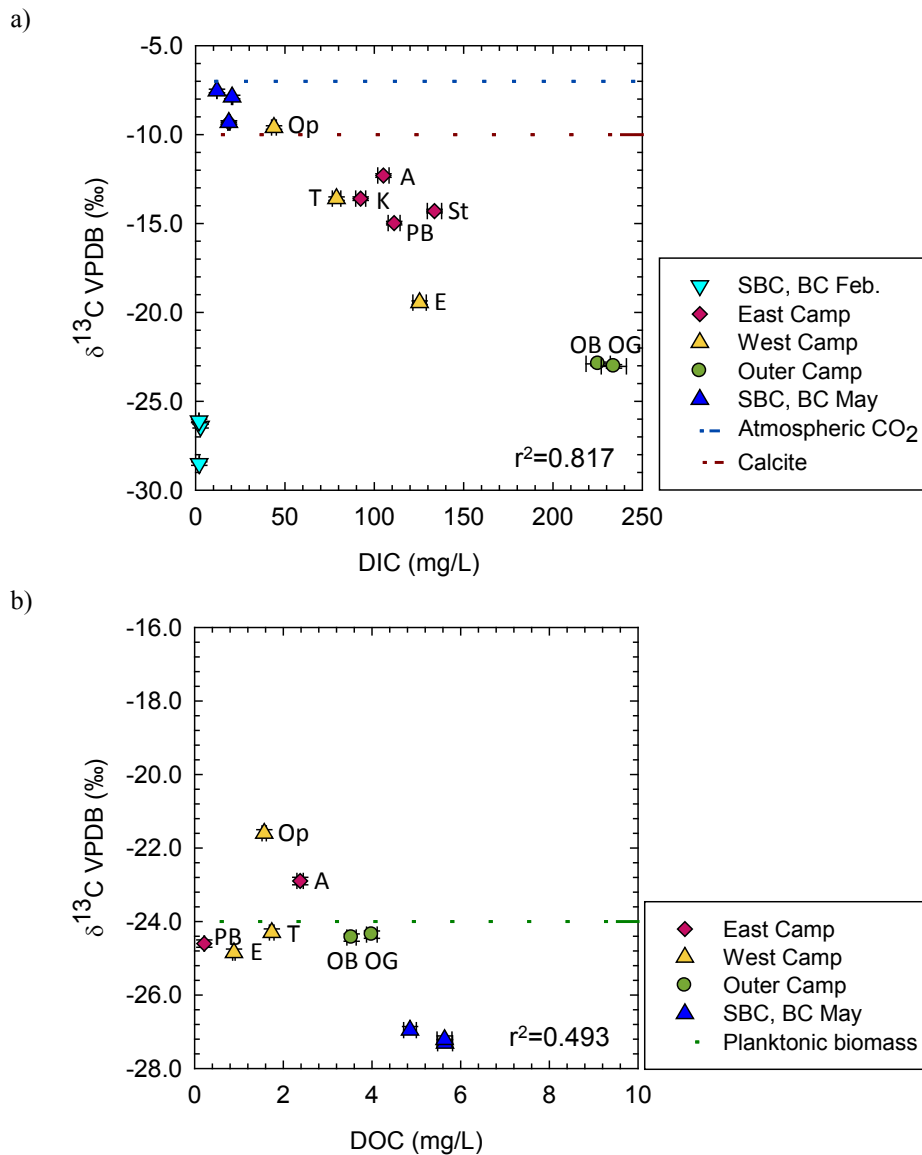


Figure 11: $\delta^{13}\text{C}_{\text{DIC}}$ and $\delta^{13}\text{C}_{\text{DOC}}$.

a) DIC concentrations and $\delta^{13}\text{C}_{\text{DIC}}$ for mines and SBC/BC. b) DOC concentrations and $\delta^{13}\text{C}_{\text{DOC}}$ values. K: Kelley, PB: Pilot Butte, St: Steward, A: Anselmo, OB: Orphan Boy, OG: Orphan Girl, E: Emma, T: Travona, Op: Ophir. $\delta^{13}\text{C}_{\text{DIC}}$ and $\delta^{13}\text{C}_{\text{DOC}}$ values relative to Vienna Pee Dee Belemnite Standard (VPDB). Atmospheric CO_2 , calcite, and planktonic biomass values are from Sacks, 1996. No data were included for SBC/BC February DOC as concentrations were below detection limit. Error bars represent $\pm 0.1\text{‰}$ for $\delta^{13}\text{C}_{\text{DIC}}$ and $\delta^{13}\text{C}_{\text{DOC}}$ and $\pm 3\%$ for DIC and DOC concentrations. Error bars are present but not visible since smaller than symbol size.

Not only did DIC show a relationship between $\delta^{13}\text{C}_{\text{DIC}}$ and concentration, but DIC also showed a trend between temperature and concentration (Figure 12). As temperature increased,

DIC concentrations increased up to 26°C. The warmest point on the graph is the Kelley mine, which showed a drop in inorganic carbon concentration.

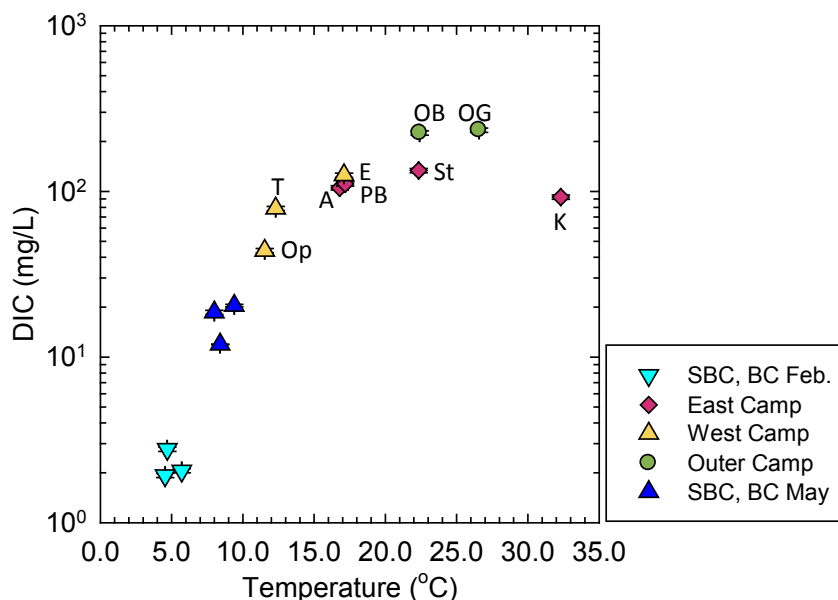


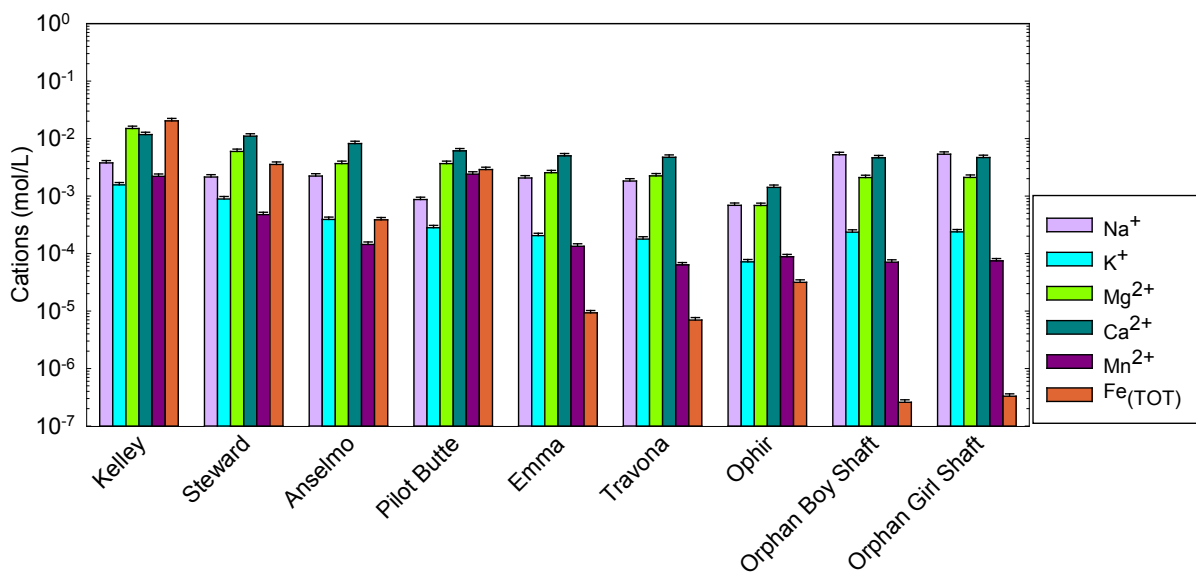
Figure 12: DIC and temperature trends.

Concentration reported in logarithmic scale. K: Kelley, PB: Pilot Butte, St: Steward, A: Anselmo, OB: Orphan Boy, OG: Orphan Girl, E: Emma, T: Travona, Op: Ophir. Error bars represent $\pm 3\%$ for DIC concentration and $\pm 0.1^\circ\text{C}$ for temperature. Error bars are present but not visible since smaller than symbol size.

Results from trace elements and major cations and anions indicate that the highest dissolved metal concentrations were located in the most acidic mines (see Figures 13a, 14a, 15a; also Appendix A, Tables XI, XII, and XIII). Major cations and anions graphs were separated from trace elements graph due to concentration differences used for analysis. Major cations and anions were on the order of one mmol/L to one $\mu\text{mol/L}$. Trace elements were on the order of 0.1 mmol/L to one nmol/L (Figures 14a, 15a, and Appendix B, Figures 32, 33, and 34) and were considered "trace" as these elements were analyzed via ICP-MS. Relative abundances provide a visual profile of the variation of metals and ions found in each mine. Iron and manganese concentrations were analyzed by both ICP-MS and ICP-OES. These two species were included in the cation graph rather than ICP-MS as the concentrations were several orders of magnitude

higher than most metals analyzed by ICP-MS. Iron and manganese cations were more abundant in the East mines than in the West and Outer (Figure 13). Anions in each mine showed the greatest variation in bicarbonate (HCO_3^-) and sulfate (SO_4^{2-}) concentrations (Figure 14). Mines with higher pH values (West and Outer) had higher concentrations of bicarbonate and lower concentrations of sulfate. The predominant trace elements in the East Camp were zinc and titanium with smaller amounts of aluminum, arsenic, and strontium (Figure 15). The West and Outer mines had higher concentrations of titanium, strontium, boron, lithium, and barium (Appendix B, Figures 32, 33, and 34).

a)



b)

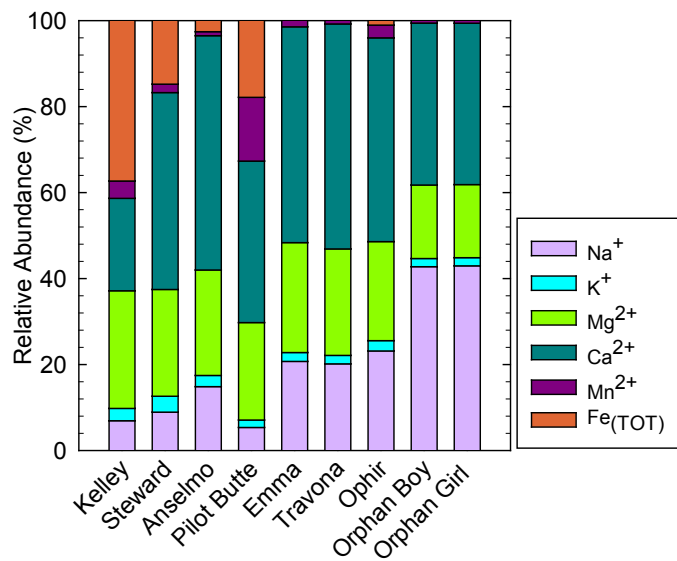
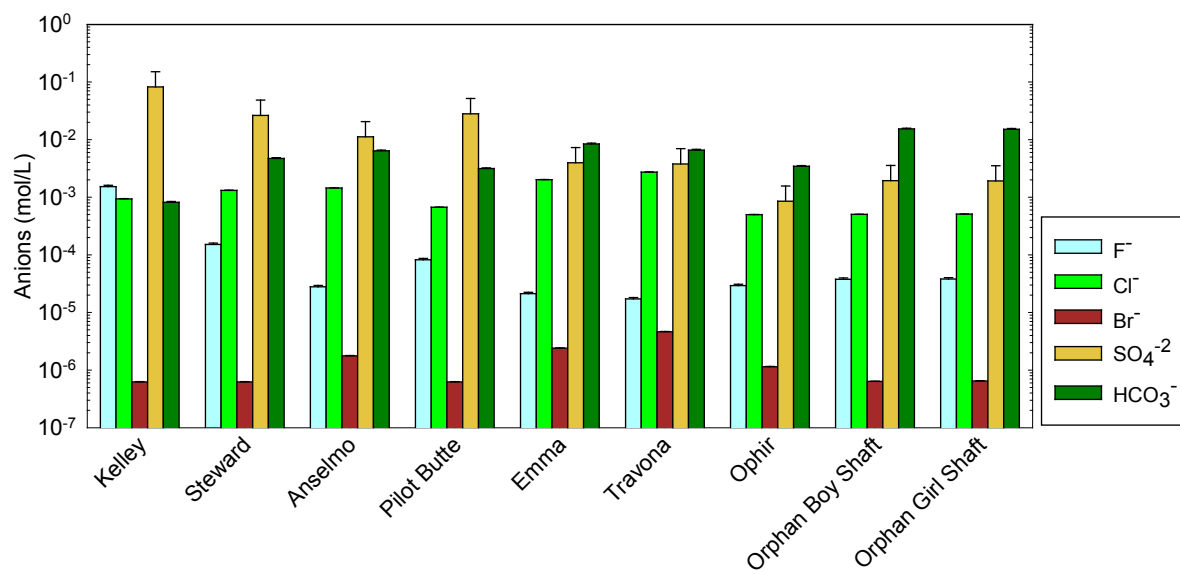


Figure 13: Total concentration and major cation relative abundances.

a) Total concentrations of major cations. Concentrations reported on log scale. See Appendix A, Table XIII for concentrations. Error bars represent $\pm 10\%$ for sodium, potassium, magnesium, calcium; $\pm 5.0\%$ for manganese; $\pm 5.4\%$ for iron. b) Relative abundances of major cations.

a)



b)

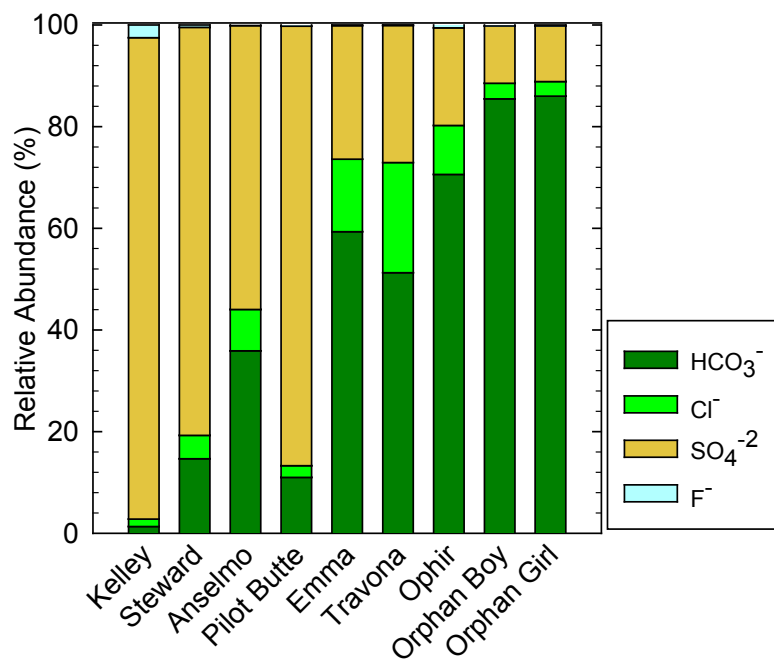


Figure 14: Total concentration and major anion relative abundances.

a) Total concentration of major anions. Concentrations on log scale. Dashed line indicates detection limit. Error bars represent $\pm 5.6\%$ for fluoride, $\pm 0.8\%$ for chloride and sulfate, and $\pm 3.0\%$ for bicarbonate. See Appendix A, Table XIV for concentrations. b) Relative abundances of anions. All anions were included, but only those $>1\%$ are included in the legend.

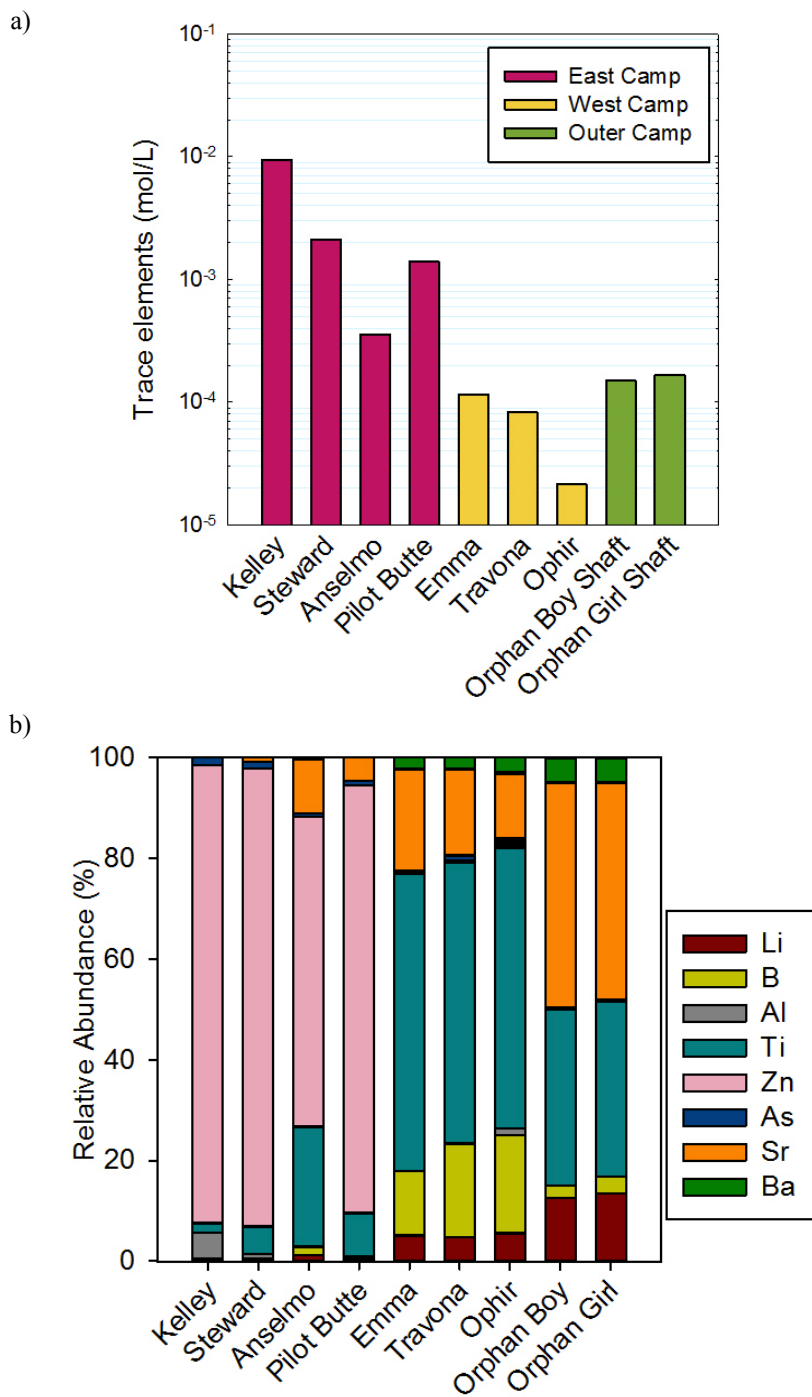


Figure 15: Total concentration and trace element relative abundances.

a) Total concentration of trace metals in mines. Concentrations on log scale. b) Relative abundances of metals in mines. All metals from Table XV were included, but only elements >0.9% were included in the legend. See Appendix B, Figures 32, 33, and 34 for total concentrations of individual metals for each mine.

Total dissolved inorganic carbon concentrations measured in the lab were used to calculate bicarbonate concentrations using the chemical reactions and equations:



$$[\text{HCO}_3^-] = \frac{K_a [\text{H}_2\text{CO}_3]}{\{\text{H}^+\}} \quad (4)$$

where $[\text{HCO}_3^-]$ is the bicarbonate concentration in mol/L, K is the acid dissociation constant of the reaction, $[\text{H}_2\text{CO}_3]$ is the DIC concentration in mol/L, and $\{\text{H}^+\}$ is the activity of the hydronium ion in mol/L obtained from pH. Acid dissociation constants at various temperatures were obtained from the GEOPIG Slop07 database in SUPCRT (Appendix A, XVI).

The dominant carbonic acid species changes from H_2CO_3 in lower pH systems to bicarbonate between 6.3 and 10.3, with carbonate dominant above pH 10.3. (Figure 16). Carbonate is not found in abundance in the mines as the highest pH value recorded was 7.87 ± 0.05 . Carbonate is present around a pH of 8 and increases with increasing pH (Figure 17). The dominant carbonic acid species in all mines is H_2CO_3 (dissolved CO_2) except for Ophir and Orphan Boy, which HCO_3^- dominates. The Eh-pH diagram represents the species that are found within the stability limits of water (the dashed blue diagonal lines). Bicarbonate concentrations from DIC results compare similarly to in-field alkalinity measurements.

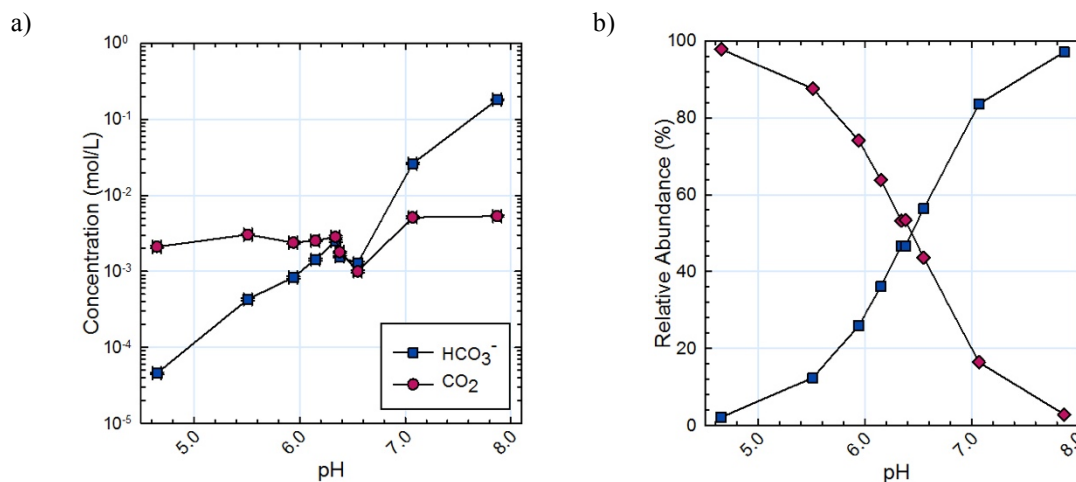


Figure 16: Carbonic acid speciation.

a) Concentrations of inorganic carbon species; all concentrations on logarithmic scale. Error bars represent ± 0.05 for pH and $\pm 3\%$ for concentration. Error bars are present but not visible since smaller than symbol size. b) Relative abundance of inorganic carbon species.

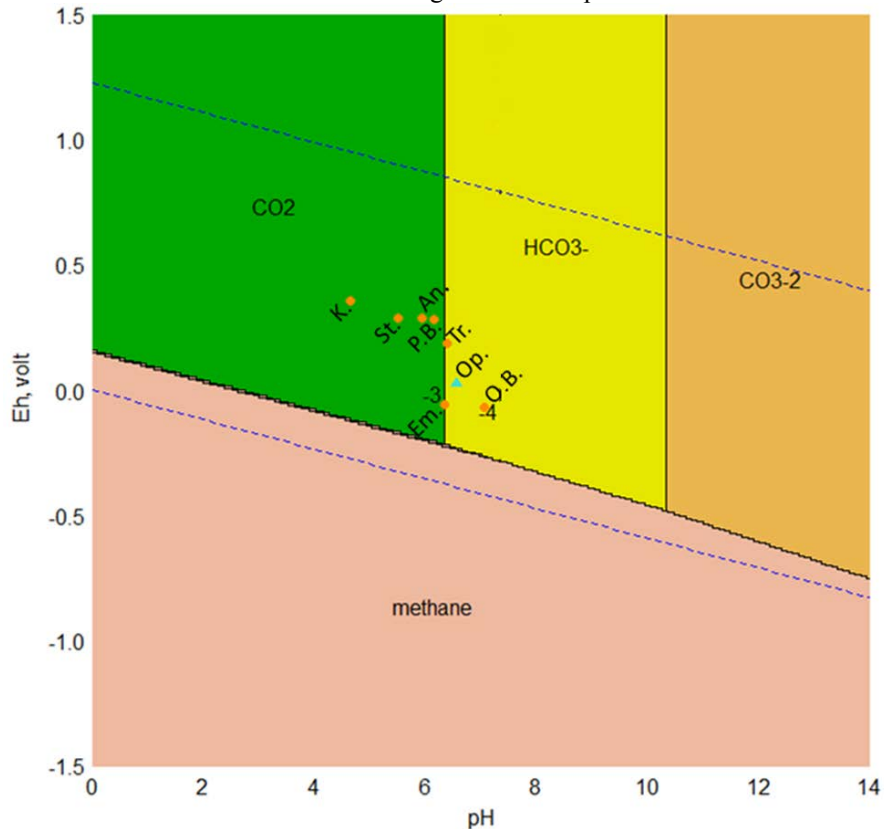


Figure 17: C-O-H Eh-pH diagram.

Temperature at 19°C, pressure at 3 bars. All Eh pH diagrams made using CHNOSZ (Dick, 2008). K: Kelley, St: Steward, An: Anselmo, P.B.: Pilot Butte, Tr: Travona, Em: Emma, Op: Ophir, O.B.: Orphan Boy. Blue dashed lines represent the stability region of water. Black solid lines represent equilibrium conditions.

The concentrations of many species decreased with increased pH. Sulfate concentrations were inversely correlated with pH (Figure 18a). Sulfide was found in the mines but did not show

a linear correlation between concentration and pH (Figure 18b). The West and Outer Camp mines ranged in sulfide concentrations from 10 nmol/L - 1 μ mol/L but still fall within the sulfate speciation section of the Eh-pH diagram (Figure 19). Recorded sulfide concentrations may not accurately represent conditions at some mines because delay and agitation between the collection and measurement may have cause volatile sulfide to escape, thus reducing the measured sulfide concentration in the sample.

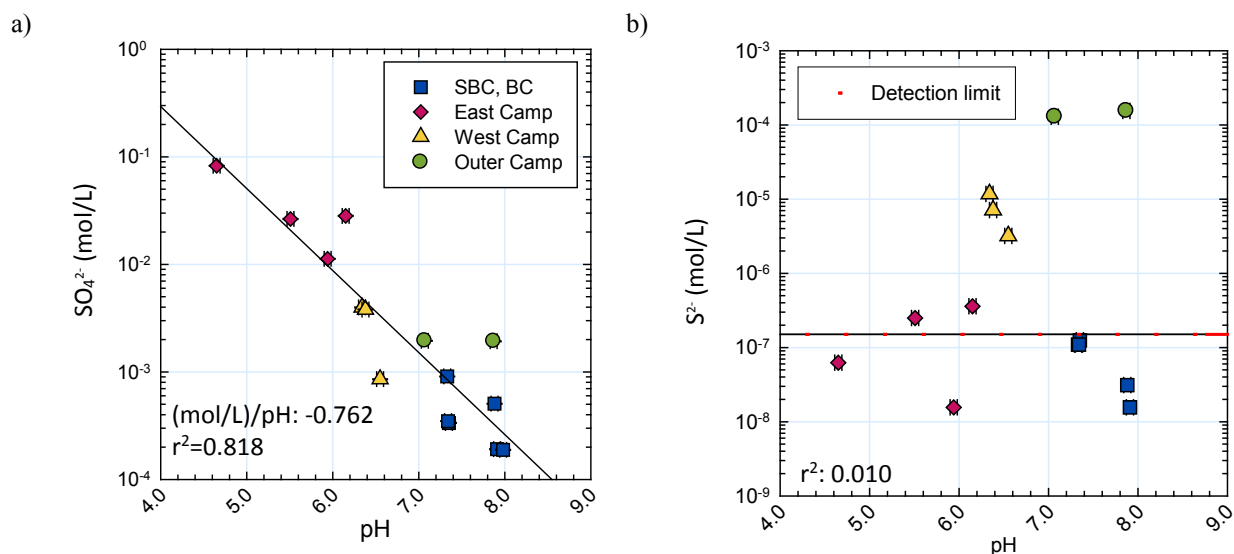


Figure 18: Sulfate and sulfide pH trends.

a) Sulfate concentration vs. pH. b) Sulfide concentration vs. pH. All concentrations on logarithmic scale. Error bars represent ± 0.05 for pH and $\pm 0.8\%$ for sulfate. Error bars are present but not visible since smaller than symbol size.

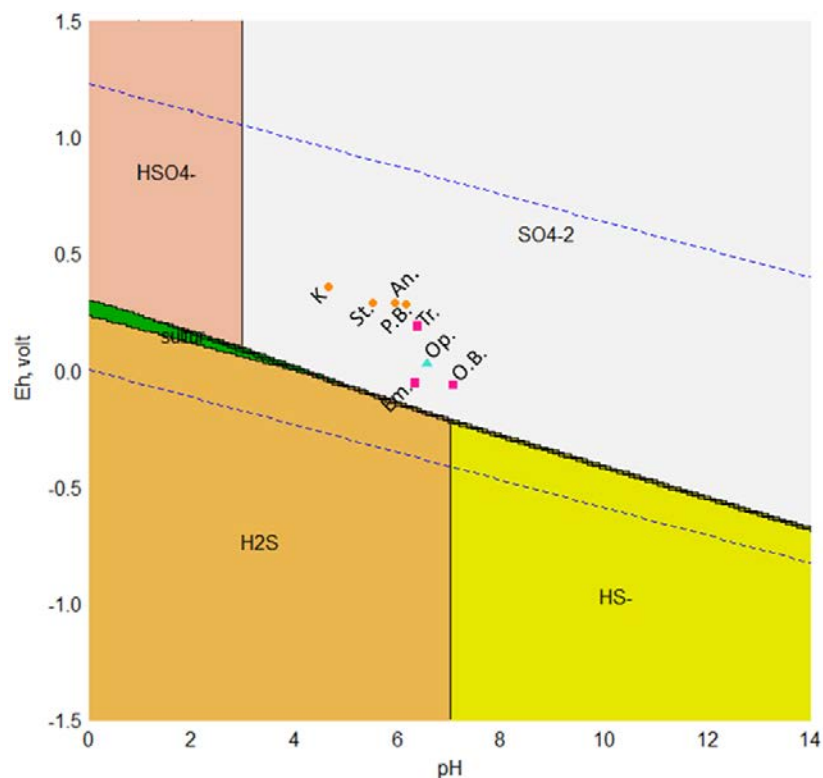


Figure 19: S-O-H Eh-pH diagram.

Temperature at 19 °C, pressure at 3 bars. Aqueous species are HSO_4^- , SO_4^{2-} , H_2S , and HS^- . S is solid. Total dissolved sulfide at 10^{-6} mol/L.

Some of the major metals and metalloids found in the mines decreased with increased pH. The only two elements that contained a linear correlation of 0.7 or greater were arsenic and iron (Figures 21a, 21c). Elements with the lowest linear correlation were lithium and strontium (Figures 20a, 21d). Barium was the only element that increased in concentration with increased pH (Figure 21e). The Eh-pH diagram of the Fe-O-H system predicted that ferrous iron is the predominant iron species in the mine (Figure 22). Oxidation reduction potential was not collected for Silver Bow and Blacktail Creeks. However, due to the pH and oxic conditions of the creek, any iron is most likely ferric.

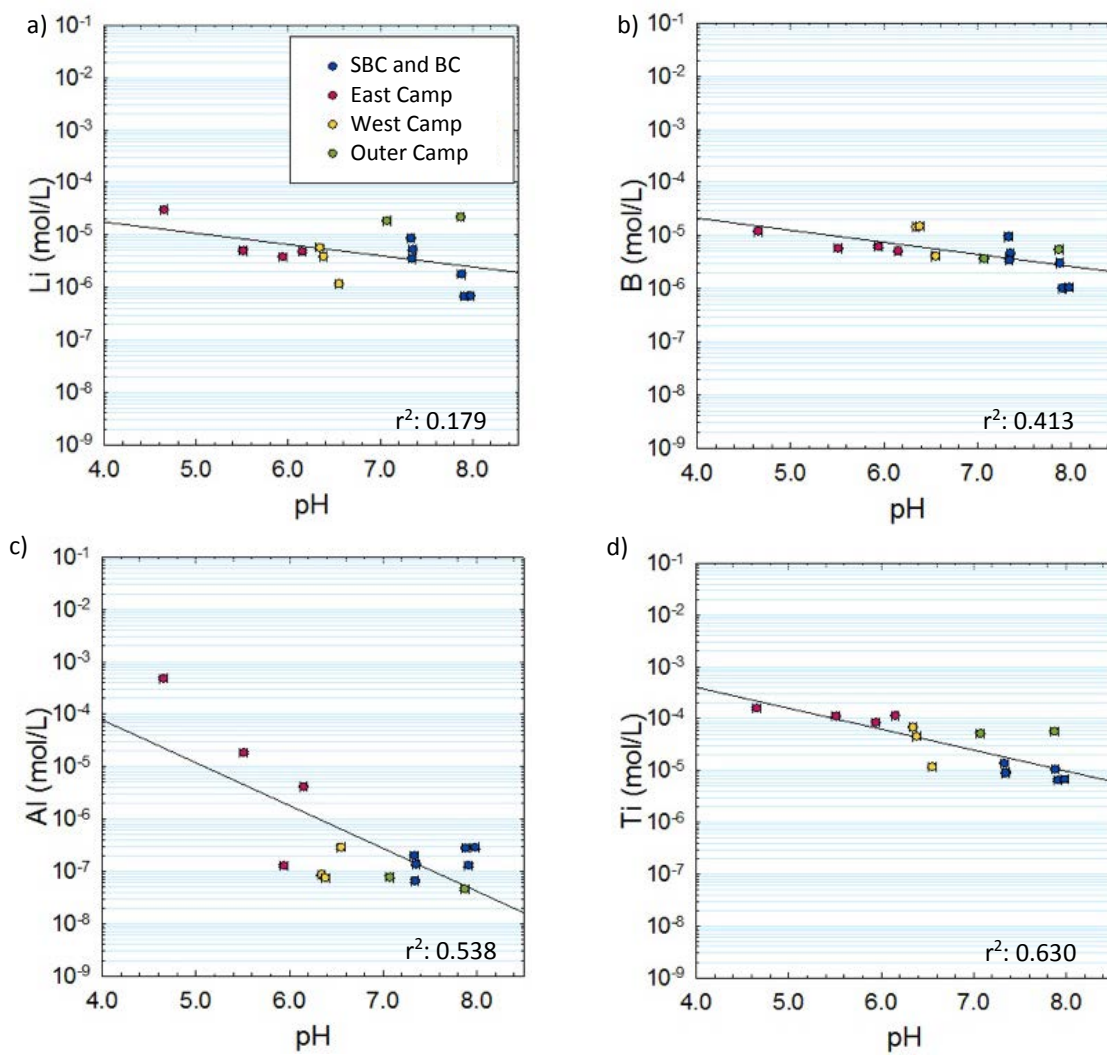


Figure 20: Total concentrations of elements vs. pH.

Total concentrations of a) lithium, b) boron, c) aluminum, d) titanium. Error bars represent instrumental error. Data are shown in Appendix A, Tables VIII and XII. Concentrations on logarithmic scale.

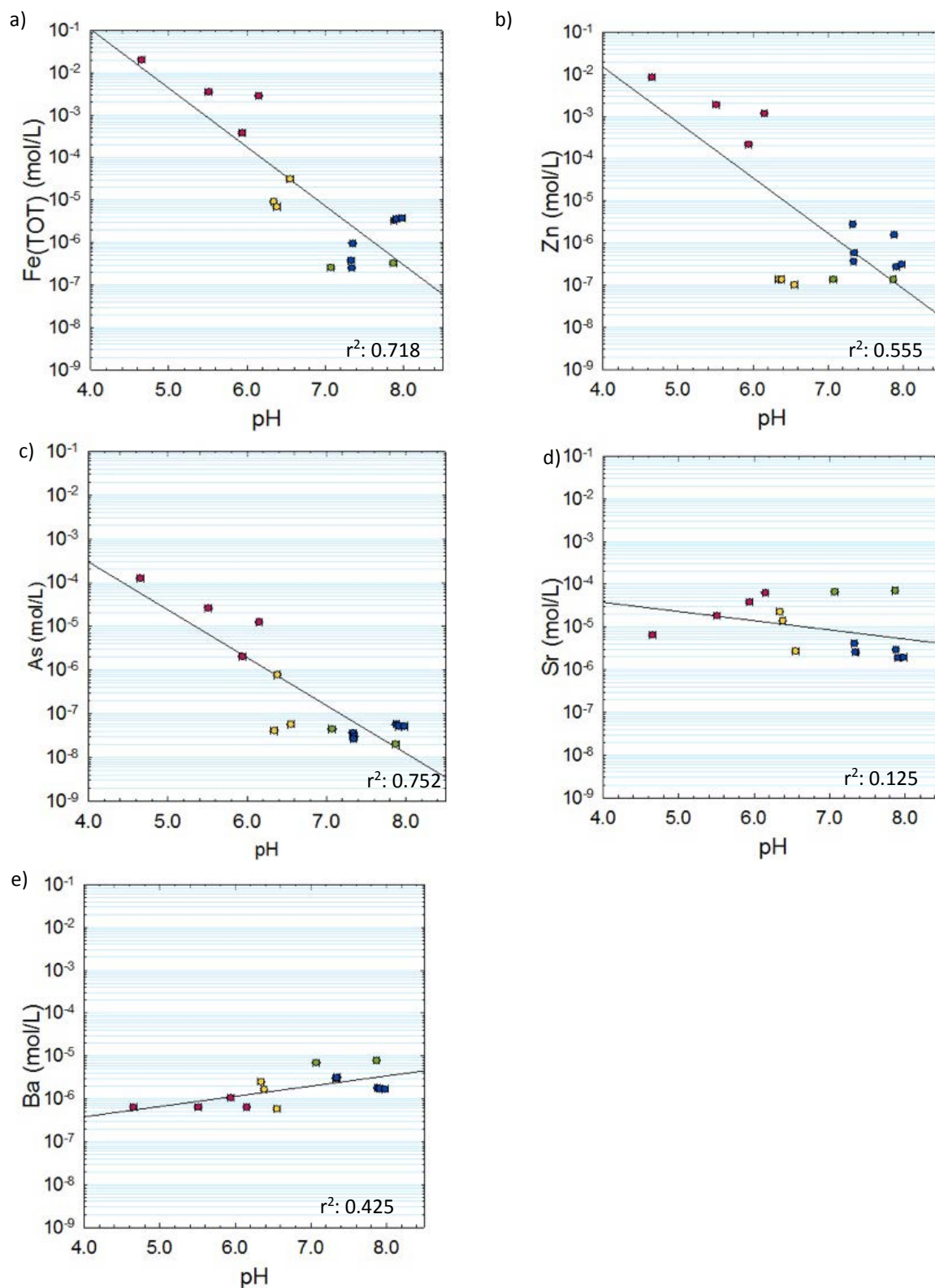


Figure 21: Total concentrations of elements vs. pH.

Total concentrations of a) iron total, b) zinc, c) arsenic, d) strontium, and e) barium. Error bars represent instrumental error. Data are shown in Appendix A, Tables VIII and XII. Concentrations on logarithmic scale.

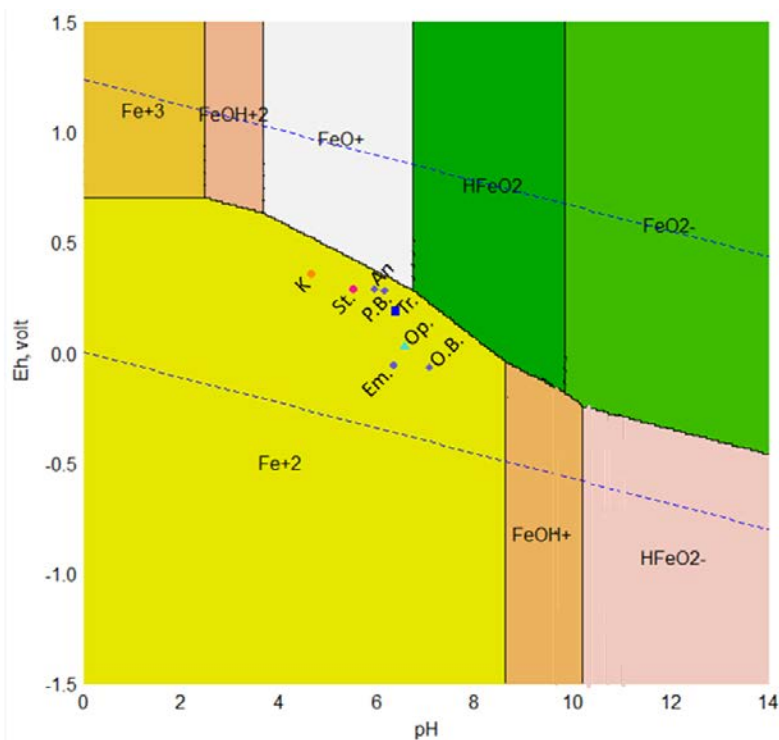


Figure 22: Fe-O-H Eh-pH diagram.

Temperature at 19 °C, pressure at 3 bars. All species are aqueous. Total dissolved iron at 10^{-3} mol/L.

3.2. PCR and Gel Electrophoresis

Gel electrophoresis of PCR products using four different 16S and 18S rRNA gene primer sets indicated that all domains of life were present in the mine waters (Appendix B, Figures 30 and 31). Bands using eukaryotic primers were found only in Orphan Boy wood samples. Archaea were present in the Orphan Boy, Steward, and Anselmo mines. All mines showed bands using universal and bacterial primers; however, the addition of PCR reagents introduced bacterial contamination. The contamination was found when viewing the gel under ultraviolet light. The negative control for bacterial and universal primers showed bands from the PCR product (Appendix B, Figures 30 and 31). The sample bands illuminated brighter than the negative control, indicating that there was a higher concentration of bacteria than contamination. The PCR product of the negative control was sequenced, and most of the contamination came from the

bacterial genus *Anaerococcus*, which is common in the human genome. To bypass the contamination from the reagents used for PCR amplification, pure DNA extract was sent to MR DNA laboratories for amplification and sequencing. At MR DNA, PCR amplification was completed on the DNA extract for all 16S and 18S rRNA primers following the sequences provided in Table V for PCR amplification and subsequent sequencing.

3.3. Sequencing Results

3.3.1. Domain Distribution

DNA sequencing for the Illumina platform was prepared by PCR amplification using both forward and reverse archaeal, bacterial, eukaryotic and universal primers for the 16S and 18S rRNA gene. Fifty nanograms of extracted and purified DNA was used for PCR amplification and the Illumina MiSeq generated an average read length of 500 bp (Dowd, n.d.). PCR amplicons from Eukarya, Bacteria, and Archaea were found in all samples at both Montana Tech and MR DNA Laboratories. The PCR amplicons and sequences from MR DNA were based on operational taxonomic unit (OTU) sequence counts. OTU is a unit that refers to the diversity and number of organisms found in a sample that contain a similar DNA sequence (such as the 16S or 18S rRNA gene). Sequenced data from PCR amplification provided counts that yielded similar abundances of Bacteria in all mines (Figure 23). Archaea was the next most abundant domain. Kelley, Emma, Travona, and Orphan Boy had the lowest counts of Eukarya, and these reads may not be taxonomically reliable (Appendix A, Table XVIII).

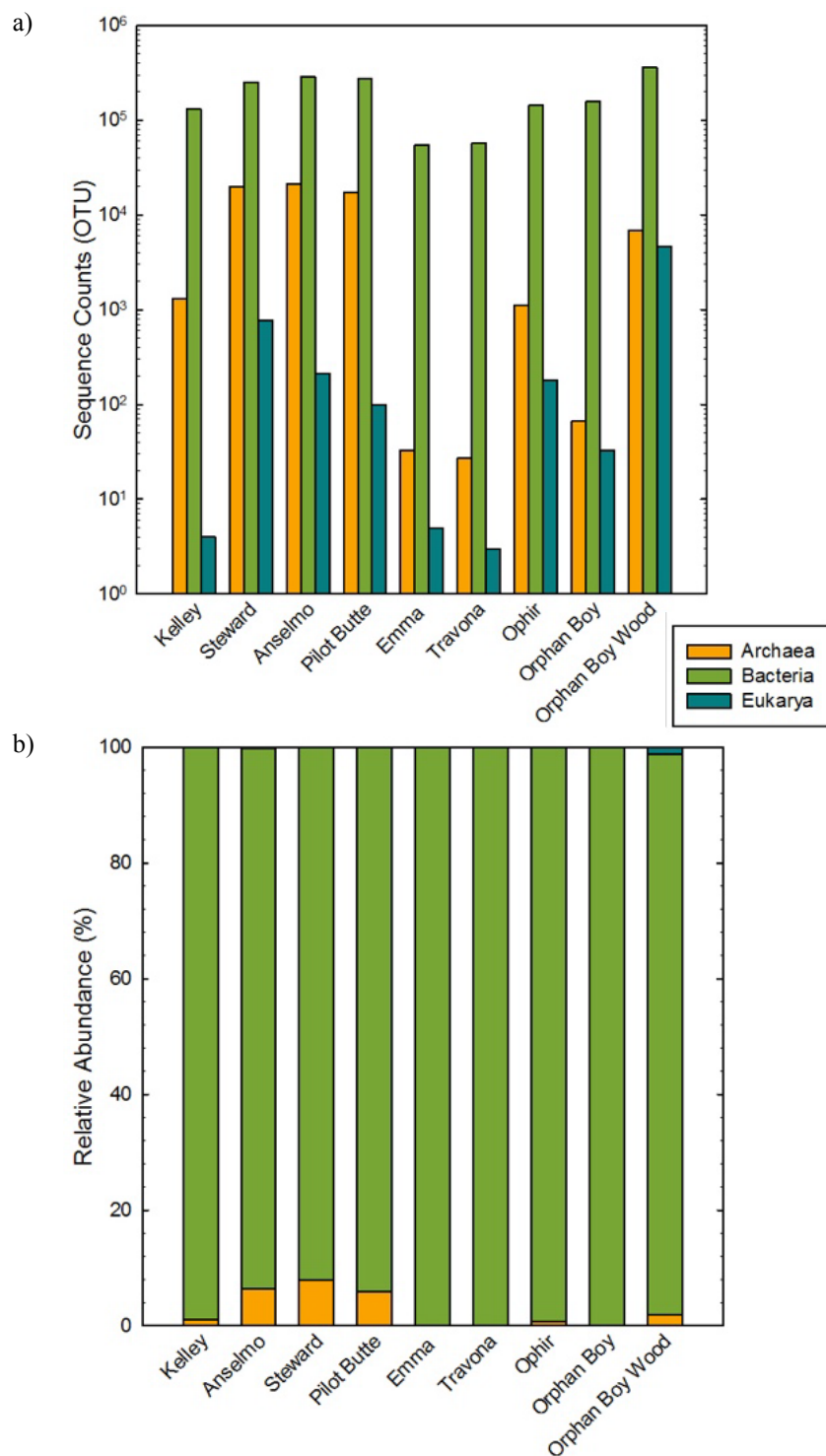


Figure 23: Domain sequence counts and relative abundance.

a) Domain sequence counts on logarithmic scale. See Appendix A, Table XVIII for sequence counts.

b) Domain relative abundance.

3.3.2. 16S rRNA Gene: Archaea

16S rRNA gene sequences belonging to the archaeal phyla were Parvarchaeota, Euryarchaeota, Thaumarchaeota, and Crenarchaeota. Figure 24 shows the relative abundance of archaeal phyla in each mine. The phylum Euryarchaeota was taxonomically ranked down to class (Figure 25). Parvarchaeota, Thaumarchaeota, and Crenarchaeota were not classified below the phylum level. Euryarchaeota is the predominant phylum in all mines except for Kelley. Ophir shows the least diversity at the phylum level as it is nearly all Euryarchaeota. Within the class ranking, Steward and Anselmo show the most diversity with seven classes while Ophir exhibits the least with only three classes. In the Kelley mine, most of the Euryarchaeota have not been identified past the phylum level.

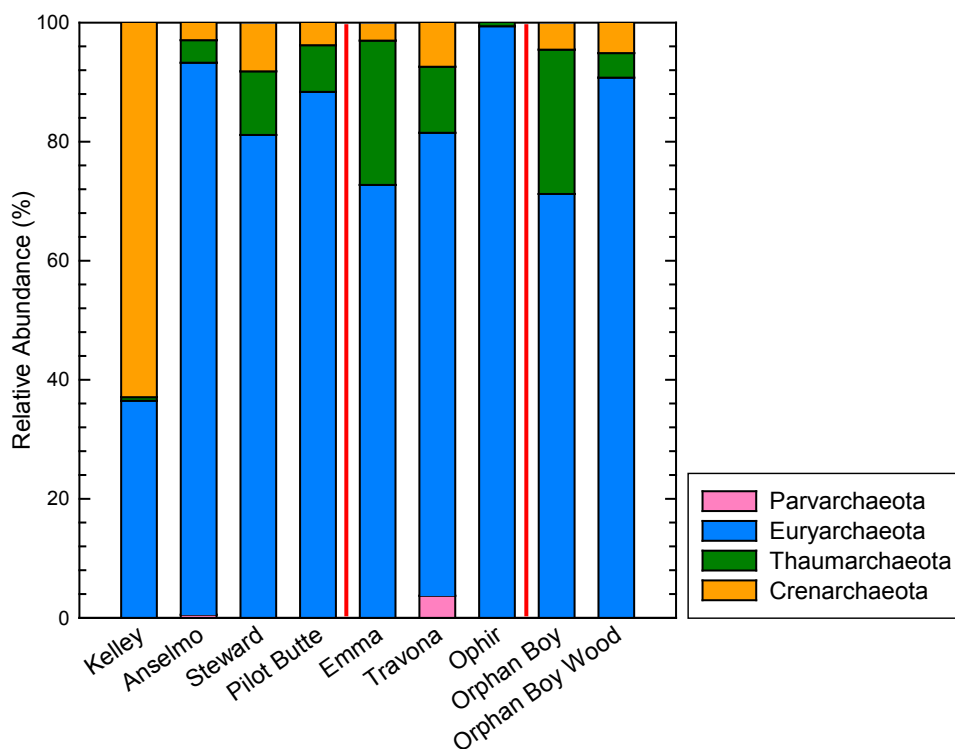


Figure 24: Relative abundance of archaeal phyla.

East Camp: Kelley, Anselmo, Steward, Pilot Butte; West Camp: Emma, Travona, Ophir; Outer Camp: Orphan Boy, Orphan Boy Wood. See Appendix A, Table XIX for sequence counts.

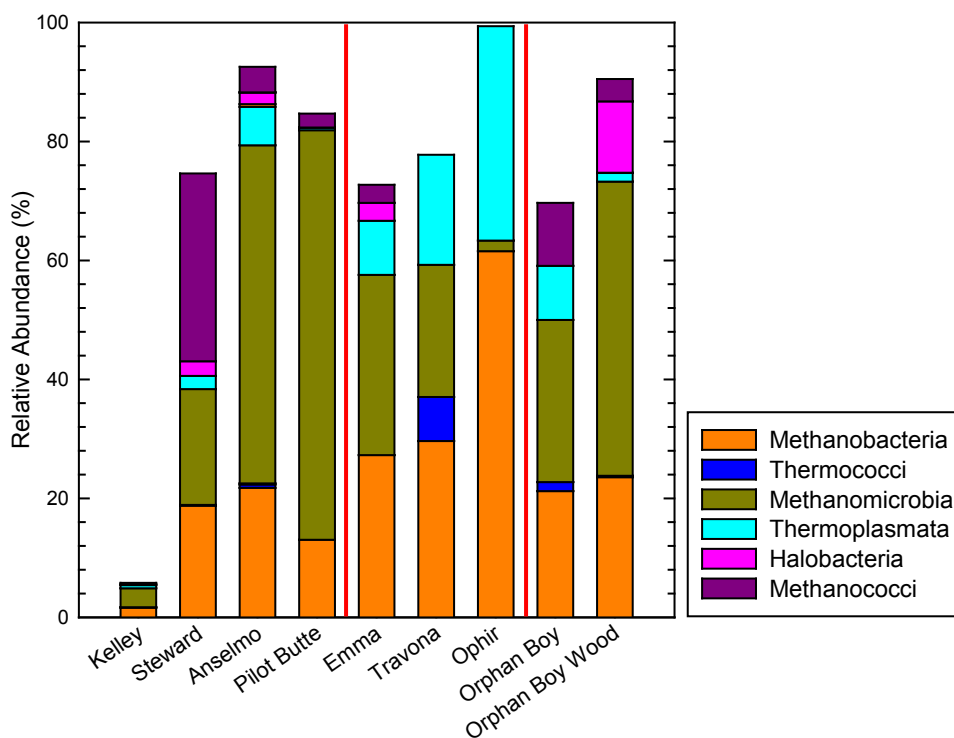


Figure 25: Relative abundance of Euryarchaeota classes.

East Camp: Kelley, Anselmo, Steward, Pilot Butte; West Camp: Emma, Travona, Ophir; Outer Camp: Orphan Boy, Orphan Boy Wood. See Appendix A, Table XIX for sequence counts.

Table VII: Archaeal phyla and classes

Phylum	Class
Euryarchaeota	Methanobacteria
	Thermococci
	Methanomicrobia
	Thermoplasmata
	Halobacteria
	Methanomicrobia
	Thermoplasmata
	Halobacteria
	Methanococci
Crenarchaeota	---
Parvarchaeota	---
Thaumarchaeota	---

3.3.3. 16S rRNA Gene: Bacteria

Bacteria were the most abundant domain in all the mines based on PCR amplification.

The most abundant phylum in most mines is Proteobacteria (Figure 26). The mines have similar

microbial compositions at the phylum level, but in varying abundances. Ophir and Orphan Boy have the most distinct bacterial fingerprints. The Emma and Travona have similar profiles, as do the Steward and Anselmo. The differences between Orphan Boy and Orphan Boy wood show that even in the same location, planktonic and surface adsorbed niches are distinct. Though the samples are from the same locations there are large differences between the planktonic and surface adsorbed niches.

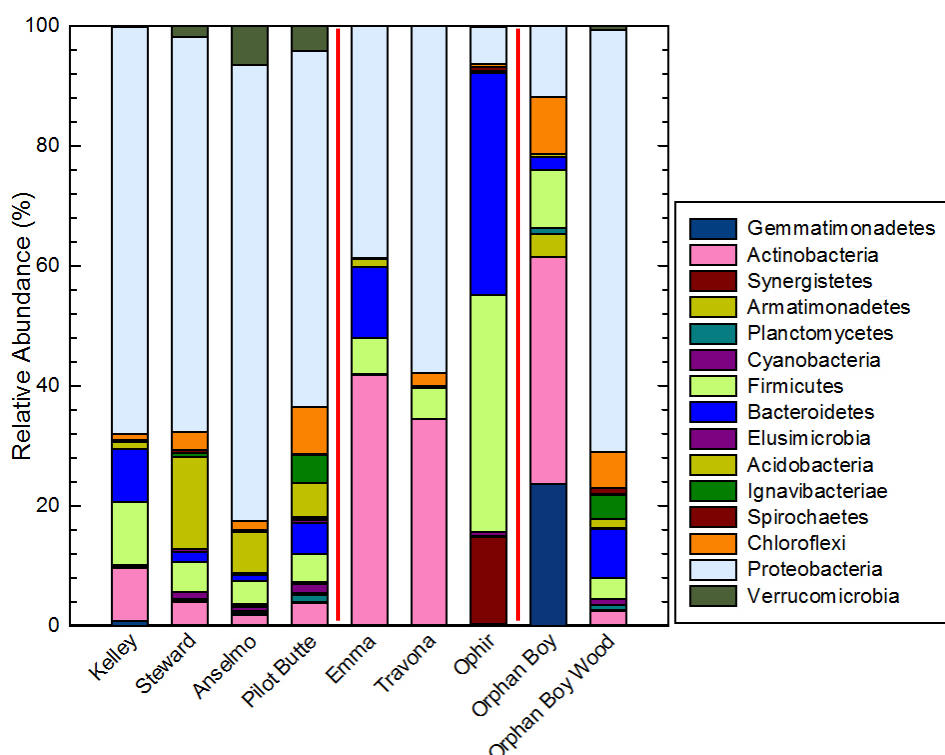


Figure 26: Relative abundance of bacterial phyla.

East Camp: Kelley, Anselmo, Steward, Pilot Butte; West Camp: Emma, Travona, Ophir; Outer Camp: Orphan Boy, Orphan Boy Wood. See Appendix A, Table XX for sequence counts.

The existence of sulfur and iron metabolizing bacteria were of interest as these organisms could contribute to bioleaching or bioremediation. The sequence counts of the genus *Desulfovibrio*, known to contain sulfate reducers, were compared to the genus *Thiobacillus*, known to contain sulfur oxidizers (Figure 27). Similarly, the sequence counts of the genera *Geobacter* and *Acidithiobacillus*, known to contain iron oxidizing bacteria were compared to the

genus sequence counts of *Nitrospira*, known to contain iron reducers (Figure 28). Table VIII summarizes the molecule or element required for both reducing and oxidizing bacteria:

Table VIII: Reducing and oxidizing bacteria genera

Metabolic requirement	Oxidizing Bacteria	Reducing Bacteria
sulfate		Desulfovibrio
sulfide	Thiobacillus	
ferrous iron	Geobacter Acidithiobacillus	
ferric iron		Nitrospira

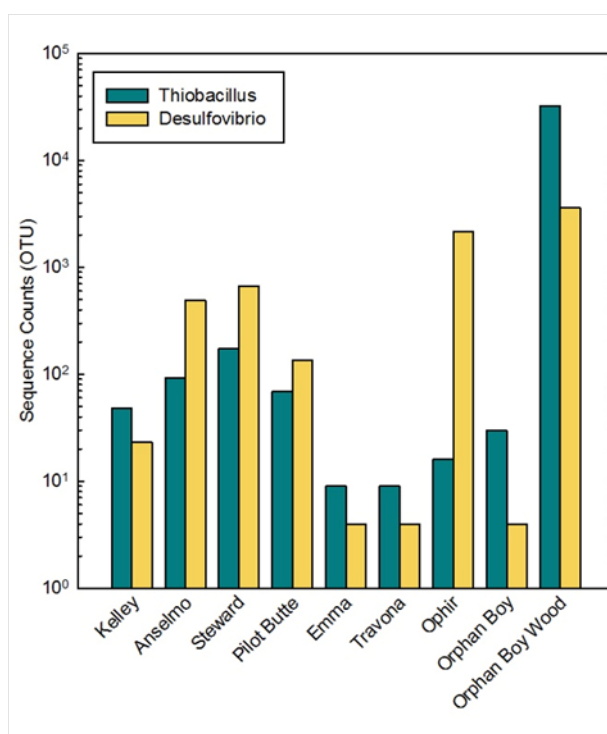


Figure 27: Sulfate reducing and sulfur oxidizing bacterial sequence counts.
Sequence count reported in log scale.

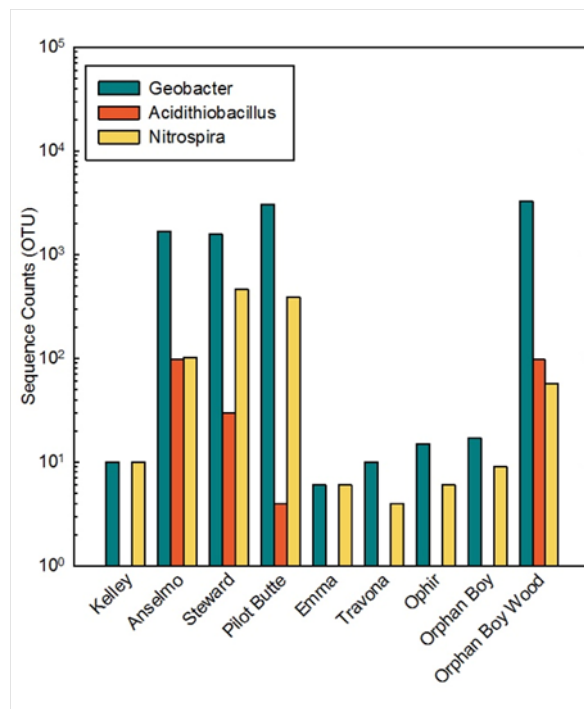


Figure 28: Iron reducing and oxidizing bacterial sequence counts.
Sequence count reported in log scale.

3.3.4. 18S rRNA Gene: Eukarya

The kingdom Eukarya was identified using the 18S rRNA gene. Eukarya was the least abundant domain in the mines; the Kelley, Emma, and Travona have the lowest sequence counts. The eukaryotic communities vary in each of the East Camp mines. Pilot Butte contains the greatest eukaryotic diversity and the Kelley has the greatest abundance of Bacillariophyta. The West Camp Travona and Ophir and the Outer Camp Orphan Boy showed the least diversity. Most sequences were not classified further than the domain Eukaryota.

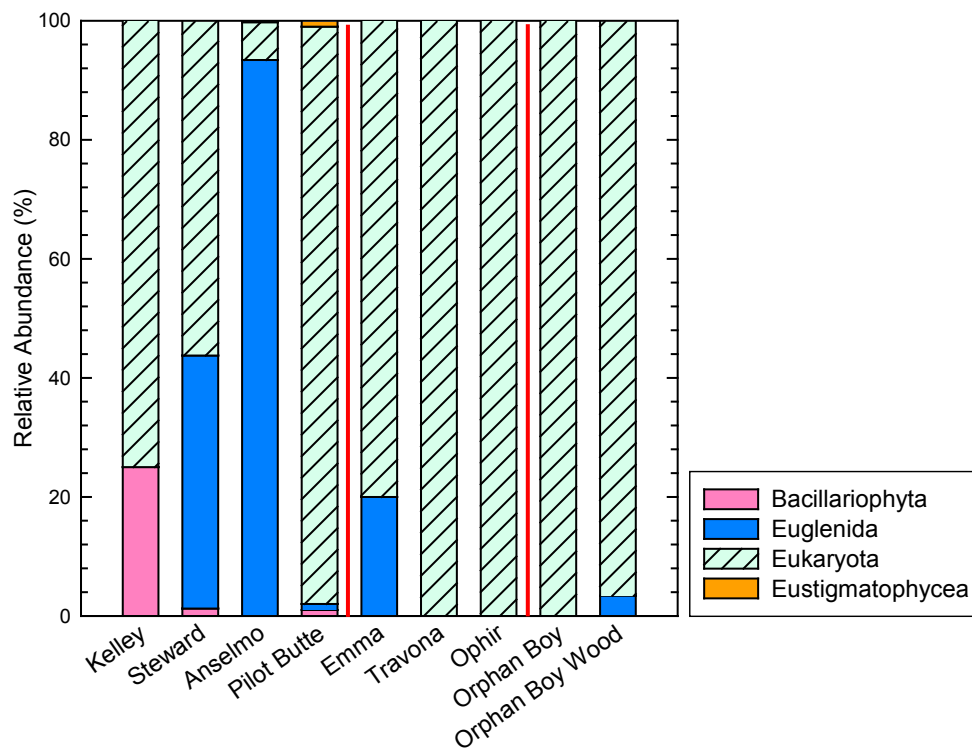


Figure 29: Eukaryotic domains and phyla.

Eukarya were identified using the 18s rRNA gene. Note the Kelley, Emma, and Travona have low eukaryotic sequence counts. Eukaryota was not classified below domain. East Camp: Kelley, Anselmo, Steward, Pilot Butte; West Camp: Emma, Travona, Ophir; Outer Camp: Orphan Boy, Orphan Boy Wood. See Appendix A, Table XXI for sequence counts.

4. Discussion

4.1. Defining the Habitat

The flooded underground mines in Butte, Montana are chemically distinct from the nearby Silver Bow and Blacktail Creeks. Conductivity and metal concentrations in the mine waters are one to three orders of magnitude higher than Silver Bow and Blacktail Creeks depending upon the location and season. Reports provided by the Montana Bureau of Mines and Geology show that water quality has changed since the initial closure of the mines in 1982 (first report Duaime and Tucci, 2008; last report Duaime, 2015). Many of these changes are from fluctuations in groundwater direction as the water levels increased, input of storm water into the mines, and pump installation in the West Camp Extraction Well (Duaime, 2015). In 2012, Dean Snyder found that apart from the Kelley mine, the pH, temperature, and metal concentrations in flooded mineshafts did not vary with depth. These findings indicated that a sample taken near the surface is representative of the deep water. However, John Metesh and Ted Duaime found that dissolved organic carbon concentrations changed vertically in the Anselmo mine, where organic carbon and cell counts were the highest at the surface of the water (Metesh and Duaime, 2002; Snyder, 2012). These studies helped shape our sampling techniques. One aliquot from each mine may not fully define the entire geochemical system of each mine shaft, nor necessarily represent the changing microbial community found in the entirety of each mine shaft, but it does provide a first step to understanding what types of microorganisms are present the system.

4.1.1. Physico-chemical Parameters

Temperature, conductivity, pH, dissolved oxygen, and oxidation reduction potential all have impacts on the microbial communities found in the mines (Figures 8, 9, 17, 19, and 22). These physico-chemical parameters showed trends across mines. Conductivity was dependent on

both temperature, pH, and the total dissolved solids. In the East Camp mines, conductivity was elevated due to the lower pH ranges, increased temperatures, and higher concentrations of dissolved metals (Figures 8, 9, and 15). In the Outer Camp, elevated conductivity and temperature coexisted with neutral to basic pH. Though pH in the Outer Camp was higher than in the East Camp, the Outer Camp has higher conductivity than the West Camp mines due to higher concentrations of dissolved species. The pH levels in the Outer Camp were similar to Silver Bow and Blacktail Creeks, but its conductivity was an order of magnitude greater than the creeks. Comparing these mines to Silver Bow and Blacktail Creeks indicate that conductivity values are influenced by the degree of water-rock interaction; the creek has not reacted as extensively with its streambed as the mine water has with the shaft. Ophir water had the lowest conductivities found in the mines, a higher pH than the other West Camp mines, and the coolest temperature (Figure 8). These differences suggest that the underground mine waters are mixing with a surficial input at this site. This mixing could either be from stormwater or groundwater. The Anselmo also is less conductive than the other East Camp mines, which may be due to mixing with stormwater inputs (Duaine, 2017, personal communication).

Lower pH ranges and warmer temperatures directly affect the abundance and types of Archaea and Bacteria in a microbial community (Baker-Austin and Dopson, 2007). The East Camp Mines, having the lowest recorded pH values and highest conductivities also had the highest Archaea OTU counts (Figure 23). Similarly, temperature and ionic strength will affect the optimum growth rate of microorganisms in a system. For example, the bacterial phylum Acidobacteria can grow at temperatures between 2-42°C with optimum temperatures between 30-35°C (Ward *et al.*, 2009). The Kelley mine had a temperature at 32.3°C, which is the optimum growth range for Acidobacteria. It was hypothesized that this mine would contain the

highest count of this phylum; instead the Steward, at a temperature of 22.41 °C, had the greatest abundance of Acidobacteria. *Ferroplasma* is the most dominant archaeal genus in extreme acid mine drainage environments, thriving in higher temperatures (around 45 °C) and elevated conductivities (around 60 mS/cm) (Bond *et al.*, 2000), but these organisms can also grow outside of their optimal physico-chemical parameters. Similar to the Acidobacteria, it was hypothesized that this genus would exist in greatest abundance in the Kelley mine as this site contained the harshest conditions based on the highest recorded temperature and conductivity. However, *Ferroplasma* was only found in Anselmo, Pilot Butte, and Steward. The Kelley should be the ideal habitat for both Acidobacteria and *Ferroplasma* based on the physico-chemical parameters, but the results do not support this idea. However, the Kelley had the greatest relative abundance of Crenarchaeota which are known as extremophiles. The Crenarchaeota is an archaeal phylum found in environments with elevated temperatures. Other factors (such as metal concentrations and carbon availability) may also contribute to the presence of absence of these organisms since they are found in mines that were not at the optimal growth parameters.

Dissolved oxygen and oxidative reduction potential also influence microbial communities as these parameters determine the potential for various electrochemical reactions. According to their dissolved oxygen concentrations, all of the mines studies were anoxic. All mines except for the Emma and Orphan Boy had a positive oxidation reduction potential (ORP) (Appendix A, Table VIII). A positive ORP value means that species at a lower electron voltage can be oxidized. In a system with limited oxygen, other oxidizing agents become the predominant electron acceptor in an environment (for example Fe^{+3} reduces to Fe^{+2} and SO_4^{-2} reduces to HS^- or other more reduced sulfur species). These oxidants are used by anaerobic Bacteria and

Archaea such as Desulfovibrionales, Desulfuromonadales, and Methanomicrobia which reduce sulfate, iron, and methane respectively (Figure 25, 26, and 27).

4.1.2. Stable Isotopes

Deuterium/hydrogen (δD) and oxygen-18/oxygen-16 ($\delta^{18}O$) in water and carbon-13/carbon-12 ($\delta^{13}C$) isotope ratios in dissolved inorganic and organic carbon give information about the source of the water, mixing, evaporation, and the extent of water-rock interaction occurring in the system. δD and $\delta^{18}O$ show that waters with a slope less than the local meteoric water line are evaporative (like surficial waters such as a creek or river system). In Silver Bow and Blacktail Creeks, water isotope values change depending on the time of year (Figure 10). In May, the points are more enriched in δD and $\delta^{18}O$ and in February the points are lower along the evaporative water line showing that the creek has seasonal changes. The May points are enriched from the addition of recent snowmelt and increased precipitation to the creek. The mine shafts plot closely between the intercept of the evaporative line and local meteoric line, which shows that the underground workings had little evaporation (Figure 10). The mine waters have not reacted with the atmosphere nor were they evaporating into the environment. As a result, circulation of waters in these mines is from the addition of ground or surficial water flowing into or through the shafts. Atmospheric exchange did not play as significant of a role in the geochemistry of the mines as it did in Silver Bow and Blacktail Creeks. The intersection between the local evaporative line and local meteoric water line is the value of recharge waters in the mine system (Gammons *et al.*, 2006). All points except for the May Silver Bow and Blacktail Creeks samples were close to this intersection (Figure 10). The isotopic values of these points mean that most water had moved downward from the surface to the ground rather than

evaporating. Anselmo shows a slight enrichment in δD and $\delta^{18}O$ values, indicating that mine water from this shaft may be mixing with surface water runoff.

Carbon isotopes give an understanding of the water-rock interactions and are an indicator of possible microbial activity. Dissolved inorganic carbon concentration is the sum of the inorganic carbon species CO_2 , HCO_3^- , and CO_3^{2-} . The carbon species present in the water is pH dependent (Figure 16). With the exception of the low DIC values for Silver Bow and Blacktail Creeks in February, inorganic carbon isotope ($\delta^{13}C_{DIC}$) values became lighter as the concentration increased. This trend was not found in organic carbon isotopes ($\delta^{13}C_{DOC}$) (Figure 11a). Gammons et al. (2009) proposed that the decrease in $\delta^{13}C$ with increase in DIC concentration in the Butte mine shafts was mainly caused by microbial respiration of organic carbon.

In Silver Bow and Blacktail Creeks, the water had not interacted with the rock as long as the mine water due to high flow rates. These waters were exposed to the atmosphere which is represented by the enriched $\delta^{13}C_{DIC}$ values. The atmosphere contains an average $\delta^{13}C_{DIC}$ of -7 ‰, which is close to the inorganic $\delta^{13}C_{DIC}$ value of the Silver Bow and Blacktail Creeks (Sacks, 1996). This value indicates that the waters exchanged with the atmosphere from evaporation in May.

$\delta^{13}C_{DIC}$ values are also affected by mineral dissolution from carbonate rocks such as calcite or rhodochrosite (a range of -7 ‰ to -30 ‰) and by microbial metabolic activity that oxidized organic carbon and created inorganic CO_2 (average -25 ‰) (Sacks, 1996). The Outer Camp mines are in equilibrium with carbonate based rocks such as calcite whereas the West and East mines have some carbonate rock, but are mostly in equilibrium with sulfate based rocks such as gypsum (Roesler, 2007). Rhodochrosite in the Orphan Boy and Girl mines are a major source of carbonate in the mines. The $\delta^{13}C_{DIC}$ value of rhodochrosite in the Butte district ranges

from -7 ‰ to -8 ‰ (Stevenson, 2015). However, the Orphan Boy and Girl mine waters were the most depleted in inorganic $\delta^{13}\text{C}_{\text{DIC}}$, with values near -23 ‰. This depleted value indicates that respiration of organic carbon by sulfate reducing bacteria, iron reducing bacteria, and other organisms take up dissolved organic carbon compounds at a $\delta^{13}\text{C}_{\text{DOC}}$ value of -25 ‰ and oxidize the DOC to DIC as CO_2 . This then produces as DIC isotopic value around -25 ‰ (Gammons *et al.*, 2009).

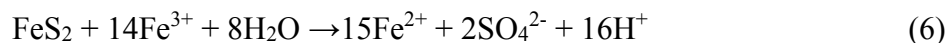
Dissolved organic carbon (DOC) values can also be an indicator of microbial activity. In general, the mines have low DOC concentrations (Figure 11b). Previous studies have hypothesized that the contribution of DOC to the water is from the timbers used to construct the shafts (Gammons *et al.*, 2009). If the organic carbon comes from the timbers, the $\delta^{13}\text{C}_{\text{DOC}}$ values would be around -25 ‰. Pilot Butte from the East Camp, Emma and Travona from the West, and Orphan Boy and Girl from the Outer have $\delta^{13}\text{C}_{\text{DOC}}$ values close to that of C3 plants (photosynthetic, temperate climate plants such as woody trees) (Kendall *et al.*, 1995). In environments with CO_2 as the predominant dissolved carbon species (such as the Kelley mine), $\delta^{13}\text{C}_{\text{DOC}}$ values are less depleted. In systems where CO_2 is limited (such as in higher pH ranges like Silver Bow and Blacktail Creeks) organic $\delta^{13}\text{C}_{\text{DOC}}$ values are more depleted (Hoefs, 2015). The exception to this is the Ophir and Anselmo. These two mines are enriched in organic $\delta^{13}\text{C}_{\text{DOC}}$ most likely due to the mixing of surficial waters (Figure 11b).

4.1.3. Major Cations, Major Anions, and Trace Elements

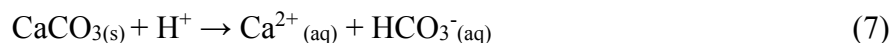
Cation concentrations and their relative abundance in the mines influence the types of microbial communities (Figure 13). Halophiles are a type of extremophile that thrive in environments with high salinity. The Anselmo, Steward, and Orphan Boy wood each had sequence counts for halophiles. Interestingly, neither the Orphan Boy water sample nor the

Kelley (which has the highest salinity and total major cations) contained halophiles. In the Kelley, high trace metal concentrations and warmer temperatures may influence the absence of halophiles. However, these parameters may be optimal for the archaeal phylum Crenarchaeota, which predominates the microbial community in the Kelley mine. In the Orphan Boy, the wood sample is a substrate that is an organic carbon source which provides a niche that is optimal for microbial diversity. Conditions in the Orphan Boy water may be too harsh for halophiles due to the elevated hydrogen sulfide concentrations and lack of available dissolved carbon. Halophiles may be higher in the Anselmo due to direct stormwater input mixing with mine water. The Steward could also have an increase in halophiles due to stormwater mixing, but a direct input from stormwater is not certain (Duaiame, 2017, personal communication).

The concentrations of two major anions found in the mines, bicarbonate and sulfate, create a separation between the chemistry and microbial communities of each mine (Figure 14). The East Camp mines are in equilibrium with gypsum which is a source of sulfate. Dissolved sulfate does not directly affect the pH in the water, but is often associated with low pH in mine waters due to pyrite dissolution. When pyrite is exposed to oxidation either by oxygen (Equation 5) or ferric iron (Equation 6), sulfide is oxidized to sulfate and hydronium ions are released, thereby decreasing pH:



Calcite is the primary source of bicarbonate in the West and Outer camps. The equilibrium constant for calcite in pure water is small ($K_{\text{eq}}=3.11 \times 10^{-9}$), but the acid-base reaction between calcite and acid proceeds quickly:



The K_{eq} for Equation 7 is 7.06×10^1 and the Gibb's free energy is -1.06×10^7 kJ/mol. These values indicate that calcium carbonate will dissociate and dissolve in water when reacted with acid. The bicarbonate product can become carbonic acid in water, which is dissolved carbon dioxide (Equation 8). When water in the mines is depressurized by bringing the sample to the surface, carbon dioxide will volatilize out of the water:



Since calcium carbonate readily dissolves in low pH waters, the pH lowers due to the formation of dissolved carbon dioxide. However, when carbon dioxide is released from the water, the pH increases.

The mines can be grouped by anion and cation abundances (Figures 14 and 15). Sulfate concentrations are greatest in the East Camp mines while bicarbonate is the predominant anion in the Outer Camp. Total iron is greatest in the East Camp mines, and calcium and sodium concentrations are relatively similar in each mine. The free energy available for microbial metabolism is based on varying concentrations of chemical constituents in the mine system. Cations and anions are also used as dissolved, bioavailable nutrients. Most organisms in water with high metal concentrations are chemoorganotrophic or chemolithotrophic and use ions other than oxygen as the terminal electron acceptor during ATP synthesis (Madsen, 2015).

Total element concentrations and relative abundance graphs of each site compare the chemical composition of each mine's habitat. The zonation between the mines is most apparent in the trace metal relative abundance plot (which ranges from 10 mmol/L – 1 nmol/L) (Figure 13). The East Camp has the greatest percentage of dissolved zinc, titanium, strontium, and arsenic whereas the West and Outer show compositions dominated by titanium, boron,

strontium, lithium, and barium. The composition can influence the types of microorganisms existing in each mine. Living organisms use zinc and strontium as micronutrients or cofactors in proteins, but arsenic is toxic (Madigan *et al.*, 2011). Additionally, high concentrations of metals can either individually or in summation have toxic effects.

4.1.4. pH Dependent Speciation

The speciation of carbon, sulfur, and many dissolved metals is pH dependent. The speciation results were as expected based on the Eh-pH diagrams (Figures 17, 19, and 22) under slightly oxic conditions. Carbon existed in the CO₂/bicarbonate area, sulfur speciated as sulfate, and iron existed as ferrous in at all the sites.

Carbon speciates as either CO₂, HCO₃⁻ or CO₃²⁻ depending upon the pH. The Butte mines do not have high enough pH values for carbonate to exist as the predominant species, so only carbon dioxide and bicarbonate are considered. An inverse trend between bicarbonate and carbon dioxide is found, and the concentration of both species are in equilibrium at a pH of 6.4 (Figure 16).

In this study, the two forms of sulfur measured were sulfate and total dissolved sulfides (H₂S/HS⁻). Sulfate concentrations showed a correlation with pH but total sulfide with pH did not (Figure 18). The sulfate trend is atypical as sulfate concentrations are not pH dependent. The observed trend is most likely due to microbial activity such as sulfate reducing bacteria that may be present in the West and Outer Camp mines and pyrite dissolution occurring in the East Camp. The elevated levels of sulfide in the West and Outer Camp mines are most likely as byproducts of sulfate reducing metabolism (Equation 9). The reaction for sulfate reduction in bacteria is:



The net acidity of mine water decreases as the sulfide will bond with divalent metal and precipitate out of the water. Alkalinity is also produced in the form of bicarbonate. Although pH is the dominant factor, sulfate reduction may help explain why the waters in the Orphan Boy and Girl system are lower in metal concentration than the other mines. However, other factors such as the abundance of carbonate minerals in the veins and lower concentration of acid producing metals (such as pyrite) also prevent the waters from becoming acidic.

Reactions producing sulfate could occur in the more acidic mines, such as the Kelley (Equation 5). This reaction is typical of surficial acid mine drainage systems. However, in the underground mines there is very little dissolved oxygen. Most of the mine waters had a measured positive electron potential, meaning that there is a greater potential for oxidation. Most likely, the reaction occurring in the underground mines is pyrite oxidation by ferric iron (Equation 6). Nearly all of the iron found in the East and West Camp water was speciated as iron(II). The source of iron(III) may come from iron that was exposed and oxidized prior to flooding or from iron oxidizing bacteria such as *Acidithiobacillus* or *Nitrospira*.

Trace elements that showed the most direct correlation between concentration and pH were total iron and arsenic (Figures 21a, 21c). These elements decreased in concentration with increased pH. This trend found in iron is due to the anoxic nature of the underground mines. Iron does not precipitate in the mines at higher pH values because of the low oxygen, otherwise iron concentrations would drop off around a pH around 3 in oxic waters (St. Clair, 2017). Arsenic trends follow typical speciation patterns where the solubility increases at lower pH values. However, arsenic speciates as an anion and is soluble at both low and high pH values. If the waters in the mines were alkaline (around 8.5), the increased pH would release arsenic anions sorbed onto iron oxides and cause arsenic concentrations to increase

(Smedley and Kinniburgh, 2002). The Orphan Boy and Girl have a pH around 8, but the lower arsenic concentration in these mines may be due to a lower abundance of arsenic in the rock.

4.1.5. Microbial Communities

Analyzing the chemical potential of a system through trace elements, cations, anions, and environmental parameters defines the habitat or niche of the microbial community. The primary purpose of this study was to investigate if similar "zones" or trends could be found in the microbial communities as seen in the chemical and geologic results. All three domains of life were considered in the diversity analysis. Furthermore, species commonly found in acid mine drainage were investigated for the potential of natural remediation in each mine, as well as bioleaching. Studying the chemical makeup of these particular organisms' niche can provide insight into the limitations and ranges of their habitability, which can be used to benefit the mining industry in both enhancing ore extraction yields and remediating metal laden waters. Archaea were detected within all mine sites. Sequence counts were similar in Steward, Anselmo, and Pilot Butte but varied in all other sites (Figure 23). Orphan Boy wood contained more Archaea than the water sample. Most of the archaeal diversity at the phylum level was similar in the mine sites, except for the Kelley, Ophir, and Travona (Figure 24). Ophir was the lowest in diversity with only Euryarchaeota. The Kelley, considered to be the most extreme environment with the warmest temperatures, lowest pH, and highest dissolved iron concentrations, was also lower in diversity, containing only Euryarchaeota and Crenarchaeota, a known extremophile. The Travona was the only mine that exhibited noticeable amounts of Parvarchaeota. Based on the biological diversity profiles of each mines, they exhibited no distinct groupings that parallel the chemical and geological zones.

Zones were apparent in the archaeal classes. Taxonomic information below the phylum level was provided only for Euryarchaeota. Similar profiles were found in the Steward, Anselmo, and Pilot Butte where Methanomicrobia, Methanobacteria, and Methanococci are the predominant archaeal classes. However, classes with smaller abundances varied between the three sites, making each community unique. Emma, Travona, Ophir, and Orphan Boy showed similar divisions in the classes with Methanobacteria, Methanomicrobia, and Thermoplasmata as the predominant components. Within the classes, Orphan Boy Wood and Kelley were most distinct. The Kelley contained Euryarchaeota that are unclassified past phylum. The wood sample from Orphan Boy contained the greatest number of Halobacteria compared to the other mines.

The predominant classes identified in the Butte mine waters within the Euryarchaeota phylum are most known for their ability to thrive in extreme conditions. Organisms in the methano- classes include methanogens which produce methane. Halobacteria can live in hypersaline conditions, however sodium and chloride concentrations in the mines are low compared to seawater. Though the conditions in the Orphan Boy mine are not considered hypersaline these organisms exist in higher concentrations on the wood rather than in the water because the wood can be used as a carbon source for metabolism. Thermoplasmata are acidophiles usually found in pH environments below 2 and warmer temperatures, such as the Richmond Mine, CA (Golyshina *et al.*, 2016). Interestingly, these Archaea were not found in the most extreme environments in Butte mines, such as the Kelley, but rather in the cooler water with lower metal concentrations such as the Emma, Travona, and Ophir.

Bacterial diversity was much higher than archaeal. Due to the large number of phyla, going below this taxonomic classification overly complicated analysis and prevented assessment

of zoning classifications. Most mines contained similar bacterial phyla in varying amounts (Figure 25). The predominant phylum in most mines was Proteobacteria, which have a wide range of metabolisms that include but are not limited to nitrogen-fixation, iron oxidation, and sulfate reduction. Proteobacteria are typically anaerobic and are classified as both chemolithoautotrophs or heterotrophs. Actinobacteria, predominant in soils, was found in all mines except for Ophir. The wood and water samples from Orphan Boy did not show similarities in their microbial communities. Orphan Boy contained Gemmatimonadetes which are not found in any of the other mines. Gemmatimonadetes are a novel phototrophic phylum similar to Cyanobacteria in that they contain carotenoids, but do not assimilate inorganic carbon. This lack of inorganic carbon uptake suggests that photosynthesis is used in addition to other metabolic pathways, thus categorizing the bacteria as photoheterotrophic (Zeng *et al.*, 2014). The Orphan Boy shaft is enclosed within a room containing a light. This light may provide a source of energy to the Gemmatimonadetes for photosynthesis.

Ophir is unique because it was the least diverse and contained Synergistes, which were unique to this mine. Ophir also had the largest concentration of Firmicutes and Bacteroidetes. Synergistes are anaerobic bacteria commonly found in wastewater treatment plants and hypersaline solutions (Gordon *et al.*, 2005). The Synergistes phylum is an example of the benefit of culture-independent studies as these bacteria are typically found at low frequencies in microbial communities (up to 1% relative abundance in 16s rRNA gene studies) (Gordon *et al.*, 2005). Thus, most Synergist sequences were found using 16S rRNA gene amplification rather than from cultivated strains. In the Ophir, 15% of the bacterial community belongs to Synergistes which is high compared to the 1% found in most microbial ecosystems. Firmicutes are anaerobic and produce hydrogen (H₂) gas as a byproduct of fermentation. This natural production of H₂ gas

is currently being studied as a renewable source for fuel while simultaneously treating wastewaters with high organic carbon (such as in distilleries) (Yu *et al.*, 2002; Mohan *et al.*, 2011). Firmicutes are also common in acid mine drainage systems and are beneficial to bioremediation as this phylum contains sulfate reducing genera such as *Sulfobacillus* (Baker and Banfield, 2003). Bacteroidetes are similar to Firmicutes in that their primary metabolic process is fermentation. Bacteroidetes live symbiotically with Firmicutes, especially in the guts of mammals (Thomas, 2011).

Sequence counts for well-studied genera of sulfate reducing bacteria and iron reducing bacteria were analyzed to compare the microbial habitat to the relative abundances of these organisms. Sulfate reducing bacteria are well known in the mining industry as a natural form of bioremediation. Additionally, iron oxidizing bacteria are useful in bioleaching but are also a detriment in uncontrolled acid mine drainage systems. The highest concentrations of *Desulfovibrio*, a well-studied genus of sulfate reducers, were found in the Orphan Boy wood and Ophir (Figure 26). Steward and Anselmo also had elevated levels of *Desulfovibrio* while Orphan Boy water was limited in this genus. The defined habitats of Orphan Boy, Steward, Anselmo, and Ophir show a great range in pH (from 5.5 to 7.8) and temperature (11.5-22.4 °C), as well as the types of dissolved anions and metals. This result shows that sulfate reducing bacteria can exist in a wide variety of habitats with varying chemical composition.

Acidithiobacillus and *Nitrospira* are two genera commonly known for their iron oxidizing metabolism (Figure 27). The Steward, Anselmo, Pilot Butte, and Orphan Boy wood all contained the highest sequence counts for these genera. Similar to *Desulfovibrio*, this result shows the large range of habitability of these genera. By observing the relative abundances of these two genera, we can suggest that iron oxidation and sulfate reduction could occur in these systems. However,

diversity analysis does not prove what metabolisms are occurring in the system, but only provides a view of the potential metabolic activities that could occur.

Eukaryotic diversity also did not replicate the same zones as the chemistry or geology of the mines (Figure 28). The Travona, Ophir, and Orphan Boy had the lowest eukaryotic diversity at the phylum level. Pilot Butte contained the highest amount of diversity with four phyla. The mines could not be grouped by eukaryotic diversity at the phylum level. Taxonomic diversity on lower orders was not analyzed due to the low relative abundances of Eukarya in the Kelley, Emma, Travona, and Orphan Boy.

The results obtained from 16S rRNA gene analysis did not concur with Metesh and Duaine's, 2002 culture findings. Dissolved organic carbon concentrations in each mine were several orders of magnitude lower and the only species that was consistent with Metesh and Duaine's finding was *Arthrobacter oxydans* (Figures 3 and 4). A greater diversity of organisms was found in this culture independent study. Though only one bacterial species was observed in both Metesh and Duaine's study and this project, this does not mean that the other bacterial species from Metesh and Duaine do not exist in the mines. Culture independent methods are beneficial as DNA can be sequenced for organisms that are difficult to grow in the lab. Culturing provides the benefit of growing organisms within the mines for experimental purposes. Also, the method used in this study does not provide information about the concentration of alive versus dead cells in the sample.

4.1.6. Microbial diversity in the Ophir

The Ophir stands out as having the most unique microbial community in relation to the other mines. This difference indicates that the Ophir is mixing with another water input either from storm or ground water. The mixed waters alter the geochemistry of the Ophir in relation to

the other West Camp mines by lowering the conductivity, temperature, and total trace elements concentration. The Ophir is also different from the other mines as it is the most enriched in both $\delta^{13}\text{C}_{\text{DIC}}$ and $\delta^{13}\text{C}_{\text{DOC}}$. These geochemical differences and water mixing provide a habitat that is optimal for bacteria that are not found in the other mines. Synergistes and Firmicutes are two strains of bacteria that live symbiotically in a variety of environments, but in lower relative abundances than found existing in the Ophir. Prior to the microbiological findings, Ophir was geochemically compared to the Travona and Emma and was hypothesized to reflect the same microbial communities due to the similarities in habitats. In spite of these geochemical similarities to other mines, the Ophir was found to be unique amongst the mines studied in terms of its microbial community.

4.1.7. Natural Amelioration?

In 2016, two abstracts were published by Schmidt and Cox discussing the possibility of natural amelioration in the mines (Schmidt and Cox, 2016a and 2016b). These abstracts stated that all nine mines showed improvement in water quality since monitoring began in 1983 but that arsenic had increased in the East Camp mines. These statements were made on the basis of an incomplete analysis of the monitoring data. Having examined the data more thoroughly and in relationship to adjustments in mine water management, it appears that natural amelioration is not taking place in the nine mines studied in this thesis. For a better understanding of how the water quality has changed in the mines with changes in water management, it is best to refer to the reports published by the Montana Bureau of Mines and Geology (Duaiame, 1998; Duaiame *et al.*, 2008; Duaiame *et al.*, 2016).

5. Conclusion and Further Studies

This study was the first 16S/18S rRNA gene microbial diversity analysis performed on the Butte mine water. The microbiological results showed that mine waters studied exhibited some similarities in microbial communities but did not contain the same separation of zones as the chemical and geological trends. Microbial similarities between mines show that microorganisms live in a large range of habitats with varying temperature, pH, conductivity, and metal concentrations. Differences in microbial diversity of the Ophir compared to other mines indicate that there is mixing with surface waters in this mine. In addition, metabolic potential for sulfate reduction and iron oxidation was observed in all mines. These findings show that the Butte underground mines have the potential to isolate organisms for use in natural remediation as well as bioleaching capabilities.

Additional work currently in progress includes metagenomic and metaproteomic analyses. Metagenomic and metaproteomic analyses provide more in-depth study information about the metabolic potential as well as activity and provide a more comprehensive picture of the water-rock-microbial interactions. Metagenomic methods sequence all DNA extracted from an environmental sample and is not limited to PCR amplification of a single 16S or 18S rRNA gene. Metaproteomic methods will provide insight into the proteins found in environmental samples. Metaproteomic analysis can provide additional information about metabolic activity and stress related changes in a microbial community. Both metagenomic and metaproteomic studies will advance the understanding and development of natural bioremediation and bioleaching.

In addition to metagenomic and metaproteomic analysis, further work is required to explore how niches and mixed waters affect microbial communities. The source of water mixing and

differences from the Ophir is currently under investigation by the Laboratory Exploring Geobiochemical Engineering and Natural Dynamics (LEGEND). Niche comparison of planktonic biomass versus differences in depth and surface should also be compared to provide an understanding of how or if the microbial communities change with depth. Additionally, seasonal work and annual work using 16S/18S rRNA genes in combination with the geochemical context can be used as a tool for monitoring changes in the water quality in relation to the mines' geochemistry.

References Cited

- Baker B. J. and Banfield J. F. (2003). Microbial communities in acid mine drainage. *FEMS Microbiol. Ecol.* **44**, 139-152.
- Baker-Austin C. and Dopson M. (2007). Life in acid: pH homeostasis in acidophiles. *Trends Microbiol.* **15**, 165-171.
- Bond P. L., Druschel G. K., and Banfield J. F. (2000). Comparison of acid mine drainage microbial communities in physically and geochemically distinct ecosystems. *Appl. Environ. Microbiol.* **66**, 4962–4971.
- Boyd E. S., Hamilton T. L., Spear J. R., Lavin M., and Peters J. W. (2010). [FeFe]-hydrogenase in Yellowstone National Park: evidence for dispersal limitation and phylogenetic niche conservatism. *ISME J.* **4**, 1485-1495.
- Brazelton W. J., Sogin M. L., and Baross J. A. (2010). Multiple scales of diversification within natural populations of archaea in hydrothermal chimney biofilms. *Environ Microbiol. Rep.* **2**, 236-242.
- Bruneel O., Duran R., Casiot C., Elbaz-Poulichet F., and Personné J.-C. (2006). Diversity of microorganisms in Fe-As-rich acid mine drainage waters of Carnoulès, France. *Appl. Environ. Microbiol.* **72**, 551-556.
- Cline J. D. (1969). Spectrophotometric determination of hydrogen sulfide in natural waters. *Anal. Chem.* **21**, 1005-1009.
- Craig H. (1961). Isotopic variations in meteoric waters. *Science.* **133**, 1702-1703.
- Dick J. M. (2008). Calculation of the relative metastabilities of proteins using the CHNOSZ software package. *Geochem. Trans.* **9**, 1-17.
- Dowd S. (n.d.). *Readme*. Shallowater, TX: MR DNA.

Duaime, T. E. (2015). August 2015 water monitoring report and data (All monitoring locations).

Montana Bureau of Mines and Geology. 1-41.

Duaime, T. E. (2017, April). Personal communication.

Duaime T. E., Icopini G. A., McGrath S. F., and Thale, P.R. (2016). Butte mine flooding operable unit water-level monitoring and water-quality sampling 2015 consent decree update Butte, Montana (1982-2015). *Montana Bureau of Mines and Geology*.

Duaime T.E., Kennelly P.J., Thale P.R. (2004). Butte, Montana: richest hill on Earth, 100 years of underground mining. *Montana Bureau of Mines and Geology*, misc. contribution. **19**, unpaginated poster.

Duaime T. E., Metesh J. J., Kerschen M. D., and Dunstan C. B. (1998). The flooding of Butte's underground mines and Berkeley Pit: 15 Years of water-level monitoring (1982-1987).

Montana Bureau of Mines and Geology.

Duaime, T. E. and Tucci N. J. (2008). History of flooding of the Butte underground mines and Berkeley Pit, water-level monitoring and water-quality sampling, 2007 consent decree update, Butte, Montana (1982-2007). *Montana Bureau of Mines and Geology*.

Edwards K. J., Bond P. L., Gihring T. M., and Banfield J. F. (2000). An archaeal iron-oxidizing extreme acidophile important in acid mine drainage. *Science*. **287**, 1796–1799.

Gammons C. H., Metesh J. J., and Snyder, D. M. (2006). A survey of the geochemistry of flooded mine shaft water in Butte, Montana. *Mine Water Environ.* **25**, 100-107.

Gammons C. H., Poulson S. R., Pellicori D. A., Reed P. J., Roesler A. J., and Petrescu, E. M. (2006). The hydrogen and oxygen isotopic composition of precipitation, evaporated mine water, and river water in Montana, USA. *J. Hydrol.* **328**, 319-330.

- Gammons C. H., Snyder D. M., Poulson S. R., and Petritz K. (2009). Geochemistry and stable isotopes of the flooded underground mine workings of Butte, Montana. *Econ. Geol.* **104**, 1213-1234.
- Godon J. J., Morinière J., Moletta M., Gaillac M., Bru V., and Delgènes J. P. (2005). Rarity associated with specific ecological niches in the bacterial world: the ‘Synergistes’ example. *Environ. Microbiol.* **7**, 213-224.
- Golyshina O. V., Kublanov I. V., Tran H., Korzhenkov A. A., Lünsdorf H., Nechitaylo T. Y., and Golyshin P. N. (2016). Biology of archaea from a novel family Cuniculiplasmataceae (Thermoplasmata) ubiquitous in hyperacidic environments. *Sci. Rep.* **6**.
- Hamidian H., Rezai B., Milani S. A., Vahabzade F., and Shafaie S. Z. (2009). Microbial leaching of uranium ore. *Asian J. Chem.* **21**, 5808-5820.
- Hoefs J. (1997). *Stable Isotope Geochemistry*. **201**. Berlin: Springer.
- Janda J. M. and Abbott S. L. (2007) 16S rRNA gene sequencing for bacterial identification in the diagnostic laboratory: pulses, perils, and pitfalls. *J. Clin. Microbiol.* **45**, 2761-2764.
- Jenkins R. E., and Lorengo J. A. (2002, January/February). Butte, Montana. *Mineralogical Record*. **33**, 4-69.
- Kendall C., Sklash M. G., and Bullen T. D. (1995). “Isotope tracers of water and solute sources in catchments”, In: S.T. Trudgill (Ed.), *Solute modelling in catchment systems*. John Wiley and Sons Ltd., New York, pp. 261-303.
- Madigan M., Martinko J., Stahl D., Clark D.P. (2011). *Brock Biology of Microorganisms*. New York, New York: Pearson Higher Ed.
- Madsen E. L. (2015). *Environmental microbiology: from genomes to biogeochemistry*. John Wiley & Sons Ltd., New York.

- Mendez-Garcia C., Mesa V., Sprenger R. R., Richter M., Diez M. S., Solano J., and Ferrer M. (2014). Microbial stratification in low pH oxic and suboxic macroscopic growths along an acid mine drainage. *ISME J.* **8**, 1259–1274.
- Mendez-Garcia C., Pelaez A. I., Mesa V., Sanchez J., Golyshina O. V., and Ferrer M. (2015). Microbial diversity and metabolic networks in acid mine drainage habitats. *Front. Microbiol.* **6**.
- Metesh J. J. (1990). *Aquifer testing and evaluation at the Travona mine and Marget Ann mine, Butte, Montana* (Doctoral thesis). (Accession No. EP32148): ProQuest Dissertations Publishing.
- Metesh J. J., and Duaine T. E. (2002). The flooding of Butte's underground mines and the Berkeley Pit: Water-quality monitoring through 2000. *Montana Bureau of Mines and Geology*.
- Meyer S. C., Goddard C. C., and Staff. (1968). Ore deposits at Butte, Montana. In: Ridge J. (Ed.), *Ore deposits of the United States, 1933-67*. New York, New York, American Institute of Mining, Metallurgical, and Petroleum Engineers. **2**, 1373-1416.
- Mohan S. V., Agarwal L., Mohanakrishna G., Srikanth S., Kapley A., Purohit H. J., and Sarma P. N. (2011). Firmicutes with iron dependent hydrogenase drive hydrogen production in anaerobic bioreactor using distillery wastewater. *Int. J. Hydrogen Energy.* **36**, 8234-8242.
- Montana Bureau of Mines and Geology. (1987). Ground Water Information Center: Berkeley Pit Water Quality. Retrieved from MBMG Data Center: <http://mbmgwic.mtech.edu/>
- Montana Bureau of Mines and Geology. (2016). Ground Water Information Center: Berkeley Pit Water Quality. Retrieved from MBMG Data Center: <http://mbmgwic.mtech.edu/>

- Montana Bureau of Mines and Geology. (2017, April 13). Ground Water Information Center. Retrieved from MBMG Data Center: <http://mbmaggwic.mtech.edu/>
- Pellicori D. A., Gammons C. H., and Poulson S. R. (2005). Geochemistry and stable isotope composition of the Berkeley pit lake and surrounding mine waters, Butte, Montana. *Appl. Geochem.* **20**, 2116–2137.
- PitWatch. (2013, July 30). *1982-2013: 31 years since pumps stopped*. Retrieved April 11, 2017, from pitwatch.org: www.pitwatch.org/31-years-since-pumps-stopped/.
- Roesler A. J., Gammons C. H., Druschel G. K., Oduro H., and Poulson S. R. (2007). Geochemistry of flooded underground mine workings influenced by bacterial sulfate reduction. *Aquat. Geochem.* **13**, 211-235.
- Sacks L. A. (1996). *Geochemical and isotopic composition of ground water with emphasis on sources of sulfate in the upper Floridan Aquifer in parts of Marion, Sumter, and Citrus Counties, Florida*. US Department of the Interior, US Geological Survey.
- Schmidt R. J., and Cox A. D. (2016a, October). *Natural amelioration in flooded mine shafts and related changes in arsenic concentrations*. Oral session presented at the Mining and Mineral Symposium, Butte, MT.
- Schmidt R. J., & Cox A. D. (2016b, December). *Geochemical changes in flooded underground mines*. Poster session presented at the American Geophysical Union, San Francisco, CA.
- Shock E. (2007). *GEOPIG SUPCRT Application Reactants*. Retrieved from <http://geopig3.la.asu.edu:8080/GEOPIG/pigopt1.html>.
- Smedley P. L., and Kinniburgh D. G. (2002). A review of the source, behaviour and distribution of arsenic in natural waters. *Appl. Geochem.* **17**, 517-568.

- Snyder D. (2012). *Vertical gradients in geochemistry of flooded mine shafts in Butte, Montana* (Master's thesis). (Accession No. 1509954): ProQuest Dissertations Publishing.
- St. Clair B. (2017). *Kinetics, Thermodynamics and Habitability of Microbial Iron Redox Cycling* (Doctoral thesis). (Accession No. 10276056): ProQuest Dissertations Publishing.
- Stevenson, Ryan. (2015). Stable isotopes of hydrothermal carbonate minerals in the Butte porphyry-lode deposits, Montana (Master's thesis). (Accession No.1599386). ProQuest Dissertations Publishing.
- Thomas F., Hehemann J. H., Rebuffet E., Czjzek M., & Michel G. (2011). Environmental and gut Bacteroidetes: the food connection. *Front. Microbiol.* **2**.
- To T. B., Nordstrom D. K., Cunningham K. M., Ball J. W., and McCleskey R. B. (1999). New method for the direct determination of dissolved Fe (III) concentration in acid mine waters. *Environ. Sci. Technol.* **33**, 807-813.
- Ward N. L., Challacombe J. F., Janssen P. H., Henrissat B., Coutinho P. M., Wu M., and Barabote R. D. (2009). Three genomes from the phylum Acidobacteria provide insight into the lifestyles of these microorganisms in soils. *Appl. Environ. Microbiol.* **75**, 2046-2056.
- Woese C. R. and Fox G. E. (1977). Phylogenetic structure of the prokaryotic domain: the primary kingdoms. *Proc. Natl. Acad. Sci.* **74**, 5088-5090.
- Yu H., Zhu Z., Hu W., and Zhang H. (2002). Hydrogen production from rice winery wastewater in an upflow anaerobic reactor by using mixed anaerobic cultures. *Int. J. Hydrogen Energy.* **27**, 1359-65.
- Zettler L. A., Messerli M. A., Laatsch A. D., Smith P. J., and Sogin M. L. (2003). From genes to genomes: Beyond biodiversity in Spain's Rio Tinto. *Biol. Bull.* **204**, 205-209.

Zeng Y., Feng F., Medová H., Dean J., and Koblížek, M. (2014). Functional type 2 photosynthetic reaction centers found in the rare bacterial phylum Gemmatimonadetes. *Proc. Natl. Acad. Sci.* **111**, 7795-7800.

Ziegler S., Dolch K., Geiger K., Krause S., Asskamp M., Eusterhues K., and Gescher J. (2013). Oxygen-dependent niche formation of a pyrite-dependent acidophilic consortium built by archaea and bacteria. *ISME J.* **7**, 1725–1737.

6. Appendix A: Raw Data

Table IX: Hydrolab field parameters for mines, Silver Bow and Blacktail Creeks.

Site	Zone	Collection Method [‡]	Date YYMMDD	pH ^a	T ^b (°C)	Con. ^c (µS/cm)	ORP ^d (V)	Alkalinity ^e (mmol/L)	DO ^f (µmol/L)
Santa	SBC	<i>In situ</i>	160215	7.33	4.69	556.6	--	--	262
Santa	SBC	<i>In situ</i>	160522	7.88	9.40	225.0	--	--	326
Slag Canyon	SBC	<i>In situ</i>	160215	7.35	4.54	350.9	--	--	291
Slag Canyon	SBC	<i>In situ</i>	160522	7.91	8.40	151.6	--	--	331
KOA	BC	<i>In situ</i>	160215	7.34	5.71	341.4	--	--	330
KOA	BC	<i>In situ</i>	160522	7.98	8.00	146.8	--	--	334
Kelley	East	Bailer	160314	4.65↑	32.31↓	6634	0.358	0.68	34.7*
Steward	East	Bailer	160315	5.51↑	22.33↓	3681	0.289	4.52	76.3*
Anselmo	East	Bailer	160314	5.94	16.79	2135	0.288	6.32	70*
Pilot Butte	East	Bailer	160523	6.15	17.18	4410	0.280	3.06	BDL
Emma	West	Pump	160523	6.34	17.10	1492	-0.570	7.20	BDL
Travona	West	Pump	160316	6.38	12.30	1296	0.187	5.82	95
Ophir	West	Pump	160316	6.55	11.53	511.2	0.270	3.56	8.75
Orphan Boy	Outer	<i>In situ</i>	160523	7.07	22.40	1987	-0.670	13.68	BDL
Orphan Girl	Outer	<i>In situ</i>	160523	7.87	26.57	1990	NA	13.08	BDL

[‡]Meter readings collected *in situ* were taken directly from the body of water. Meter readings from bailer methods are approximate due to the time between sample collection and analysis (pH and temperature were continuously changing. Arrows indicate direction of change). Pump meter readings were taken after all parameters stabilized. Not all errors were recorded for each parameter, so error ranges are approximate.

^a Error: ±0.04 (maximum flux in readings)

^b Error: ±0.01 °C (maximum flux in readings)

^c Conductivity; error ±0.5 µS/cm (maximum flux in readings)

^d Oxidation reduction potential; error ±0.001 V (maximum flux in readings)

^e Alkalinity; error ±0.02 mmol/L (method sensitivity)

^f Dissolved oxygen; error ±60 µmol/L (maximum flux in readings). Detection limit 5µmol/L.

* DO levels are falsely high due to bailing method

BDL: below detection limit

Table X: Spectrophotometry data.

Site	SiO ₂ ^a ($\mu\text{mol/L}$)	Fe ^{+2b} ($\mu\text{mol/L}$)	Sulfide ^c ($\mu\text{mol/L}$)
Santa 160215	376	120	BDL
Santa 160522	---	0.45	BDL
Slag Canyon 160215	428	4.4	BDL
Slag Canyon 160522	BDL	0.33	BDL
KOA 160215	404	BDL	BDL
KOA 160522	514	0.21	BDL
Kelley	Int.	24000	BDL
Steward	Int.	4700	0.25
Anselmo	558	340	BDL
Pilot Butte	Int.	230	0.36
Emma	Int.	230	12
Travona	298	6.8	7.1
Ophir	335	47	3.2
Orphan Boy	Int.	Int.	130
Orphan Girl	225	Int.	150

^a Detection limit: 17 $\mu\text{mol/L}$

^b Detection limit: 3.6×10^{-2} $\mu\text{mol/L}$

^c Detection limit: 0.2 $\mu\text{mol/L}$

Int: matrix interference

BDL: below detection limit

Table XI: Stable isotopes.

Site	δD^a (‰)	$\delta^{18}\text{O}^b$ (‰)	$\delta^{13}\text{C}_{\text{DIC}}^b$ (‰)	$\delta^{13}\text{C}_{\text{DOC}}^b$ (‰)
Santa Feb.	-137	-17.3	-26.4	BDL
Santa May	-128	-15.9	-7.9	-27.0
Slag Canyon Feb.	-137	-17.4	-26.1	BDL
Slag Canyon May	-129	-16.5	-7.5	-27.3
KOA Feb.	-137	-17.4	-28.5	BDL
KOA May	-130	-16.6	-9.3	-27.2
Kelley	-142	-17.6	-13.6	-22.3*
Steward	-138	-17.6	-14.3	-18.2*
Anselmo	-136	-17.1	-12.3	-22.9
Pilot Butte	-140	-17.8	-15.0	-24.6
Emma	-135	-17.4	-19.4	-24.8
Travona	-136	-17.4	-13.6	-24.3
Ophir	-137	-17.7	-9.6	-21.6
Orphan Boy	-140	-17.5	-22.9	-24.4
Orphan Girl	-140	-17.7	-23.0	-24.4

BDL: below detection limit; if carbon concentrations were too low, isotopic values were not obtained.

*Compromised values due to ethanol contamination. Value is isotopically heavy.

^a Error ± 1 ‰ (instrument sensitivity)

^b Error ± 0.1 ‰ (instrument sensitivity)

Table XII: Dissolved carbon concentrations in mines and Silver Bow and Blacktail Creeks.

Site	DIC mg/L	DOC mg/L
Santa 160215	2.78	BDL
Santa 160522	20.4	4.8
Slag Canyon 160215	1.9	BDL
Slag Canyon 160522	11.9	5.6
KOA 160215	2.0	BDL
KOA 160522	18.6	5.6
Kelley	92.4	8.2*
Steward	133.7	7.6*
Anselmo	105.1	2.4
Pilot Butte	111.1	0.2
Emma	125.3	0.9
Travona	78.9	1.7
Ophir	43.9	1.6
Orphan Boy	225.3	3.5
Orphan Girl	234.1	4.0

DIC: dissolved inorganic carbon; detection limit 1 mg/L

DOC: dissolved organic carbon; detection limit 0.1 mg/L

BDL: below detection limit.

Error for DIC and DOC: $\pm 3\%$ (instrument sensitivity)

*DOC samples contaminated from ethanol and are falsely high

Table XIII: Major cation concentrations in mines.

Site	Na ⁺ (mmol/L)	K ⁺ (mmol/L)	Mg ⁺² (mmol/L)	Ca ⁺² (mmol/L)	Mn ⁺² (mmol/L)	Fe _(TOT) (mmol/L)
Kelley	3.8	1.6	14.9	11.7	2.20	20.30
Steward	2.1	0.9	6.0	11.0	0.48	3.55
Anselmo	2.2	0.4	3.7	8.2	0.14	0.38
Pilot Butte	0.9	0.3	3.7	6.1	2.40	2.89
Emma	2.1	0.2	2.5	5.0	0.13	0.01
Travona	1.8	0.2	2.2	4.7	0.06	0.01
Ophir	0.7	0.1	0.7	1.4	0.09	0.03
Orphan Boy	5.2	0.2	2.1	4.6	0.07	BDL
Orphan Girl*	5.3	0.2	2.1	4.7	0.07	BDL
Error (%)	10.	10.	10.	10.	5.0	5.4

Errors from instrument sensitivity.

Table XIV: Major anion concentrations in mines

Site	F ⁻ (mmol/L)	Cl ⁻ (mmol/L)	HCO ₃ ^{-*} (mmol/L)	SO ₄ ⁻² (mmol/L)
Kelley	1.53	0.94	0.82	82.50
Steward	0.15	1.32	4.73	26.40
Anselmo	0.03	1.45	6.41	11.20
Pilot Butte	0.08	0.67	3.16	28.20
Emma	0.02	2.02	8.46	3.98
Travona	0.02	2.74	6.60	3.80
Ophir	0.03	0.50	3.46	0.86
Orphan Boy	0.04	0.51	15.40	1.95
Orphan Girl	0.04	0.51	15.20	1.93
Error (%)	5.6	0.8	3.0	0.8

Bicarbonate value calculated from pH, temperature, the acid dissociation constant total DIC concentration. Errors from instrument sensitivity.

Table XV: Trace element concentrations in mines.

Site	Li ($\mu\text{mol/L}$)	Be ($\mu\text{mol/L}$)	B ($\mu\text{mol/L}$)	Al ($\mu\text{mol/L}$)	Ti ($\mu\text{mol/L}$)	V ($\mu\text{mol/L}$)	Co ($\mu\text{mol/L}$)	Ni ($\mu\text{mol/L}$)
Kelley	30.50	1.37	12.10	486.00	160.00	0.16	7.48	18.30
Steward	5.06	BDL	5.80	18.60	112.00	BDL	1.04	2.17
Anselmo	3.89	BDL	6.23	0.13	85.20	BDL	0.09	0.29
P. Butte	4.90	BDL	5.13	4.16	115.00	BDL	0.69	2.40
Emma	5.82	BDL	14.60	0.09	68.00	BDL	BDL	0.16
Travona	3.92	BDL	15.20	0.08	45.70	BDL	BDL	BDL
Ophir	1.18	BDL	4.15	0.29	11.90	BDL	BDL	BDL
O. Boy	18.90	BDL	3.71	0.08	52.30	0.04	BDL	BDL
O. Girl	22.30	BDL	5.48	0.05	57.40	0.04	BDL	BDL
Error (%)	4.2	3.7	4.0	5.6	3.8	4.4	4.1	4.1
Detection limit ($\mu\text{mol/L}$)	0.22	0.22	0.22	0.01	0.30	0.02	0.02	0.08
Site	Cu ($\mu\text{mol/L}$)	Zn ($\mu\text{mol/L}$)	As ($\mu\text{mol/L}$)	Se ($\mu\text{mol/L}$)	Rb ($\mu\text{mol/L}$)	Sr ($\mu\text{mol/L}$)	Mo ($\mu\text{mol/L}$)	Cd ($\mu\text{mol/L}$)
Kelley	0.69	8550.00	125.00	0.69	2.20	6.53	0.30	0.79
Steward	BDL	1920.00	26.20	BDL	0.92	18.50	BDL	BDL
Anselmo	BDL	220.00	2.05	BDL	0.30	38.40	BDL	BDL
P. Butte	BDL	1180.00	12.50	BDL	0.70	63.20	BDL	BDL
Emma	BDL	BDL	0.04	BDL	0.19	22.90	BDL	BDL
Travona	BDL	BDL	0.79	BDL	0.14	14.00	BDL	BDL
Ophir	BDL	BDL	0.06	BDL	0.07	2.72	BDL	BDL
O. Boy	BDL	BDL	0.05	BDL	0.22	67.20	BDL	BDL
O. Girl	BDL	BDL	BDL	BDL	0.23	71.20	BDL	BDL
Error (%)	4.3	4.8	3.8	4.6	3.0	3.8	3.9	4.0
Detection limit ($\mu\text{mol/L}$)	0.30	0.14	0.01	0.29	0.05	0.22	0.21	0.14
Site	Cs ($\mu\text{mol/L}$)	Ba ($\mu\text{mol/L}$)	Nd ($\mu\text{mol/L}$)	W ($\mu\text{mol/L}$)	U ($\mu\text{mol/L}$)	Total ($\mu\text{mol/L}$)		
Kelley	0.07	BDL	0.61	0.06	0.03	9402.86		
Steward	BDL	BDL	BDL	BDL	BDL	2110.29		
Anselmo	BDL	1.07	BDL	BDL	0.08	357.73		
P. Butte	0.06	BDL	BDL	BDL	0.09	1388.82		
Emma	BDL	2.51	BDL	BDL	0.08	114.39		
Travona	BDL	1.67	BDL	BDL	0.07	81.56		
Ophir	BDL	BDL	BDL	BDL	BDL	20.37		
O. Boy	BDL	7.02	BDL	0.14	0.12	149.78		
O. Girl	BDL	7.94	BDL	0.16	0.12	164.91		
Error (%)	3.0	3.8	4.1	3.2	4.1			
Detection limit ($\mu\text{mol/L}$)	0.04	0.60	0.10	0.04	0.01			

BDL: below detection limit. Errors from instrument sensitivity.

Table XVI: Log K values for carbonic acid reaction in equation 4

Site	Temperature (°C)	Log K
Kelley	32.31	-6.310
Steward	22.33	-6.363
Anselmo	16.79	-6.397
Pilot Butte	17.18	-6.397
Emma	17.10	-6.397
Travona	12.30	-6.439
Ophir	11.53	-6.439
Orphan Boy	22.40	-6.363
Orphan Girl	26.57	-6.339

Log K obtained from SUPCRT using reaction (2) (Shock, 2007)

Table XVII: Nanodrop results and DNA yields

Sample	Extraction Yield (ng DNA/L H ₂ O)	260/280*	Concentration (ng/μL) ^{a,b}	Total Extracted (ng)
Kelley	9.45	1.65	23.5	2350
Steward	15.5	1.77	46.6	4660
Anselmo	18.7	1.63	36.9	3690
Pilot Butte	6.13	2.05	17.7	1770
Emma	9.53	1.40	14.3	1430
Travona	2.71	1.63	6.2	620
Ophir	6.55	2.26	9.5	950
Orphan Boy	3.78	1.72	19.3	1930
Water				
Orphan Boy	--	1.91	16.1	1610
Wood				

* ideal 260/280 ratio is ~1.8

^a Accuracy: ±3.0%

^b Detection limit: 2ng/μl

Table XVIII: Domain distribution by sequence count

	Archaea OTU	Bacteria OTU	Eukarya OTU	Total hits OTU
Kelley	1292	130263	4	131559
Steward	19816	250539	772	306623
Anselmo	21340	286035	214	72093
Pilot Butte	17194	273539	99	290832
Emma	33	54340	5	54378
Travona	27	56908	3	56938
Ophir	1116	142497	179	143792
Orphan Boy	66	156313	33	156412
Orphan Boy Wood	6850	358149	59	369646

Distribution counts are from 16S and 18s rRNA gene analysis from PCR product. OTU counts based on 97% similarity.

Table XIX: Archaeal classes and phyla sequence counts.

Phylum/Class	Kelley	Steward	Anselmo	Pilot				Orphan Boy	Orphan Boy Wood
				Butte	Emma	Travona	Ophir		
Methanobacteria	21	4648	3724	2241	9	687	8	14	1613
Thermococci	1	116	13	0	0	0	2	1	17
Archaeoglobi	0	40	9	0	0	0	0	0	0
Parvarchaeota	0	110	5	5	0	0	1	0	0
Methanomicrobia	41	12131	3856	11841	10	20	6	18	3388
Thermoplasmata	7	1380	441	73	3	402	5	6	99
Thermoprotei	0	97	0	0	0	0	0	0	3
Euryarchaeota	396	135	1281	626	0	0	0	1	20
Halobacteria	2	416	486	5	1	0	0	0	822
Methanopyri	0	5	0	0	0	0	0	0	0
Methanococci	3	920	6260	403	1	0	0	7	258
Thaumarchaeota	8	808	2118	1348	8	6	3	16	281
Crenarchaeota	813	534	1623	652	1	1	2	3	349

Table XX: Bacterial phyla sequence counts.

Phylum	Kelley	Steward	Anselmo	Pilot				Orphan Boy	Orphan Boy Wood
				Butte	Emma	Travona	Ophir		
Acidobacteria	1422	38245	19947	15668	744	41	371	663	5405
Actinobacteria	11592	9708	4869	10004	22662	19571	358	59050	8251
Aquificae	1	0	25	0	0	0	0	0	36
Armatimonadetes	4	19	17	12	11	5	8	5909	24
Bacteroidetes	11659	4197	2687	14337	6436	94	52788	3485	29514
Caldiserica	0	4	3	1	0	0	0	0	0
Candidatus									
Saccharibacteria	0	0	0	0	0	0	0	0	0
Chlamydiae	3	225	230	848	3	2	3	1	408
Chlorobi	1	223	79	1045	0	0	1	2	25
Chloroflexi	1503	7487	4270	21246	65	1232	754	14689	21675
Chrysiogenetes	0	0	1	3	0	0	0	0	0
Cloacimonetes	0	0	0	0	0	0	0	0	4
Cyanobacteria	369	2937	1999	4045	6	3	788	16	3174
Deferribacteres	0	0	0	0	0	0	98	0	35
Deinococcus									
Thermus	2	15	122	542	1	1	2	3	95
Dictyoglomi	0	8	37	128	0	0	1	0	52
Elusimicrobia	4	1063	672	1380	1	2	133	1	89
Fibrobacteres	2	1	0	5	0	1	91	0	2
Firmicutes	13672	12406	10997	12656	3229	2919	56306	15026	12215
Fusobacteria	0	1	7	2	0	0	0	0	193
Gemmatim-									
onadetes	988	286	400	207	72	33	73	37074	287
Ignavibacteriae	340	1855	371	12815	6	6	21	34	14647
Lentisphaerae	0	60	105	292	0	1	75	0	423
Nitrospinae	0	0	18	0	0	0	0	0	68
Nitrospirae	11	158	1032	388	6	4	7	11	318
Planctomycetes	103	601	1012	3261	15	12	242	1672	2615
Proteobacteria	88233	164960	217666	162381	21042	32931	8752	18614	251864
Spirochaetes	7	1194	354	551	4	2	829	5	3861
Synergistetes	45	93	187	182	14	27	20447	25	112
Tenericutes	1	88	419	81	0	0	50	0	155
Thermodesulfo-									
bacteria	0	0	5	0	0	0	0	0	298
Thermotogae	0	3	21	4	0	0	0	0	7
Verrucomicrobia	301	4702	18483	11455	23	21	299	33	2297

Table XXI: Eukaryotic phyla and domain sequence counts.

	Kelley	Steward	Anselmo	Pilot				Orphan Boy	Orphan Boy Wood
				Butte	Emma	Ophir	Travona		
Bacillariophyta	1	1	0	1	0	0	0	0	0
Euglenida	0	34	721	1	1	0	0	0	2
Eukaryota	3	45	49	96	4	179	3	4	57
Eustigmatophyceae	0	0	2	1	0	0	0	0	0

7. Appendix B: Supplemental Data

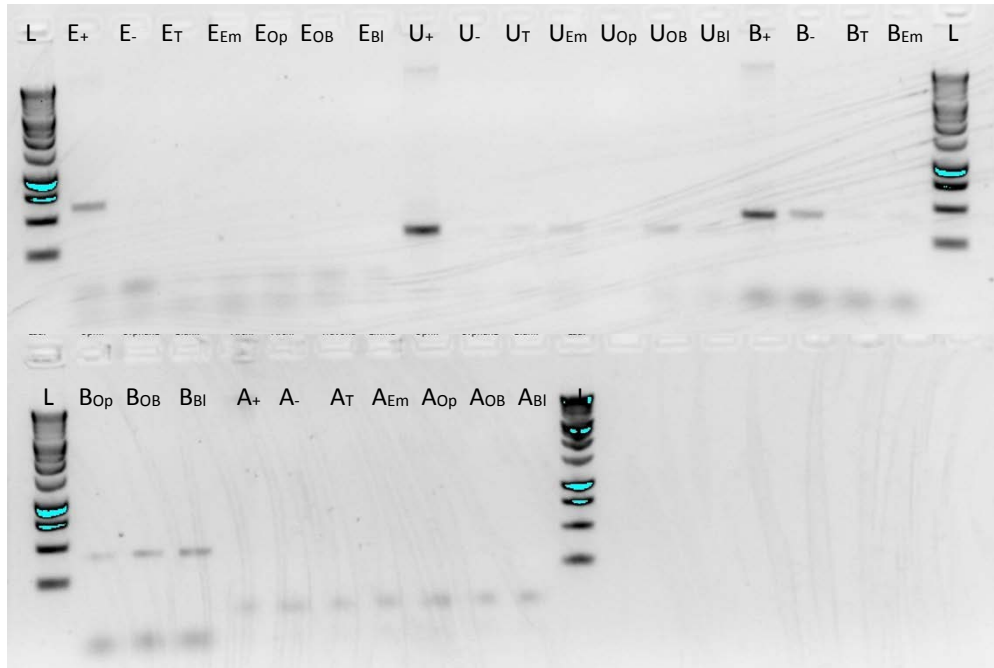


Figure 30: Gel electrophoresis of mine samples (set 1).

L:ladder, E:Eukarya, U:Universal, B:Bacteria, A:Archaea, +:positive control, -:negative control, T:Travona, Em:Emma, Op:Ophir, Bl:Stevivex blank. Bands on gel are from PCR products.

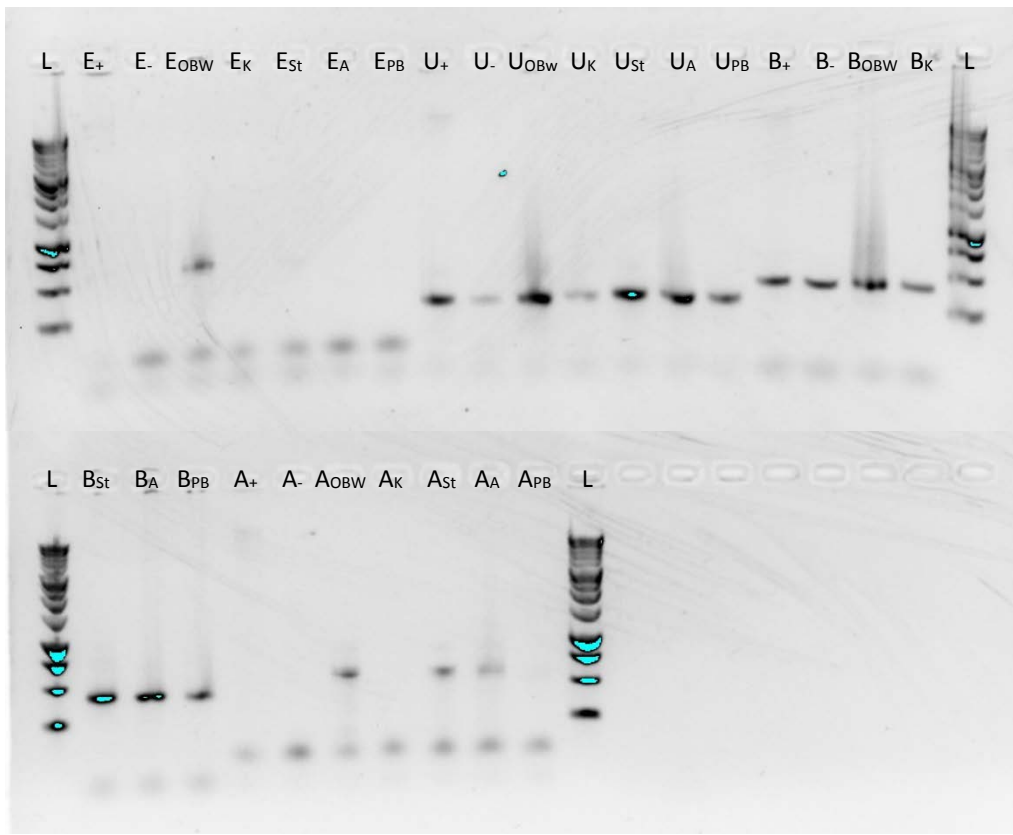


Figure 31: Gel electrophoresis of mine samples (set 2).

L:ladder, E:Eukarya, U:Universal, B:Bacteria, A:Archaea, +:positive control, -:negative control, OBW:Orphan Boy Wood, K:Kelley, St:Steward, PB:Pilot Butte. Bands on gel are from PCR products.

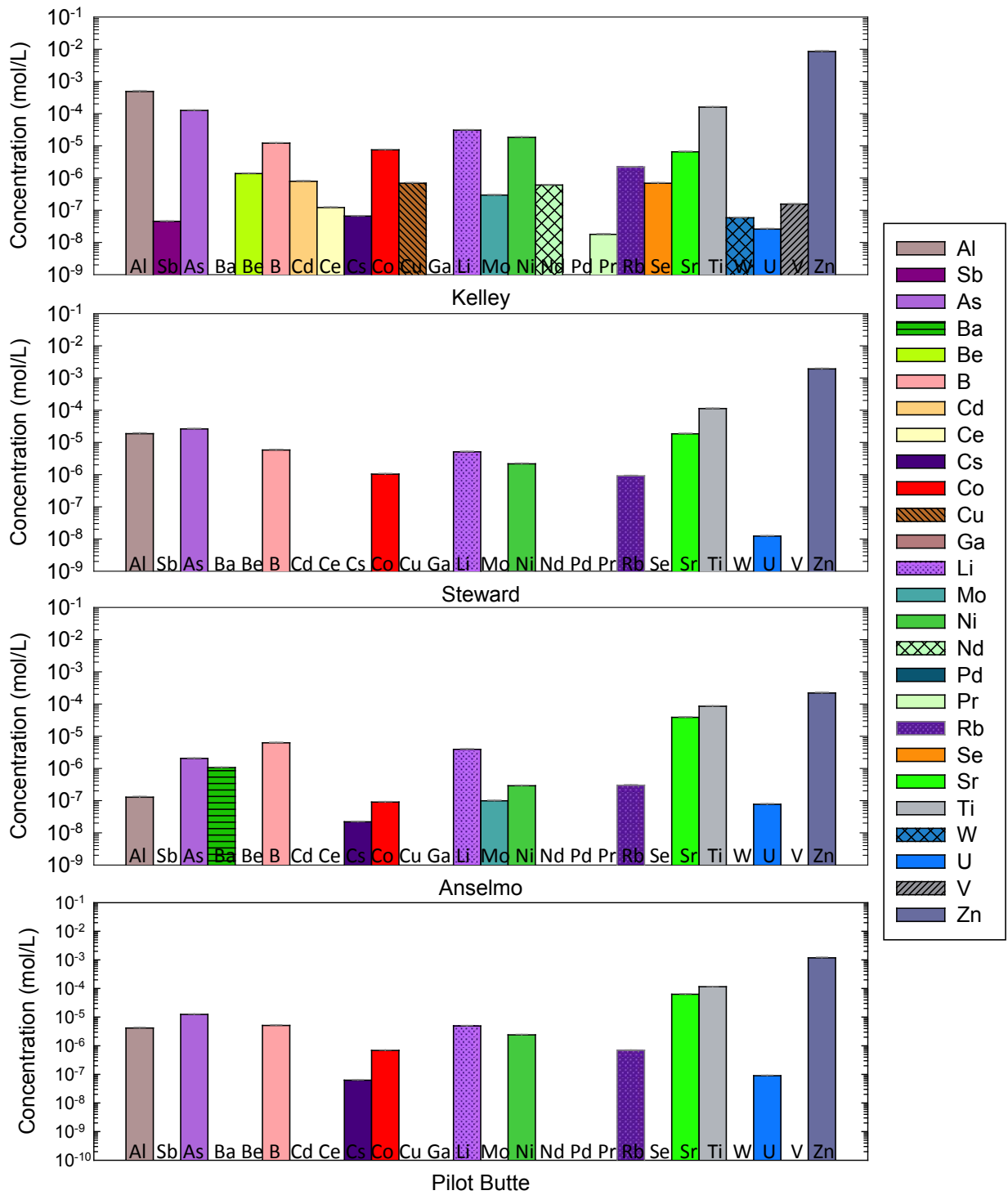


Figure 32: East Camp trace element concentrations

Error bars represent instrumental error for each element. Detection limits vary by element. See Table XV for each element's error and detection limit. Concentrations reported in logarithmic values.

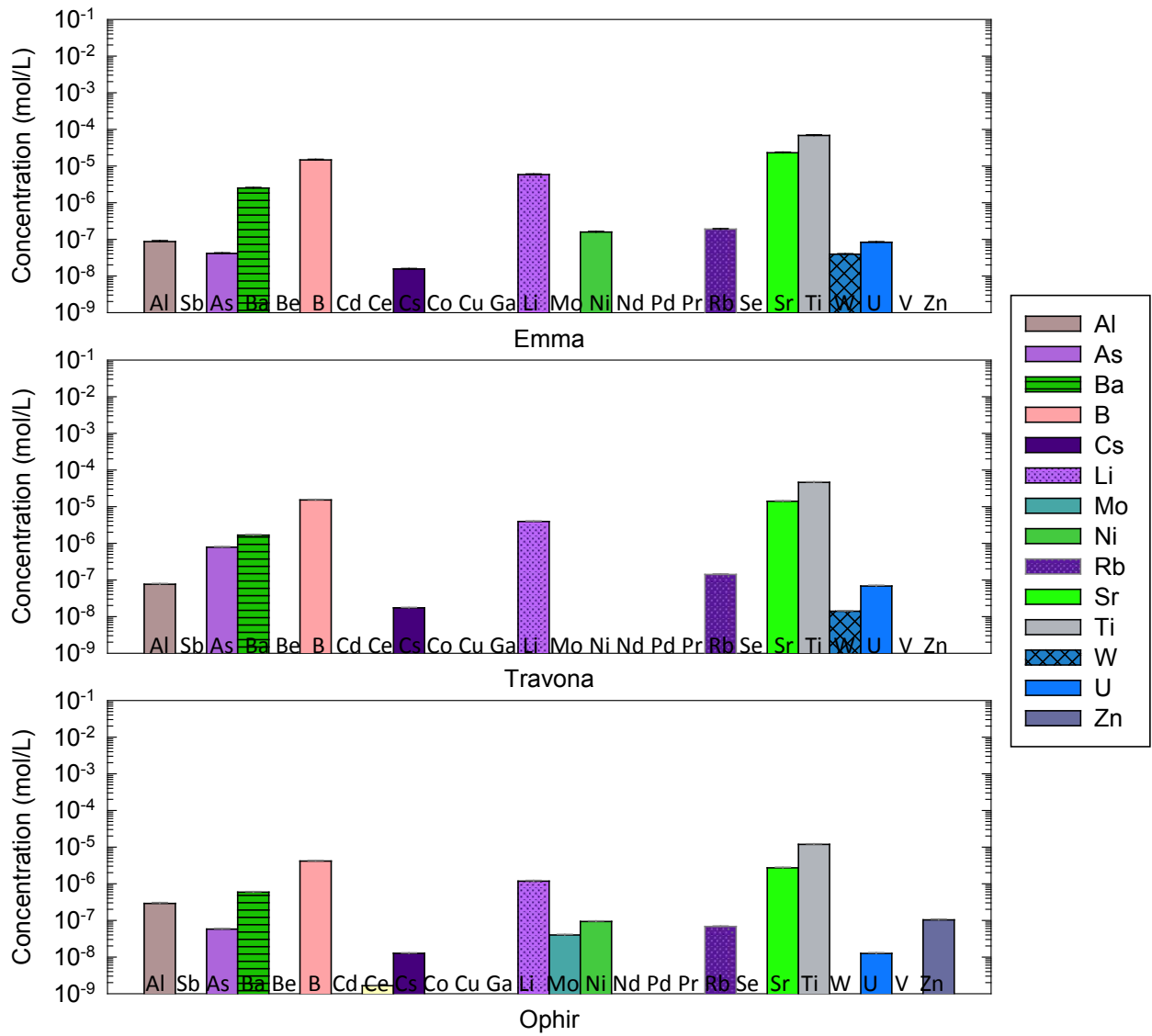


Figure 33: West Camp trace element concentrations

Error bars represent instrumental error for each element. Detection limits vary by element. See Table XV for each element's error and detection limit. Concentrations reported in logarithmic values.

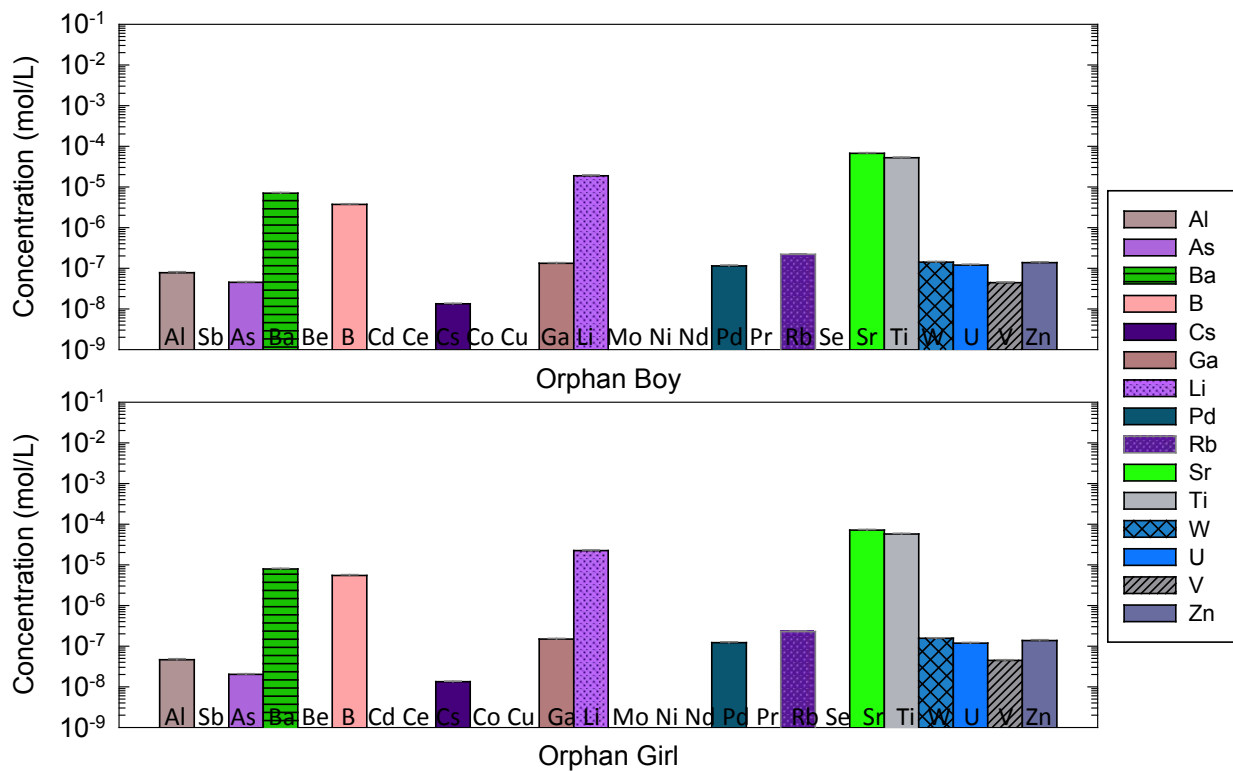
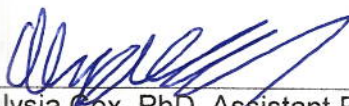


Figure 34: Outer Camp trace element concentrations

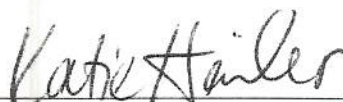
Error bars represent instrumental error for each element. Detection limits vary by element. See Table XV for each element's error and detection limit. Concentrations reported in logarithmic values.

SIGNATURE PAGE


This is to certify that the thesis prepared by Renee Johanna Schmidt entitled "Biogeochemical Interactions in Flooded Underground Mines" has been examined and approved for acceptance by the Department of Chemistry and Geochemistry, Montana Tech of the University of Montana, on this 29th day of June, 2017.




Alysia Cox, PhD, Assistant Professor
Department of Chemistry and Geochemistry
Chair, Examination Committee



Katie Hailer, PHD, Associate Professor and Department Head
Department of Chemistry and Geochemistry
Member, Examination Committee



Marisa Pedulla, PhD, Professor
Department of Biological Sciences
Member, Examination Committee



Chris Gammons, PhD, Professor
Department of Geological Engineering
Member, Examination Committee